

**Faculdade de Engenharia da Universidade do Porto**



# **Analysis of Bone Damage during Drilling Processes**

Maria Goreti Antunes Fernandes

Programa Doutoral em Engenharia Mecânica

October 2017



# **Analysis of Bone Damage during Drilling Processes**

by

Maria Goreti Antunes Fernandes

A thesis submitted in conformity with the requirements for the  
Doctoral Degree in Mechanical Engineering by the Faculty of  
Engineering of the University of Porto

## **Supervisor:**

Renato Manuel Natal Jorge

Associate Professor, Department of Mechanical Engineering, Faculty of Engineering,  
University of Porto, Porto, Portugal

## **Co-Supervisor:**

Elza Maria Morais Fonseca

Assistant Professor, Department of Applied Mechanics, Polytechnic Institute of  
Bragança, Bragança, Portugal

Porto, October 2017



*“Aprender é a única coisa de que a mente nunca se cansa, nunca tem medo e nunca se arrepende.”*

*Leonardo da Vinci*



# Agradecimentos

É revigorante ver o resultado final daquilo que foi uma longa caminhada de conhecimentos, desafios, incertezas medos mas sobretudo conquistas. Símbolo daquilo que reúne não só toda uma dedicação e gosto pela investigação mas sobretudo a partilha da sabedoria e o compilar de vários contributos, sem os quais este trabalho simplesmente não existia.

Em primeiro lugar desejo expressar os meus agradecimentos sinceros ao meu orientador Professor Renato Manuel Natal Jorge. Obrigada pela oportunidade, confiança depositada em mim e sobretudo por toda a sua dedicação e esforço em proporcionar as melhores soluções e condições de trabalho essenciais para a realização e conclusão desta tese.

De seguida, um reconhecimento especial à minha coorientadora Professora Elza Maria Morais Fonseca. Os meus mais genuínos agradecimentos pela sua constante orientação, total disponibilidade e sobretudo pela motivação e amizade que sempre manteve presente, não só durante este percurso mas também durante grande parte da minha vida académica. Sem dúvida uma referência e símbolo de inspiração para mim.

A eles, orientador e coorientadora, quero exprimir que foi e será sempre uma honra poder trabalhar e sobretudo aprender junto daqueles que considero serem exemplo de dedicação e sucesso.

Referir também o importante apoio de todas as instituições envolvidas, sobretudo o INEGI (Instituto de Engenharia Mecânica e Gestão Industrial), bem como a FEUP (Faculdade de Engenharia da Universidade do Porto) e o IPB (Instituto Politécnico de Bragança). Agradeço as excelentes condições de trabalho e todas as ferramentas fornecidas para o desenvolvimento desta tese de doutoramento.

Agradecer às Professoras Maria Isabel Ribeiro Dias (CITAB-Centro de Investigação e de Tecnologias Agroambientais e Biológicas da Universidade de Trás-os-Montes e Alto Douro) e Maria Cristina Manzanares Céspedes (Unidade de Anatomia e Embriologia Humana da Faculdade de Medicina da Universidade de Barcelona) por proporcionarem todas as condições e ferramentas necessárias à realização dos ensaios experimentais em tecido ósseo de bovino e osso humano cadavérico, respetivamente.

Aos técnicos de laboratório, Jorge Meireles e Luísa Barreira do Instituto Politécnico de Bragança pela colaboração e disponibilidade prestada durante os ensaios experimentais.

Para terminar, obrigada a todos os meus amigos, especialmente aqueles que estiveram mais presentes durante esta minha etapa: João Pires, Joana Calejo, Daniela Correia, Ana Lousada e Ana Catarina Lopes. Obrigada pela amizade, carinho, boa disposição e conversas partilhadas.

Aos meus pais, irmãos e David um agradecimento especial pelo apoio, alegria, motivação constante e sobretudo por sempre estimularem a minha evolução profissional e pessoal. São eles que, incondicionalmente, me apoiam e apoiaram e sem eles certamente não seria a pessoa que sou hoje. Serei eternamente grata.

A todos, sem exceção, muito obrigada!



# Abstract

Bone drilling is an essential step in a broad range of clinical interventions. The success of these clinical operations depends of the drilling procedure quality in view to minimize associated injuries to the bone and surrounding tissue. Studies have shown that the bone damage is directly related with the drilling parameters, particularly, drill speed, feed-rate, applied force, drilling depth, drill bit geometry, the use or not a cooling system and also the bone type. Therefore, a thorough understanding of different materials and cutting parameters is essential to reduce the bone damage and help the health professionals in the success of these drilling surgeries.

In the present thesis, a comprehensive research was performed including numerical analysis and experimental tests of the thermal and mechanical aspects of bone tissue, with applications to the drilling situations. The effects of different drilling parameters on the temperature field and generated stresses were investigated taking into account the engineering and biological principles.

A work programme of experimental tests was conducted, using synthetic bone (polyurethane foam materials with different densities) and biological materials (bovine femurs and human cadaveric tibiae). Thermocouples and infrared thermography were used to measure the temperature during the experimental tests, and also linear strain gauges to measure the deformations during the drilling process.

Computational modelling of bone drilling included thermal and mechanical models to analyse the thermomechanical behaviour of bone tissue. The numerical models are able to predict the stresses and temperature distribution, during the perforation for a given material similar to bone characteristics, with a typical drill bit geometry and cutting conditions such as drill speed, feed-rate, drilling depth and use of cooling system. Additionally, novel dynamic models based on real geometries of human bone tibia were

developed. Comparative studies were performed for the developed numerical models and the results validated through the experimental tests. The magnitude and variation tendency of drilling temperatures and stresses obtained by both methodologies are in agreement.

The main outcome of this thesis is a detailed understanding of the bone drilling processes, contributing for the application of optimum drilling parameters that will minimise the bone damage due the invasive procedure. The results contribute to a comprehensive understanding of thermomechanical aspects of bone drilling process and associated predictive models. The developed models can be used to simulate, in a realistic manner, the drilling process under different aspects and to provide an important tool that will enable for the health professionals to plan an accurate and safe surgery with better post-surgery patient recovery.

## Resumo

A furação do tecido ósseo é um procedimento cirúrgico essencial em diversas intervenções clínicas. O sucesso destas cirurgias depende da qualidade do processo de furação, sendo objetivo principal a minimização das lesões associadas ao tecido ósseo e tecidos circundantes. Estudos efetuados têm demonstrado que a lesão óssea está diretamente relacionado com os parâmetros de furação, mais especificamente a velocidade de rotação da broca, velocidade de avanço, força aplicada, profundidade do furo, geometria da broca, o uso ou não de um sistema de arrefecimento e também o tipo de osso. Por conseguinte, a compreensão aprofundada dos diferentes materiais e dos parâmetros de corte envolvidos nestes processos é essencial na redução da lesão óssea e no auxílio aos profissionais de saúde para o sucesso nessas cirurgias.

Na presente tese foi realizada uma pesquisa abrangente que inclui a análise numérica e ensaios experimentais sobre os aspetos térmicos e mecânicos do tecido ósseo, com aplicações nos processos de furação. Os efeitos dos diferentes parâmetros de furação sobre o aumento da temperatura e tensões geradas foram investigados sob o ponto de vista da engenharia e da biologia.

Realizaram-se um conjunto de ensaios experimentais com recurso a osso sintético (materiais em espuma de poliuretano com diferentes massas volúmicas) e materiais biológicos (fémures de bovino e tíbias humanas cadavéricas). Foram utilizados termopares e a termografia para a medição da temperatura durante os ensaios experimentais, e ainda utilizada a extensometria para o registo das deformações durante o processo de furação.

A modelação computacional da furação óssea inclui modelos de materiais térmicos e mecânicos para analisar o comportamento termomecânico do tecido ósseo. Os modelos numéricos são capazes de prever as tensões e a distribuição da temperatura durante a

furação, considerando as características do osso, a geometria da broca e as condições de corte, tais como velocidade de rotação, velocidade de avanço, profundidade do furo e a utilização ou não de um sistema de arrefecimento. Além disso, foram desenvolvidos novos modelos dinâmicos baseados em geometrias obtidas de tíbias humanas. Foram efetuados estudos comparativos entre os modelos numéricos desenvolvidos e os resultados experimentais. A tendência obtida e verificada no campo das temperaturas e das tensões, ao longo da furação, através das diferentes metodologias, estão em concordância.

O principal resultado desta tese é obter uma análise detalhada dos processos de furação óssea, contribuindo para a implementação de parâmetros de furação ideais que minimizem a lesão no tecido ósseo e a agressividade no procedimento. Os resultados contribuem para uma compreensão abrangente dos aspetos termomecânicos do processo de furação e dos modelos preditivos associados. Os modelos desenvolvidos podem ser utilizados para simular, de forma realista, a furação sob diferentes aspetos e fornecer assim, uma ferramenta importante que permitirá aos profissionais de saúde planear uma cirurgia mais precisa e segura, e que possibilite uma melhor recuperação pós-cirúrgica ao paciente.

# Table of Contents

<b>CHAPTER I.....</b>	<b>1</b>
General Introduction and Motivations.....	1
1.1 Background and Motivation .....	3
1.2 Thesis Objectives.....	6
1.3 Thesis Structure .....	7
References.....	9
<b>CHAPTER II.....</b>	<b>13</b>
Literature Overview.....	13
2.1 Bone Tissue.....	15
2.1.1 Mechanical properties of cortical bone .....	17
2.1.2 Mechanical properties of trabecular bone .....	21
2.1.3 Thermal properties of bone tissue .....	22
❖ Specific heat of bone tissue .....	23
❖ Thermal conductivity of bone tissue .....	23
2.2 Bone Drilling in Medicine .....	26
2.2.1 Bone damage induced by drilling .....	26
❖ Mechanical damage in bone drilling .....	27
❖ Thermal osteonecrosis in bone drilling .....	29
2.2.2 Effects of drilling parameters on bone .....	31
❖ Drill bit specifications .....	32
❖ Drill parameters.....	39
2.2.3 Temperature measurement in bone drilling .....	48
❖ Thermocouples .....	49
❖ Infrared thermography.....	51
2.2.4 Numerical modelling in bone drilling .....	52

❖ Thermal models.....	53
❖ Mechanical models.....	54
References.....	56
<b>CHAPTER III.....</b>	<b>71</b>
Thermal analysis during bone drilling using rigid polyurethane foams: numerical and experimental methodologies* .....	71
Abstract.....	73
1 Introduction.....	75
2 Experimental Methodology .....	76
3 Numerical Analysis.....	80
4 Results and Discussion .....	83
5 Conclusions.....	88
Acknowledgments .....	88
References.....	88
<b>CHAPTER IV.....</b>	<b>91</b>
Three-dimensional dynamic finite element and experimental models for drilling processes* .....	91
Abstract.....	93
1 Introduction.....	95
2 3D Dynamic FE Model.....	97
2.1 Material properties .....	98
2.2 Element removal and contact interactions .....	99
3 Experimental Setup.....	100
4 Results and Discussion .....	102
5 Conclusions.....	106
Declaration of conflicting interests.....	106
Funding .....	106
References.....	107
<b>CHAPTER V .....</b>	<b>111</b>
Thermo-mechanical stresses distribution on bone drilling: Numerical and experimental procedures* .....	111
Abstract.....	113
1 Introduction.....	115
2 Thermo-mechanical Model of Drilling.....	117

2.1 Material properties .....	118
2.2 Contact interaction and failure criteria.....	121
3 Experimental Validation .....	121
3.1 Strain measurement.....	122
3.2 Temperature control.....	122
4 Results and Discussion .....	125
4.1 FE results.....	125
4.2 Experimental results and FE model validation .....	126
5 Conclusions.....	127
Declaration of conflicting interests .....	128
Funding .....	128
References.....	128
<b>CHAPTER VI.....</b>	<b>133</b>
Thermal analysis in drilling of <i>ex vivo</i> bovine bones* .....	133
Abstract.....	135
1 Introduction.....	137
2 Temperature Evolution in the Drilling of <i>ex vivo</i> Bovine Bones and Foam Blocks .....	139
2.1 Bovine bones samples preparation.....	139
2.2 Experimental setup in bovine bones samples.....	141
2.3 Experimental setup in polyurethane foam blocks .....	142
2.4 Analysis of the experimental results: bovine bones and foam blocks.....	143
3 Temperature Evolution Inside of the Bone .....	145
3.1 Temperature measurement system.....	145
3.2 Temperature evolution inside of the polyurethane foam blocks .....	146
4 Conclusions.....	149
Acknowledgments .....	150
Conflict of interest statement.....	150
References.....	150
<b>CHAPTER VII.....</b>	<b>155</b>
<i>Ex vivo</i> experimental and numerical study of stresses distribution in human cadaveric tibiae* .....	155
Abstract.....	157
1 Introduction.....	159

2 Materials and Methods.....	160
2.1 Numerical model of human tibia.....	160
2.1.1 Material and constitutive models .....	162
2.1.2 Contact and material failure criteria.....	164
2.2 Experimental validation .....	164
3 Results and Discussion .....	166
3.1 Comparison of the numerical and experimental results .....	167
4 Conclusions.....	168
Acknowledgments .....	169
Conflict of interest statement.....	169
References.....	169
<b>CHAPTER VIII.....</b>	<b>173</b>
Concluding Remarks and Future Directions.....	173
8.1 Introduction.....	175
8.2 Conclusions and remarks .....	175
8.3 Future directions .....	177
<b>APPENDIXES .....</b>	<b>179</b>



# List of Figures

## CHAPTER II:

Figure 1. (a) Classification of bones according to their shape and (b) schematic image of a long bone with its basics components. (Adapted from [6, 9]).....	16
Figure 2. Hierarchical structural distribution of bone tissue. (Adapted from [10]).....	17
Figure 3. Illustration of load-displacement curve for a bone sample. (Adapted from [11]) .....	18
Figure 4. Illustration of tensile stress-strain curve. (Adapted from [12]).....	19
Figure 5. The anisotropic behaviour of cortical bone tissue. (Adapted from [13]).....	19
Figure 6. Comparison of compressive stress-strain curve high and low bone density. (Adapted from [23]).....	21
Figure 7. Correlation between density and elastic modulus in tensile (filled circles) and compression (empty circles) of trabecular bone tissue. (Adapted from [32]) .....	22
Figure 8. Stages of Osteonecrosis. (Adapted from [93]).....	30
Figure 9. Geometry of a twist drill bit and its drill bit tip. (Adapted from [98]).....	32
Figure 10. Cooling systems: (a) external and (b) internal cooling. (Adapted from [144]) .....	44

## CHAPTER III:

Figure 1. Test Blocks from Sawbones: (a) C+D, (b) C-D, (c) T+D, (d) T-D. ....	77
Figure 2. Schematic illustration of the thermocouples positions.....	77
Figure 3. Geometrical model of block from Sawbones.....	79
Figure 4. Drilling process of biomechanical blocks.....	79
Figure 5. Finite element mesh to the numerical model. ....	82

Figure 6. The mean value of temperature-time history in the drill bit during the drilling process. ....	83
Figure 7. Time-temperature history in the block C+D: (a) side A, without external cooling, (b) side A, with external cooling, (c) side B, without external cooling, (d) side B, with external cooling. ....	84
Figure 8. Temperature during drilling at 440 s: (a) C+D, (b) C-D, (c) T+D, (d) T-D. ..	85
Figure 9. Thermal images of the drill bit, C+D: (a) before and (b) after drilling; C-D: (c) before and (d) after drilling. ....	87
Figure 10. Thermal images of the drill bit, T+D: (a) before and (b) after drilling; T-D: (c) before and (d) after drilling. ....	87

#### CHAPTER IV:

Figure 1. Geometric representation of the drill bit and the biomechanical block. ....	97
Figure 2. FE model of the drill bit, biomechanical block and applied boundary conditions. ....	98
Figure 3. (a) Biomechanical test block from Sawbones and (b) instrumented block... ..	100
Figure 4. Geometrical model of the block and identification of the holes. ....	101
Figure 5. (a) Drilling process and (b) distance between the edge of the drilled hole and the stain gauge. ....	102
Figure 6. Temperature distribution on the block top surface. ....	102
Figure 7. Distribution of von Mises stresses (MPa) at different point-in-times ( $V_f = 25$ mm/min). ....	103
Figure 8. Distribution of von Mises stresses (MPa) at different point-in-times ( $V_f = 50$ mm/min). ....	103
Figure 9. Distribution of von Mises stresses (MPa) at different point-in-times ( $V_f = 75$ mm/min). ....	104
Figure 10. Comparison of normal stress (MPa) in numerical and experimental tests at different times of drilling.....	104
Figure 11. Variation of normal stresses for different feed-rates at depth = 30 mm. ....	105

#### CHAPTER V:

Figure 1. (a) FE model of drilling and (b) boundary conditions. ....	118
Figure 2. Flow stress for the Cowper-Symonds model. ....	120

Figure 3. (a) Solid rigid polyurethane foam and (b) installation of the linear strain gauges. .....	122
Figure 4. (a) Geometrical model and (b) thermocouples position.....	123
Figure 5. Temperature data applied in the Fe model. ....	124
Figure 6. Experimental drilling process. ....	124
Figure 7. Distribution of von Mises stress (MPa) at different feed-rates and drill speeds (3 mm of depth). ....	125
Figure 8. Normal stresses $\sigma_{zz}$ (MPa) in experimental and FE models with (a) feed-rate and (b) drill speed. ....	126
Figure 9. Maximum normal stresses $\sigma_{zz}$ (MPa) with (a) feed-rate and (b) drill speed. ....	127

## CHAPTER VI:

Figure 1. Samples preparation for the experimental tests in <i>ex vivo</i> bovine bones. ....	140
Figure 2. Fresh bovine femur (a), sample cut from mid-diaphysis (b) and wrapped with gauze swabs in physiological saline solution (c). ....	141
Figure 3. Drilling operations of bovine bones. ....	142
Figure 4. Biomechanical foam blocks: B11 and B12. ....	142
Figure 5. Drilling process of biomechanical blocks. ....	143
Figure 6. Polyurethane foam block and illustration of the thermocouple positions. ....	145
Figure 7. Temperature evolution at different feed rates and positions of thermocouples. .....	147
Figure 8. Temperature evolution at different drill speeds. ....	148

## CHAPTER VII:

Figure 1. Human cadaveric tibiae and sample dimensions. ....	161
Figure 2. (a) Human cadaveric tibia, (b) 3D CAD model and (c) FE model. ....	161
Figure 3. (a) FE model of bone drilling and (b) mesh and boundary conditions. ....	162
Figure 4. Instrumentation of human bone tibiae. ....	165
Figure 5. Experimental setup on human cadaveric tibiae. ....	166
Figure 6. Comparison of the von Mises stresses (MPa) obtained for drill speeds of 900 and 1370 rpm and 2.5 mm drilling depth. ....	166
Figure 7. Comparisons of normal stress (MPa) from FE model and experiments at different drilling steps (a) and at maximum drilling depth of 3 mm (b). ....	168



# List of Tables

## CHAPTER II:

Table 1. Mechanical properties of cortical bone tissue by different tests. (Based from [13]) .....	20
Table 2. Mechanical properties (MPa) of trabecular bone from compression tests. (Based from [13]) .....	21
Table 3. Specific heat of bone tissue reported in the literature. ....	23
Table 4. Thermal conductivity of cortical bone reported in literature.....	24
Table 5. Parameters involved in bone drilling.....	32
Table 6. Some experimental studies of heat measured using thermocouples. ....	50
Table 7. Some experimental studies of heat measured using infrared thermography....	51

## CHAPTER III:

Table 1. Tagging of thermocouples.....	78
Table 2. Drilling processing parameters.....	78
Table 3. Parameters used for thermal images acquisition. ....	79
Table 4. Thermal properties of the drill bit and bone.....	80

## CHAPTER IV:

Table 1. Drilling parameters used in FE simulation.....	98
Table 2. Isotropic material properties and Cowper-Symonds parameters used in drilling simulations.....	100
Table 3. Tagging of strain gauges. ....	101

## **CHAPTER V:**

Table 1. Material properties and Cowper-Symonds parameters used in numerical simulations.....	120
Table 2. Parameters used for thermal images acquisition. ....	123

## **CHAPTER VI:**

Table 1. Parameters used for the thermal image acquisition.....	141
Table 2. Parameters used in drilling tests.....	143
Table 3. Variation of temperature from drill bit, before and after drilling.....	144
Table 4. Thermocouple labelling.....	146
Table 5. Parameters used in drilling experiments.....	146

## **CHAPTER VII:**

Table 1. Material properties and Cowper-Symonds parameters. ....	163
--	-----

# **CHAPTER I**

## **General Introduction and Motivations**





## 1.1 Background and Motivation

Bone is a highly dynamic tissue and the main constituent of the human skeletal system. Its structure differs from the connective tissues in rigidity and hardness [1]. Although the bone is a self-repairing structural material, bone loss or bone fracture continues to be one of the most common public health concerns due to the automobile and motorcycle accidents, sports injuries, falls from a height, ageing population and others diseases. Hard tissue cutting is a common practice in medical and dental fields (e.g. neurosurgery, orthopaedic, trauma and maxillofacial surgeries) to bone repair and fracture reconstruction. The main bone cutting operations are drilling [2], sawing [3] and grinding [4]. Although all of these procedures have an important role in clinical practice, bone drilling is one of the most important surgical operation in the medicine history [5].

Holes perforation into the bone have been used in our societies from the earliest times and they are considered the oldest surgical procedure. The first operation that involved bone drilling was called cranial trepanation, which literally means drilling through the skull. This prehistoric procedure was first identified in 1865 by E. George Squier and became a common and crucial surgery technique throughout many civilizations [6, 7].

Until recently, bone drilling was not considered from technical point of view. The focus was merely to perform the surgical operation by intuitively controlling the parameters for minimal or no damage to the bone tissue without any understanding of the machining process fundamentals [8]. However, the progress of medicine in conjunction with the technology require the development and improvement of the drilling procedures with minimally invasive techniques for the patients. The importance of this subject has motivated the research on bone drilling and the development of recent reviews [9, 10]. Many investigations have been carried out to study the tool materials, mechanical aspects of drilling and their biological and cellular impact on the bone tissue. Dahotre and Joshi [8] indicated an increased from 100 to 10000 published papers over the years of 1940 to 2016 in the field of conventional and laser based bone machining (including drilling, sawing, grinding and milling).

Despite the efforts and the progress, bone drilling is still largely conducted by the surgeon using hand drills, which means a blind operation with unknown hole depth and a feed-rate manually controlled by the surgeon. Such mostly conventional way of surgery is associated with human and tool attributes and hence leaves tremendous room for further

development and improvement of operating tools and techniques. In addition, the reported cases of implant failures and post-operative problems associated to the drilling process continue to be a significant public health problem in the health care system and show the need for improvements in this field [11, 12]. In the year of 1998, Piattelli et al. [13] reported eight cases of failed implants due to suspected thermally induced bone necrosis. Later in 2008, Augustin et al. [14] indicated that the implant failure rate for leg osteosynthesis ranges between 2.1% and 7.1%. They noted that one of the causes is the increase in bone resorption around the implanted screws from thermal osteonecrosis caused by preparative drilling. Abayazid et al. [15] reported that the failure rate of dental implant in the lower jaw is 7.65% in 10 years period and three times higher in the maxilla. More recently, Elangovan and Allareddy [11] have provided detailed information on the nationally representative estimates of hospital based emergency department visits attributed to dental implant failures in the United States. During the period of their studies (years 2008–2010), a total of 1200 emergency department visits were due to dental implant failures. Its conclusions indicate that 31.7% of the visits were related to osseointegration failures and 30.4% were due to post-osseointegration mechanical failures. According to the authors, two etiological factors that can lead to the implant failures are tissue trauma (possibly from overheating the bone during placement) and mechanical overloading.

The clinical problems coupled with the importance to reduce the bone damage risk during drilling procedures were the main motivations for the realization of this thesis. After the research subject has been identified, it was necessary to determine the main research lines and the main challenges and contributions on this domain. For this purpose, a bibliographic review of all relevant studies on bone drilling was conducted, including the different methods used, results and conclusions made by the various researches. Literature review reveals that the main problems associated to the bone damage are the cut effort and the heat generation during drilling. High loads with high speed velocity and tool vibrations may result in drill overrun, damages to the bone microstructure, which can lead to the crack formations and even bone fracture [16]. The heat causes bone cell damage and can result in thermal necrosis [17]. Problems like clogging or built up edge are also associated to bone drilling. These problems are all linked with the drilling parameters [18, 19]. If parameters such as drill speed and feed-rate are not selected properly, the drilling load induces bone damage, which lead to surgical complications.

Therefore, determination of optimal parameters is crucial to the success of this surgeries and further evolution of the patients. In fact, there are a significant number of studies dedicated only to this issue. However, most works available in the literature provide an experimental approach with special attention to thermal effects. The studies on strain and stress distribution during drilling have not been reported so far. An investigation of this effects can contribute significantly for minimizing bone tissue injury during drilling. Even about the experimental works on thermal damage, there still remains a lack of consensus in the literature regarding to critical temperature values and their time durations. The extensive variables number involved and the large discrepancies in the obtained results from different methods complicate the concluding remarks statement. Furthermore, the literature available so far has been concentrating on artificial or animal bones, and relatively few research has been completed on the human bone. Indeed, some animals can resemble the human properties but none of them is equal to the human bone. This inherent disparity in mechanical and thermal properties of specimens taken from different bones results in differences in the results subject to almost identical drilling conditions in repeated experiments [20].

In 2013, Pandey and Panda [10] conducted a literature review of all relevant investigations carried on bone drilling and concluded that there are several significant factors influencing the process on which no general agreement is yet been made, or are not investigated and need an evaluation in the future. They suggested that the further improvement in bone drilling is possible, including the drilling parameters optimization. The advances of technology and computational models in recent decades have contributed to the study and improvement of new drilling techniques. The modelling of drilling process using finite element analysis (FEA) may be considered as a promising and reliable technique for understanding of bone drilling, as well as, in the study and definition of the best drilling conditions. There are studies on literature that describe finite element (FE) models to study the behaviour of the bone under several drilling conditions [21-25]. However, it is complicated to reach a numerical model to simulate the real drilled bone due to the complexity of the material properties inherent to the cutting material separation. Marco et al. [26] performed a review of the main contributions in modelling of bone cutting with special attention to the bone mechanical behavior. They concluded that is difficult to find complete models of bone drilling including chip removal simulation and capable to predict the thermomechanical damage. In the author's opinion, the available models are still far from clinical application and a strong effort is still needed

in this field. Moreover, the high computational cost of the complete three-dimensional (3D) approach is the major drawback.

Based on the literature review, it has become clear that the accuracy of the developed models to predict the bone damage requires a combination of experimental and numerical methods. It is important to compile different methodologies to achieve real results and extrapolate these results to clinical situations. Developing accurate FE models of bone drilling could be a potential tool of significant improvement of the process and possible substitute for experimental work as it eliminates high costs of the equipment as well as potential health risks associated with biological materials.

In general, the main challenges in this field are the numerical modelling of the bone drilling, that includes the dynamic characteristics of this processes and chip removal; the lack of experimental data on the strain and stress distribution during drilling and the lack of consensus among the available published works; and, lastly, the lack of experimental validation for the developed numerical models. The described challenges are the main motivation for the present research, which provides a comprehensive experimental and numerical study of bone drilling taking into account the engineering and biological principles.

## **1.2 Thesis Objectives**

The main objective of this thesis is to analyse the conventional drilling process with the purpose to reduce the bone damage risk and to contribute for a better knowledge of the involved parameters in the drilling process and their effects. A comprehensive research including experimental tests and numerical modelling for thermal and mechanical analysis of bone drilling is carried out, in order to predict the strain, the stress and temperature distribution for a given drilling conditions, drill bit geometry and material properties of the bone tissue. It is expected that the final findings of this work will be a useful tool on the selection of drilling parameters and an additional support for the health professionals in the decision-making process before drilling.

To achieve the described purpose, the following specific aims were defined in this thesis:

1. Development of experimental methodologies using engineering materials (synthetic bone with properties similar to the human bone) and biological materials (bovine bones and human cadaveric bones) to study the inherent

- variation in mechanical and thermal properties of bones taken from different species;
2. Measurement of temperature distribution in the cutting tool and within the bone tissue during drilling through the use of a thermographic camera and thermocouples;
  3. Development of an experimental model to measure the strain and calculate the respective stress distribution during bone drilling through the use of strain gauges;
  4. Study the influence of different drilling parameters (feed-rate, drill speed, hole depth, irrigation system and bone density) on bone temperature and stress distribution during bone drilling;
  5. Development of a 3D FE model to simulate the thermal behaviour of the bone tissue and to predict the temperature distribution during drilling. The effect of different parameters is analysed through a thermal and transient analysis;
  6. Development of a 3D dynamic elasto-plastic FE model with the element removal scheme to simulate the mechanical behaviour of the bone and to predict the strain and the stress distribution during drilling. The FE model aims to incorporate the geometric and dynamic characteristics involved in the drilling processes;
  7. Development of a 3D dynamic elasto-plastic FE model with the element removal scheme to simulate the thermo-mechanical behaviour of the bone and to predict the respectively stress distribution during drilling. The FE model aims to incorporate the geometric and dynamic characteristics involved in the drilling processes and the developed temperature inside of material;
  8. Development of a new 3D dynamic elasto-plastic FE model, using a real geometry of human cadaveric tibia, captured by 3D handheld scanner. The FE model was optimised to best represent the human bone response of drilling procedures.
  9. Validation of the FE models based on a comparison with the experimental results.

### 1.3 Thesis Structure

The present thesis has been organized into eight chapters and two main parts. First part include Chapter I and II. Chapter I includes the thesis subject with the main issues and concerns on the drilling interventions. The main motivations and overall objectives are presented. Chapter II provides to the reader a bibliographic review on mechanical and

thermal properties of bone tissue, as well as a comprehensive review of the most relevant investigations carried on bone drilling. The main findings are described and compared. The second part is composed for six chapters with the most important published papers (or under review) and a last chapter with the general conclusions and future perspectives. The sequence of papers is organized in the following chapters:

**Chapter III.** First paper, entitled “*Thermal analysis during bone drilling using rigid polyurethane foams: numerical and experimental methodologies*”, describes an experimental and numerical methodology to study the thermal behaviour of the bone tissue during drilling. The effect of some drilling parameters on temperature distribution during drilling is analysed and the 3D thermal FE model is presented.

This paper was published in *Journal of the Brazilian Society of Mechanical Sciences and Engineering*, by the authors Maria Goreti Fernandes, Elza Fonseca and Renato Natal Jorge.

**Chapter IV.** Second paper, entitled “*Three-dimensional dynamic finite element and experimental models for drilling processes*”, describes an experimental and numerical methodologies to study the mechanical behaviour of the bone tissue during drilling. The effect of some drilling parameters on strain and stress distribution during drilling is analysed and the 3D mechanical FE model is presented.

This paper was published in *Proceedings of the Institution of Mechanical Engineers, Part L: Journal of Materials: Design and Applications*, by the authors Maria Goreti Fernandes, Elza Fonseca and Renato Natal Jorge.

**Chapter V.** Third paper, entitled “*Thermo-mechanical stresses distribution on bone drilling: numerical and experimental procedures*”, describes an experimental and numerical methodologies to study the thermo-mechanical behaviour of the bone tissue during drilling. The effect of some drilling parameters on temperature, strain and stress distribution during drilling is analysed and the 3D thermo-mechanical FE model is presented.

This paper was published in *Proceedings of the Institution of Mechanical Engineers, Part L: Journal of Materials: Design and Applications*, by the authors Maria Goreti Fernandes, Elza Fonseca and Renato Natal Jorge.

**Chapter VI.** Fourth paper, entitled “*Thermal analysis in drilling of ex vivo bovine bones*”, describes a set of experimental methodologies to study the temperature generation during drilling of synthetic bone (solid rigid polyurethane foams) and animal bone (bovine origin). The effect of different drilling parameters, such as feed-rate, drill speed and hole depth were evaluated.

This paper was published in *Journal of Mechanics in Medicine and Biology*, by the authors Maria Goreti Fernandes, Elza Fonseca, Renato Natal Jorge, Mário Vaz and Maria Isabel Dias.

**Chapter VII.** Fifth paper, entitled “*Ex vivo experimental and numerical study of stresses distribution in human cadaveric tibiae*”, describes a new dynamic FE model of bone drilling based on the real geometry of human cadaveric tibia from handheld 3D scanner. The numerical model was validated with experimental tests on human cadaveric tibiae.

This paper was submitted to the *Computer Methods in Biomechanics and Biomedical Engineering* by the authors Maria Goreti Fernandes, Elza Fonseca, Renato Natal Jorge and Maria Cristina Manzanares Céspedes.

Finally, there is the Appendix containing the consent forms signed by all authors.

## References

1. Jee WSS (2001) Integrated bone tissue physiology: anatomy and physiology. In: Cowin SC (Eds), *Bone Mechanics Handbook*. Second Edition, New York: CRC Press, pp. 1-34.
2. Fox MJ, Scarvell JM, Smith PN, Kalyanasundaram S, Stachurski ZH (2013) Lateral drill holes decrease strength of the femur: an observational study using finite element and experimental analyses. *J Orthop Surg Res* 8-29.
3. Tawy GF, Rowe PJ, Riches PE (2016) Thermal Damage Done to Bone by Burring and Sawing With and Without Irrigation in Knee Arthroplasty. *J Arthroplasty* 31:1102-1108.

4. Zhang L, Tai BL, Wang G, Zhang K, Sullivan S, Shihb AJ (2013) Thermal model to investigate the temperature in bone grinding for skull base neurosurgery. *Med Eng Phys* 35(10):1391-1398.
5. Wang W, Shi Y, Yang N, Yuan X (2014) Experimental analysis of drilling process in cortical bone. *Med Eng Phys* 36(2):261- 266.
6. Andrushko VA, Verano JW (2008) Prehistoric Trepanation in the Cuzco Region of Peru: A View into an Ancient Andean Practice. *Am J Phys Anthropol* 137(1):4-13.
7. Finger S, Fernando HR (2001) E. George Squier and the discovery of cranial trepanation: a landmark in the history of surgery and ancient medicine. *J Hist Med Allied Sci* 56 (4):353-381.
8. Dahotre N, Joshi S (2016) *Machining of bone and hard tissues*. Springer International Publishing, Switzerland, pag.5. ISBN: 978-3-319-39158-8 (e-Book).
9. Augustin G, Zigman T, Davila S, Udiljak T, Brezak D, Babic S (2012) Cortical bone drilling and thermal osteonecrosis. *Clin Biomech* 27:3313-325.
10. Pandey RK, Panda SS (2013) Drilling of bone: A comprehensive review. *J Clin Orthop Trauma* 4:15-30.
11. Elangovan S, Allareddy V (2016) Estimates of Hospital Based Emergency Department Visits due to Dental Implant Failures in the United States. *J Evid Based Dent Pract* 16(2):81-85.
12. Daokar SS, Agarwal G (2016) Orthodontic Implant Failure: A Systematic review. *International Journal of Oral Implantology & Clinical Research* 7(1):1-6.
13. Piattelli A, Piattelli M, Mangano C, Scarano A (1998) A histologic evaluation of eight cases of failed dental implants is bone overheating the most probable cause? *Biomaterials* 19(7-9):683-690.
14. Augustin G, Davila S, Mihoci K, Udiljak T, Vedrina DS, Antabak A (2008) Thermal osteonecrosis and bone drilling parameters revisited. *Arch Orthop Trauma Surg* 128:71-77.
15. Abayazid M (2010) *Modelling heat generation and temperature distribution during dental surgical drilling*. M.Sc. Thesis, Delft University of Technology, Netherlands.
16. Li S, Wahab AA, Demirci E, Silberschmidt VV (2014) Penetration of cutting tool into cortical bone: Experimental and numerical investigation of anisotropic mechanical behaviour. *J Biomech* 47:1117-1126.
17. Hillery MT, Shuaib I (1999) Temperature effects in the drilling of human and bovine bone. *J Mater Process Technol* 92-93:302-308.



18. Soriano J, Garay A, Aristimuño P, Iriarte LM, Eguren JA, Arrazola PJ (2013) Effects of Rotational Speed, Feed rate and Tool Type on Temperature and Cutting Forces When Drilling Bovine Cortical Bone. *Machine Science and Technology* 17(4):611-636.
19. Fonseca EMM, Magalhães K, Fernandes MGA, Barbosa MP, Sousa G (2014) Numerical Model of Thermal Necrosis due a Dental Drilling Process. In: R Natal, et al (eds) *Biodental Engineering II*, London: Taylor & Francis Group, CRC Press 2013, pp.69-73.
20. Lee J, Ozdoganlar B, Rabin Y (2012) An experimental investigation on thermal exposure during bone drilling. *Med Eng Phys* 34:1510-1520.
21. Davidson SR, James DF (2003) Drilling in bone: modelling heat generation and temperature distribution. *J Biomech Eng* 125(3):305-314.
22. Tu YK, Hong Y, Chen YC (2009) Finite element modeling of kirschner pin and bone thermal. *Life Science Journal* 6(4): 23-27.
23. Sezek S, Aksakal B, Karaca F (2012) Influence of drill parameters on bone temperature and necrosis: A FEM modelling and in vitro experiments. *Comp Mater Sci* 60:13-18.
24. Lughmani WA, Bouazza-Marouf K, Ashcroft I (2013) Finite element modelling and experimentation of bone drilling forces. *J Phys Conf Ser*, p. 451.
25. Wang Y, Cao M, Zhao X, Zhu G, McClean C, Zhao Y, Fan Y (2014) Experimental investigations and finite element simulation of cutting heat in vibrational and conventional drilling of cortical bone. *Med Eng Phys* 36(11):1408-1415.
26. Marco M, Rodríguez-Millán M, Santiuste C, Giner E, Henar Miguélez M (2015) A review on recent advances in numerical modelling of bone cutting. *J Mech Behav Biomed Mater* 44:179-201.



## **CHAPTER II**

### **Literature Overview**



## 2.1 Bone Tissue

The skeletal system is made up of individual bones and connective tissues [1]. Bone, as the main constituent of the human skeleton, is considered a complex biological tissue with a unique capacity to heal and regenerate without the formation of scar tissue [2]. Its excellent characteristics of stiffness and hardness allow the human skeleton to perform important tasks such as locomotion, protection of soft tissues and mineral homeostasis [1].

On a morphological viewpoint, bone tissue is divided in macroscopic and microscopic structures. Macroscopically, bone is classified according to their long shape, short, flat, sesamoid and irregular (Figure 1(a)). Long bones are used as the classical model for the macroscopic structure of bone and characterised for being longer than wider. In these group are included the majority of the bones from lower and upper limbs such as humerus, femur and tibia. Short bones are characterised by their width and length comparable. In these group are included small bones such as carpal and tarsal bones, patellae and sesamoid bones. Its main function is to assist in shock absorption by spreading the load. Flat bones on the other hand are associated to protection functions for body organs. Its thinner and flatted structure provides broad section for protection or muscular attachment. In this group are included the bones from cranial, rib cage and sternum parts. Sesamoid bones also contain functions of protection and are usually found in locations where tendons intersect the ends of long bones such as knee joints. The protection of these tendons from an excessive mechanical load is the main function of sesamoid bones. Lastly, irregular bones include vertebrae, sacrum, coccyx, and hyoid bone. As its name suggests, irregular bones do not have a particular shape characteristic to be classified as long or short or flat [3-6].

Despite these different morphologies, all adult bones are classified into cortical (or compact) bone and trabecular (or cancellous) bone. These two type of bones are very different from each other, especially in their development, architecture, function, blood supply, proximity to the bone marrow and magnitude of age-dependent changes and fractures [1]. Basically, cortical bone is a dense and solid mass with only microscopic channels. They form the outer shell of all bones and represent 80% of the adult human skeleton. Its main functions are associated to their mechanical strength and comprise the protection and support of the skeleton [1].

The rest 20% of the human skeleton comprises of trabecular bone, which is a much softer and porous tissue. Its structure helps in damping of physical shocks and load transmission with the help of joints [7]. However, the distribution of cortical and trabecular bone vary greatly between individual bones, according to site and relate to the need for mechanical support.

As stated above, long bones serve as the classical model for the best visualization of macroscopic bone structure. A typical long bone is composed of three different regions: diaphysis (central cylindrical shaft), two epiphyses (wider and rounded ends) and the metaphysis (conical regions that connect the diaphysis with each epiphysis) (Figure 1 (b)). The diaphysis is composed primarily of cortical bone whereas the epiphysis and metaphysis are composed mostly of trabecular bone with a thin cortical layer.

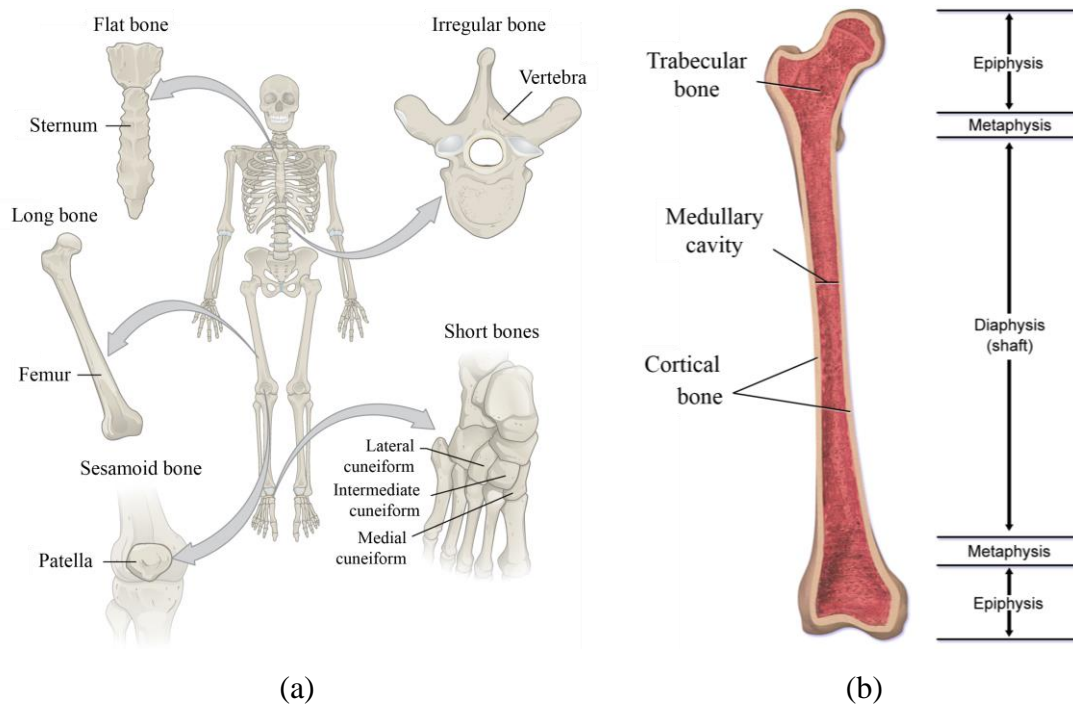


**Figure 1.** (a) Classification of bones according to their shape and (b) schematic image of a long bone with its basic components. (Adapted from [6, 9])

The bone structure is hierarchical in nature with different features on many levels of scale. Figure 2 demonstrate the length scale distribution of bone structure. Microscopically, there are many additional structures that form the cortical and trabecular bone. Briefly, the main bone microstructures (from 10 to 500  $\mu\text{m}$ ) are the osteons, lamellae, canaliculi and Haversian canals. Beyond the microstructure, there is the nanostructure (from a few hundred nanometers to 1  $\mu\text{m}$ ) that consists of collagen fibres that make up the osteons.

Finally, there is the sub-nanostructure (below a few hundred nanometers) where molecular structure of constituent elements are identified, such as mineral, collagen, and non-collagenous organic proteins. This hierarchically organized structure has an irregular arrangement and different orientation, making the bone a heterogeneous and anisotropic material [10].

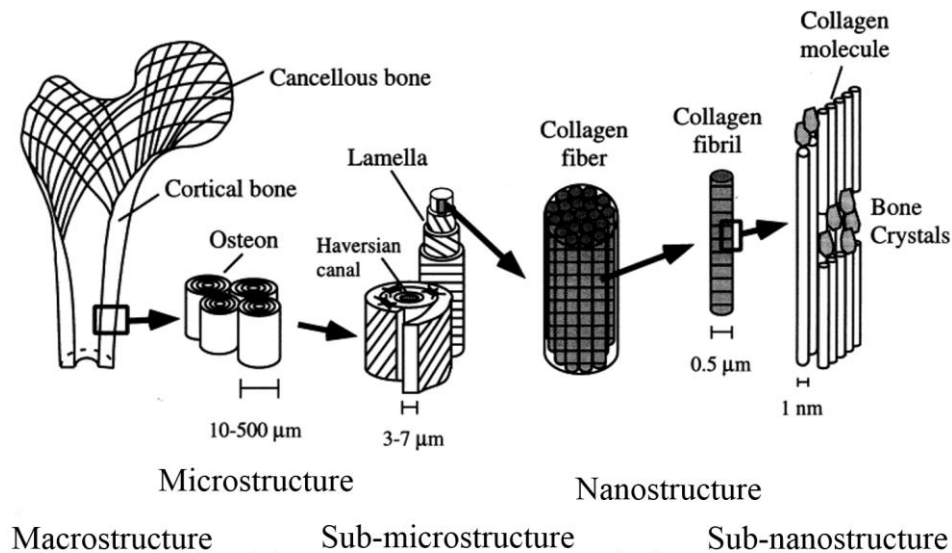


**Figure 2.** Hierarchical structural distribution of bone tissue. (Adapted from [10])

It has been shown that the various types of the bone described earlier heavily influence the thermophysical properties of the bone tissue [3, 10]. Therefore, it is important to understand the bone structure, and in turn the bone properties in order to get an insight into the bone response towards machining operation. In addition, predictive models for bone drilling require complete and accurate input of bone tissue properties. The wide range of materials and structural features makes the bone properties selection more difficult. Factors such as age, gender, dietary habits and even geographic location also contribute to variety of these properties [3]. According this, the following subsections are dedicated to the thermophysical properties of both cortical and trabecular bone tissues.

### 2.1.1 Mechanical properties of cortical bone

Mechanical properties of bone tissue have been a topic discussed of several researchers over time. Currently, a wide range of mechanical testing techniques have been defined to measure the bone properties. Depending on the bone type, there are different testing methods that can be implemented.

For cortical bone tissue, uniaxial tensile or compressive tests and three-point or four-point bending are used for measuring its mechanical properties [1]. From these mechanical tests, several properties can be quantified, including the stiffness ( $S$ ), the ultimate load that corresponds to the load at failure, the energy or work to failure ( $U$ ) and ultimate displacement (Figure 3).

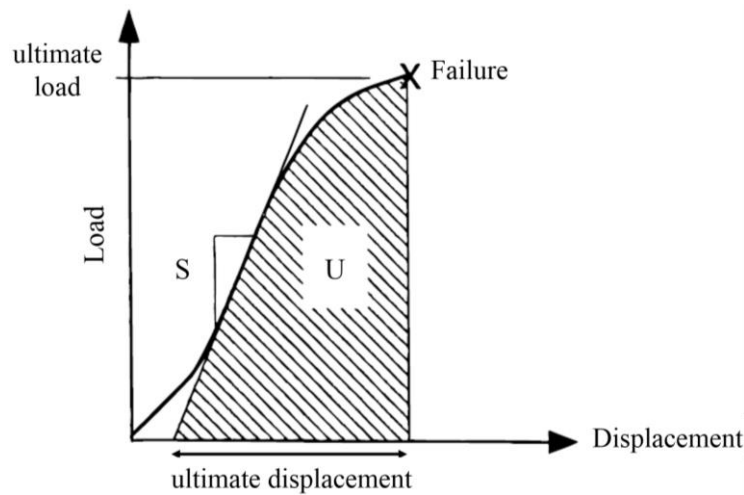


**Figure 3.** Illustration of load-displacement curve for a bone sample. (Adapted from [11])

If load is converted to stress and displacement converted to strain, the curve of bone mechanical behaviour will be called the stress-strain curve [1]. In this curve, there are important mechanical properties that can be identified such as elastic modulus or Young's modulus, yield stress and ultimate stress, as shown in Figure 4. In a summarized manner, the stress-strain curve is characterized by an initial linear region before yield (called elastic region) and a post-yield nonlinear region (called plastic region) that contain the ultimate stress and the failure point. The slope of the stress-strain curve within the elastic region represent the Young's modulus (material stiffness). Yield stress is the transition to nonlinear behaviour, which means that the stress begin to cause permanent damage to the bone structure; and the maximum stress and strain that the bone can sustain are called the ultimate stress (or strength) and ultimate strain, respectively [1, 12]. These properties are strongly dependent on the loading mode (tensile, compression, bending, or shear) and determine the mechanical response of the bone tissue to the drilling operations [3, 12].



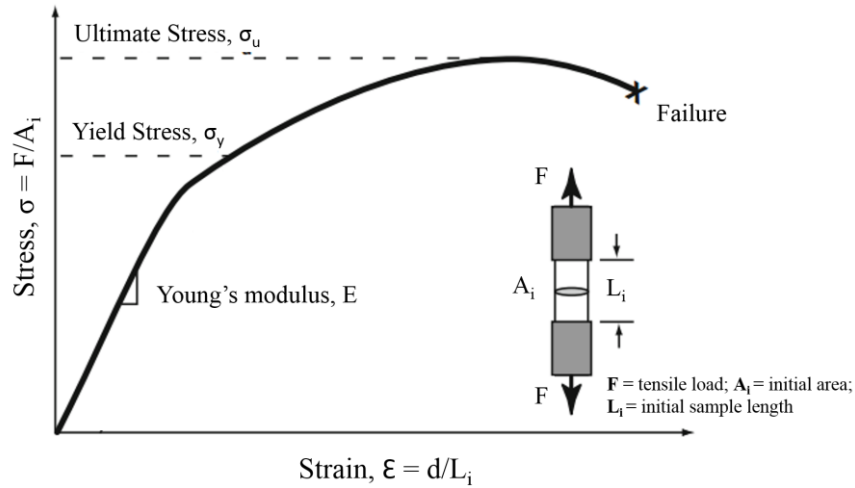


**Figure 4.** Illustration of tensile stress-strain curve. (Adapted from [12])

The properties of human cortical bone from long bones such as tibia, femur and humerus have been found to vary between subjects, although the density was the same [10]. As heterogeneous and anisotropic material, cortical bone exhibits different mechanical properties depending on loading directions of the test method (Figure 5).

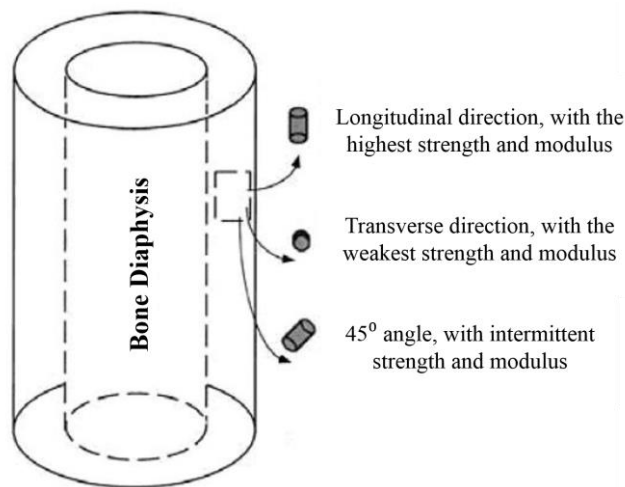


**Figure 5.** The anisotropic behaviour of cortical bone tissue. (Adapted from [13])

According to previous studies, the elastic modulus is different depending on the direction. The longitudinal direction (0° normally the weight direction) elastic modulus is the highest while the transverse (90° lateral directions) elastic modulus is the lowest. The angles between 0° and 90° have intermittent magnitudes [13].

According to the author Guo [14], the orthotropic or transversely isotropic constitutive relation describes cortical bone elastic properties fairly well.

The bone is also considered viscoelastic material, that exhibits both creep and stress relaxation. The ultimate strength, energy to failure and fracture toughness of bone tissue are rate dependent [15]. There are numerous studies in the literature dedicated to this topic. In Table 1, the strength and elastic modulus from cortical bone tissue by compressive, tensile and torsional tests are summarized together.

**Table 1.** Mechanical properties of cortical bone tissue by different tests. (Based from [13])

Test	Bone Type	Strength (MPa)	Elastic Modulus (GPa)	Ref.
Compression	Human femur	167-215 <sup>a</sup>	14.7-19.7 <sup>a</sup>	[16]
	Human tibia	183-213 <sup>a</sup>	24.5-34.3 <sup>a</sup>	[17]
	Bovine femur	240-295 <sup>a</sup>	21.9-31.4 <sup>a</sup>	[16]
	Bovine tibia	228 ± 31	20.9 ± 3.26	[16]
Tensile	Human femur	107-140 <sup>a</sup>	11.4-19.7 <sup>a</sup>	[16]
	Human tibia	145-170 <sup>a</sup>	18.9-29.2 <sup>a</sup>	[17]
	Bovine femur	129-182 <sup>a</sup>	23.1-30.4 <sup>a</sup>	[16]
	Bovine tibia	152 ± 17	21.6 ± 5.3	[16]
Torsion	Human femur	—	3.1-3.7 <sup>a</sup>	[16]
	Human tibia	66-71 <sup>a</sup>	—	[18]
	Bovine femur	62-67 <sup>a</sup>	—	[16]
Bending	Human femur	103-238 <sup>a</sup>	9.82-15.7 <sup>a</sup>	[19]
	Cattle femur	228 ± 5	19.4 ± 0.7	[20]

<sup>a</sup> Range of average values from different subjects; Mean ± SD

Material density is another bone property highly variable which makes it difficult to accurately determine them (Figure 6). The density of cortical bone is considered the wet weight divided by the specimen volume and is a function of porosity and mineralization of the bone materials [13]. However, there are two concepts of density: apparent density and material density. The apparent density is known as the ratio of wet mineralised mass to the volume occupied by the tissue. The material density is known as the mineralised mass over the volume occupied by the material itself. According to the author An [13], the apparent density and the material density are basically the same for the cortical bone, because there is no marrow space in compact bone.

Huiskes [21] summarized the density measurements of cortical bone from three investigations. It was found the range values of 1.86 g/cm<sup>3</sup> to 2.9 g/cm<sup>3</sup> with an average of 2.2 g/cm<sup>3</sup>. The authors Spatz et al. [22] determined the mechanical properties of cortical bone from mammals, birds and antler bone and found an average apparent density of approximately 1.9 g/cm<sup>3</sup>.

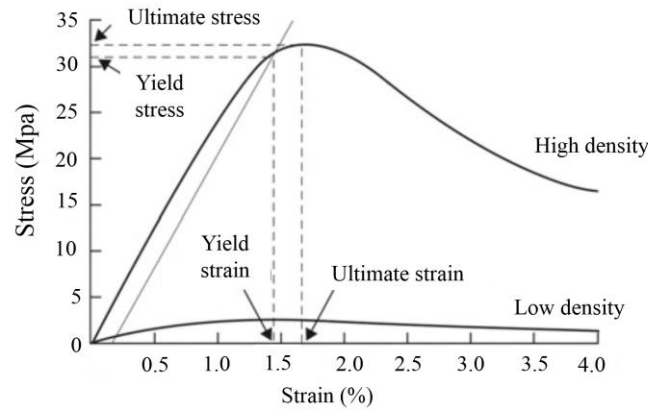


**Figure 6.** Comparison of compressive stress-strain curve high and low bone density. (Adapted from [23])

### 2.1.2 Mechanical properties of trabecular bone

As mentioned earlier, trabecular bone presents a structure more porous than cortical bone. This characteristic makes the trabecular bone lends itself to a mechanical description by both structural and material properties [13]. Measure and test the mechanical properties of trabecular bone tissue is much harder than the cortical bone, due to its extremely small dimension of individual trabeculae [14]. The properties are determined by several major factors such as structural density, trabecular connectivity, location and function [13].

The most common tests to measure the properties of trabecular bone are compression, tensile or bending tests [13]. Previous studies have been shown that the strength and elastic modulus by tensile tests present lower values than compression tests. Kaplan et al. [24] developed methods for tensile tests on the bovine fresh/frozen trabecular bone samples and concluded that the strength by tensile is approximately 60% of the value by compression. Keaveny et al. [25] analysed the elastic modulus of trabecular bone from bovine tibiae and found that the elastic modulus by tensile is approximately 70% of the value by compression test. The ranges of strength and elastic modulus to the trabecular bone tissue found in the literature are 1.5 to 38 MPa and 10 to 1570 MPa, respectively [13]. Table 2 summarizes some mechanical properties of trabecular bone found in the literature.

**Table 2.** Mechanical properties (MPa) of trabecular bone from compression tests. (Based from [13])

Bone Type	Ultimate Strength	Elastic Modulus	Ref.
Human distal femur	$5.6 \pm 3.8$	$298 \pm 224$	[26]
Human femoral head	$9.3 \pm 4.5$	$900 \pm 710$	[27]
Bovine distal femur	$8.5 \pm 4.2$	$117 \pm 61$	[28]
Dog femoral head	$12 \pm 5.8$	435	[29]
Pork vertebral body	$27.5 \pm 3.4$	$1080 \pm 470$	[31]
Bovine proximal tibia	—	$648 \pm 430$	[32]

As regard to the density of trabecular bone tissue, mechanical tests have shown a strong correlation between the mechanical properties of trabecular bone, both strength and stiffness, and its structural density. Figure 7 shows the correlation between elastic modulus and density of trabecular bone tissue.

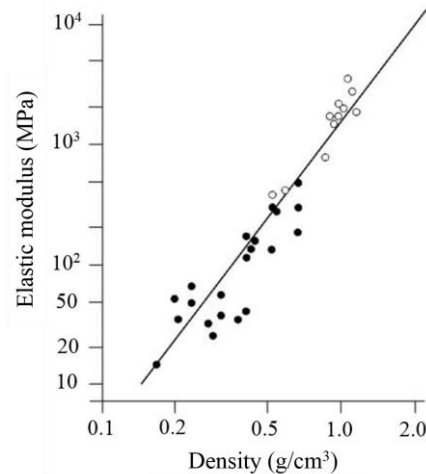


**Figure 7.** Correlation between density and elastic modulus in tensile (filled circles) and compression (empty circles) of trabecular bone tissue. (Adapted from [32])

### 2.1.3 Thermal properties of bone tissue

Besides the mechanical properties, during bone drilling the thermal effect also comes into play giving a temperature rise. This effect is critical from bone damage point of view and can result in bone necrosis, which mean irreversible death of bone cells, and in turn can lead to infection and reduced mechanical strength [35, 36]. The bone necrosis occurs when the temperature increases above a threshold and its extent depends on temperature rise and duration [37]. To assess the temperature rise during bone drilling, through experimental and numerical models, it is important to know the geometry, the heat input and the thermal properties of bone tissue. The main properties governing thermal effects during bone drilling are specific heat (a measure of how easily a material heats up), thermal conductivity (the ability of a material to transport heat) and thermal expansion coefficient [34]. Compared with others materials, such as metals, the bone presents a poor thermal heat transport, that makes the properties of specific heat and thermal conductivity have an inverse relationship with the temperature rise.

Unlike the mechanical properties, measurements of thermal bone properties are more difficult to obtain. The thermal behaviour is difficult to study, sensitive to test conditions, specimen preparation and it is an anisotropic material [33, 34].

Although several researchers have calculated the thermal properties of the bone tissue, a search of the literature reveals that these properties are a challenge to find, and are not always in agreement [1, 34].

#### ❖ *Specific heat of bone tissue*

Specific heat of the material is defined as the energy required to raise the temperature of a system by 1 °C. The effect of heat on bone tissue during the drilling procedure depends on drilling parameters, temperature and time of exposure. According to the Karmani [34], the maximum temperature reached by a sample depends on balance between heat gain and heat loss. When these two phenomena are equal, the sample is in equilibrium state. This equilibrium state means that the temperature reached by a sample is function of exposure temperature and thermal conductivity [34]. During the drilling procedures on bone tissue is impossible to achieve the temperature equilibrium, since the exposure times are usually too short. For the situations of non-equilibrium state, the heat generated is function of the exposure temperature and time for a constant value of specific heat capacity [38]. Some values for specific heat of bone tissue have been mentioned by several authors in their research. The values reported in the literature are summarized in Table 3.

**Table 3.** Specific heat of bone tissue reported in the literature.

Bone type	Specific heat (J/kg K)	Ref.
Human cortical bone (fresh)	$1.26 \times 10^3$	[39] reported in [40]
Human cortical bone (fresh)	$1.26 \times 10^3$	[38] reported in [40]
Calf trabecular bone (fresh)	$1.15-1.73 \times 10^3$	[41] reported in [40]
Elephant bone (dry)	$1.17 \times 10^3$	reported in [34]
Ox bone (fresh)	$1.13 \times 10^3$	
Ox bone (dry)	$1.17 \times 10^3$	
Dog bone (fresh)	$1.26 \times 10^3$	
Dog bone (dry)	$1.09 \times 10^3$	

Most researchers use a specific heat for bone tissue equal to  $1.26 \times 10^3$  J/kgK [42-44].

#### ❖ *Thermal conductivity of bone tissue*

Thermal conductivity of the material is defined as the amount of heat conducted through a material per unit area, per unit Kelvin and per unit length of heat transfer. Various researchers have reported this parameter for bone tissue (Table 4).

The reported results range from about 0.2 W/mK to around 12.8 W/mK [33, 45]. A wide variation in the quantitative results, test methods and procedures were found in the literature. There are numerous possible reasons for this variability, which includes differences in bone samples, fresh or dry conditions of measurement, directions of heat flow, variation in experimental procedure and equipment [46].

**Table 4.** Thermal conductivity of cortical bone reported in literature.

Bone Type	Conductivity (W/mK)	Ref.
Human samples (fresh)	0.38	[47] reported in [40]
Bovine samples (dry)	0.601	[48]
Bovine samples (fresh)	2.27	
Bovine and caprine samples	0.888-3.08	[49]
Human samples (dry)	3.56-4.9	[38]
Human femur (longitudinal direction)	11-12.8	[33]
Human femur (radial direction)	9.0-9.75	
Human femur (circumferential direction)	8.75-9.75	
Human femur (dry)	0.16-0.24	[45]
Human femur (fresh)	0.26-0.34	
Equine foreleg samples (dry)	0.70	[50]
Equine foreleg samples (fresh)	0.80	
Bovine femur (longitudinal direction)	0.58	[35]
Bovine femur (radial direction)	0.54	
Bovine femur (circumferential direction)	0.53	
Bovine femur (dry, longitudinal)	0.54	[46]

Vachon et al. [48] and Kirkland [49] were among the first researchers to obtain the thermal conductivity of cortical bone tissue. These authors used a “thermal comparator technique” (device that compares the cooling rates of two heated copper spheres in air) to obtain values of thermal conductivity from cortical bone samples. However, Davidson and James [35] questioned the reliability of these results since the device used for Vachon et al. was sensitive to contact pressure.

According Davidson and James, this problem, together with the problem that the measurement of conductivity is not straightforward with this type of device, makes it difficult to assess the reliability of the data from these authors.

Lundskog [38] investigated the thermal properties of cortical bone from different species. Two thermocouples were used to measure the temperature drop from a known heat flux.

However, according to the authors Zhang et al. [46], the heat flow through the samples was affected due the drilled holes performed to accommodate the thermocouples (including possible microcracks in samples).

Zelenov [33] used experimental methods to measure the thermal conductivity of human femur in different directions, through a hot plate technique. This technique measures the heat input and the resulting temperature drop, for one-dimensional steady-state heat transfer across the bone specimens.

The results presented by Lundskog and Zelenov were also questioned by Davidson and James [35]. According to the authors, the lack of information with regard to description of their apparatuses and to assume that the heat flow through the specimen was equal to the heat generated by a heating element, leads to believe that the results have errors of unknown magnitude [35].

Biyikli et al. [45] obtained the thermal conductivity through the experimental tests at various positions along the length of human femur. This author used insulation and measured the heat flow directly. According to the Davidson and James [35], these are essential requirements for the determination of thermal conductivity and so, can be considered as the most reliable data available.

Moses et al. [50] obtained experimental values for the thermal conductivity of equine cortical bone, through the guarded hot plate apparatus. They used different saturated and dry samples.

Later, Davidson and James [35] improved the experimental tests of Biyikli et al. [45] to measure the thermal conductivity of cortical bone tissue and to determine its variation with heat flow direction. They found that the directional differences were small, concluding that the bovine cortical bone could be treated as thermally isotropic.

Finally, Zhang et al. [46] used an analytic and experimental approach to establish stress and thermal conductivity correlation in bovine cortical bone as a function of nanomechanical compressive stress changes using Raman Thermometry. They found a thermal conductivity in the range from 0.45 to 0.64 W/mK, with an average of 0.54 W/mK. These results are in the range of the values reported by Chato [47], Moses et al. [50] and Davidson and James [35], which vary from 0.38 to 0.70 W/mK.

## 2.2 Bone Drilling in Medicine

Bone drilling procedure is an essential step in a broad range of clinical interventions including: orthopaedics, neurosurgery, dentistry, plastic and reconstructive surgery, craniomaxillofacial, among others. The success of these surgical operations is dependent upon the quality of the drilling procedure in view to minimize associated injury to the surrounding tissue [51, 52]. In a summarized manner, bone drilling is a machining operation in which a revolving cutting tool is fed along its axis of rotation into the bone producing a hole. The main purpose to create holes in the bone tissue is to accommodate screws or other threaded devices for rigid fixation, which is provided by the integration of bone (cortical and/or trabecular) with the screw threads [53].

Nowadays, bone drilling is a surgical procedure increasingly necessary. Studies have shown an extensive increase in the ageing population and the prevalence of bone diseases is going to increase significantly as a consequence [54]. Due the human aging and associated diseases, improved bone drilling methods are necessary to understand the drilling mechanics effects in its entirety.

At start, when the present work has begun, the majority of the published studies focused on bone drilling, were done in dentistry. Meanwhile, other orthopaedic/traumatological articles have been developed and published, but with numerous contradictions between them [55]. At initial phase of this work, a bibliographical review was made to understand which are the main ambiguities and failures on bone drilling and define the possible contributions to optimise the drilling process. Following subsection covers the essential details about bone drilling, its parameters, limitations and complications that affect the quality and integrity of bone tissue.

### 2.2.1 Bone damage induced by drilling

Bone drilling is an old medical procedure, nevertheless, the penetration of a sharp tool into bone tissue continues to be a clinical and surgical challenge, as many pertinent questions still remain without solutions.

As a manual method, drilling require a high level of dexterity and an extensive training, due the difficulties arising from vibration and the risk of drill bit breakage during perforation [56]. In addition, drilling operations leads to damaging effects within the bone tissue apart from the material removal. Theses damages can be broadly classified as mechanical and thermal damages.



Improvements are constantly underway and new methods need to be defined to analyse and minimize the damages. The following topics briefly explores the mechanical and thermal effects caused by bone drilling in general.

❖ *Mechanical damage in bone drilling*

Bone is considered a hard biological material, however, an excessive force generated by a cutting tool can lead to bone physical damage. These damages can occur in the form of cracking, surface roughness, and volumetric changes that, in turn, can produce postoperative complications [57-59]. Some researchers have concluded that the magnitude of the damage is related with the forces generated by movement of the tool and consequently with drilling parameters and the type of bone tissue [60, 61]. As a result of bone composite nature, the mechanical load direction critically determines its response to the drilling operation. Under the action of moving tools the stress begin to accumulate up to reach the limit of ultimate tensile strength supported by bone tissue. Once the limit has been reached, the bone fails. Typically, these failures begin with formation of cracks. These cracks can propagate through the bone cross section and damage the surrounding tissues [3]. In addition, based on drill bit geometry and cutting parameters, the drilling action can produce different surface finish on the bone tissue. Researches have shown that the surface roughness has influence on the mechanical properties of bone as well as the bone healing [62, 63]. Although the volume removal is a necessary action in drilling processes, other secondary effects act as harmful.

Another important factors in these processes is that drilling are implemented by hand drills, which means that the bone drilling force and feed-rate are manually controlled by the surgeon. Thus, the cutting effort sensed by the surgeon is personal and depends on the tool feed-rate, the bone quality and the cutting tool type. Development of methodologies to predict the drilling forces and relating with mechanical damage are essential for improving the drilling processes.

According to the author Lee et al. [64], since the late 1950s, experimental studies on bone drilling have been conducted to determine optimal drilling conditions and drill bit geometries. Various studies examined the effect of drill speed, feed-rate and other drilling parameters on thrust force and torque during bone drilling [64]. The majority of studies have indicated that large forces experienced during bone drilling play significant challenges to effective application of bone drilling [64].

The use of uncontrolled forces may result in drill breakthrough, drill-bit breakage, excessive heat generation and bone mechanical damage, producing irreversible damages to surrounding tissues and may promote crack formation, which could conduct to prosthetic or bone failure [59, 64-67].

Jacob et al. [68] focused their studies on experimental methodologies on drilled bovine tibia samples using different drill point geometries under different conditions of feed-rate and drill speed, while measuring torque and thrust. They found that high drill speeds commonly results in lower drilling forces but the higher feed-rates were seen to produce higher thrust forces and torques. However, Albrektsson [69] and Thompson [70] observed that the high drill speeds to cause increased trauma, while the authors Abouzgia and James [71] measured the drill speed, applied force and energy consumed during drilling in bovine cortical bone specimens and concluded that drilling at high speed and with a large force may be desirable because bone temperature is reduced.

Wiggins and Malkin [72] also investigated the effect of drilling parameters for three types of drill bits and they concluded that higher feed-rates produce higher thrust forces and torques. Soriano [60] and Krause [73] studied the effect of the feed-rate on the cutting force and they concluded that high feed-rates provided the greatest reduction in cutting forces and energy spending.

A review of studies about the drill bit geometry have shown strong relation between the geometry type and bone drilling forces [74, 75]. Hobkirk and Rusiniak [76] observed that the smaller point angles (i.e., sharper drill tip) produced lower forces, but also increased the unwanted drill breakthrough. Farnworth and Burton [76] have also analysed the drill bit geometry and they found that the twist drill bits with larger (fast) helix angles provoked lower drilling forces and also allowed more effective chip removal. The authors also noted that the large helix angles can also cause drill breakthroughs and increase the bone trauma [76].

Beside the experimental methodologies, the development of numerical models based on experimental models calibration also have been used to predict the drilling forces. Alam et al. [78] developed a finite element model of bone cutting to predict the cutting forces as a function of cutting parameters and comparison with experimental results. For orthopaedic bone surgery, they recommended low cut depth and cutting tool with sharp edge to reduce the cutting forces.

Lughmani et al. [79, 80], developed a numerical model for prediction the thrust forces during the bone drilling and, subsequently, they improved the model by incorporating a constitutive material damage law to predict drilling forces in cortical bone with experimental validation. Through his studies, they observed that the thrust force increased with an increase in feed-rate, while the torque decreased with an increase in drill speed. Similarly, the thrust force decreased with an increase in drill speed, while the effect of feed-rate on the torque was negligible.

Many other authors have focused their studies on develop predictive tools capable of simulating the bone drilling process with the cutting parameters involved, being the modelling of these process still a challenge. A review on advances in numerical modelling of bone drilling will be discussed further below.

Apart from mechanical effects, due to mechanical and thermal stresses, the temperature rise as undesirable side effect in drilling process is associated with biological and cellular damage of the bone tissue. In the following the essential details about heat generated during drilling and its effects on bone tissue will be described.

#### ❖ *Thermal osteonecrosis in bone drilling*

Heat growth during bone drilling leads to substantial rise in the bone temperature. Such a rise in temperature can lead to thermal injury or osteonecrosis (irrecoverable damage) in the tissues subjected to heat. In clinical terms, osteonecrosis means irreversible death of the bone cells when the temperature increase above a threshold [36]. According to the authors Augustin et al. [55], the first studies about thermal necrosis, as a result of elevated temperature, was reported in 1925 when have described local effects of frictional heat during orthopaedics operations. Years later, Anderson and Finlayson proposed the term “aseptic necrosis” for the local cauterization observed in bone after pin insertion [81]. In 1958, Thompson [70] studied low drill speeds (125-2000 rpm) by histology and measuring the bone temperature *in vivo*. Rafel, in 1962, studied the temperature changes during high drill speeds (200 rpm and above) [82]. More recently, the spatial distribution of elevated temperature has been studied in real time using the thermocouples [83-87] or infrared thermography [88-90] as indirect methods to determine the thermal necrosis [91]. However, a precise temperature threshold for thermal necrosis of human bone is still unclear and the study of causes and effects remains a major challenge [55].

Currently, it is known that the osteonecrosis may result in the collapse of the architectural bone structure, leading to joint pain, bone destruction and function loss [92].

Beaulé and Amstutz concentrated their studies in total hip arthroplasty and what the implications are in respect of osteonecrosis.

Figure 8 show an example of four stages of osteonecrosis, represented by these authors. The first stage presents a normal stage and in the last stage is visible the progressive loss of articular cartilage and collapse of the femoral head.

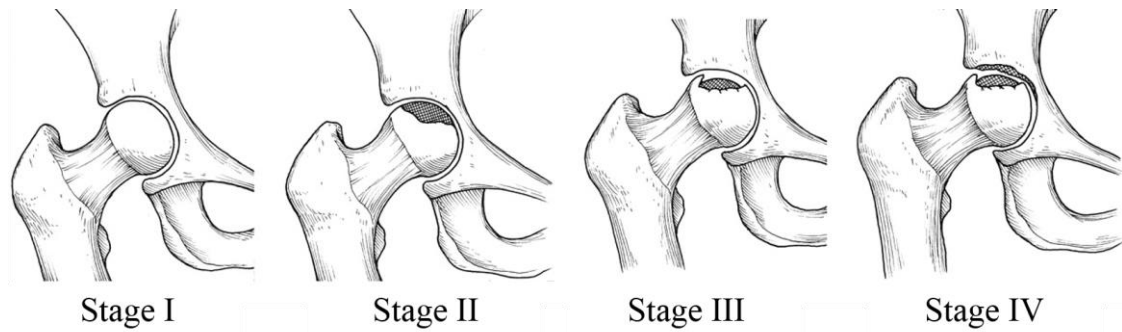


**Figure 8.** Stages of Osteonecrosis. (Adapted from [93])

The magnitude of the damages depend of the temperature range and the exposure time. Over the years, studies have been showed that an increase in temperature above 70 °C causes immediate damage to the bone tissue.

One of the first and most detailed studies about temperature threshold was done by Moritz and Henriques [94]. They investigated the time-temperature thresholds required to produce damage on the dermal and epidermal layers of human and porcine skin over a wide temperature range (44 °C to 100 °C). According to them, the temperature above 70 °C destroys the epithelial cells instantly, and the same for 50 °C when the tissue is exposed for 30 seconds or more. The study found that as the temperature increased, the amount of time required to initiate thermal necrosis decreased.

Bonfield and Li [95] studied the deformation characteristics of dog femora under on temperature range of -58 °C to 90 °C and they found irreversible changes in the bone structure to the temperatures higher than 50 °C.

Lundskog [38] showed through his studies on rabbits that a temperature of 55 °C for 30 seconds will induces irreversible death of the bone cells. They established a threshold temperature of 50 °C at 30 seconds exposure. In the years of 1983 and 1984, Eriksson et al. published several studies on the determination of threshold for osteonecrosis in rabbit bones [37, 96, 97]. They also studied the effects of defined temperature rise on bone regeneration and found that heating the titanium implants to 47 °C or 50 °C during 60 s

caused a significant decrease in the bone formation, while no significant effects were detected when the heating was done to 44 °C for 60 seconds [97, 98].

Based upon the published experimental results, the thermal damage on bone tissue starts at around 45 °C with critical damages for temperatures above 55 °C. However, these studies were not conducted on human bone tissue, and therefore, the exact threshold temperature for the death of the human bone is unknown. The majority of the authors believes that an average temperature of 47 °C for 1 min as threshold, above which the necrosis of the human bone will take place [36]. Accumulation of heat during bone drilling is usually due the friction between the cutting tool and the bone [34].

Through these studies it has been widely demonstrated the importance of controlling the heat produced during bone drilling to avoid osteonecrosis and subsequently the surgical failures and postoperative problems. Improving our understanding to the relationship between drilling conditions and resulting temperatures field are an essential step to identify the most favourable conditions to minimize the injuries.

Although several researches have been done in this field, there are still an existing disagreement over how the drill bit geometry, force, drill speed and feed-rate affect the heat generated during drilling.

Through the bibliographical survey, it is evident that the subject of osteonecrosis is complex and discussion continues on how the results of such experiments should be reflected in clinical practice.

### **2.2.2 Effects of drilling parameters on bone**

Independently from bone type undergoing the drilling, the choice of parameters also plays a key role in determining the overall success of the surgeries. The most important parameters reported in the literature can be divided in two major categories. The first one is related to the specifications of the drill bit and the second one is related to the drilling parameters. It is important to indicate that these parameters did not influence the drilling efficiency individually. All drilling parameters are interrelated [55]. In general, it is accepted that the applied force should not exceed the safe limit of material (fracture strength, thermal strength, and necrosis temperature) [3].

Table 5 specifies the both groups that influence the drilling performance. In the last few decades many researchers have investigated the influence of these parameters in order to minimize the changes of bone damage during drilling procedures.

**Table 5.** Parameters involved in bone drilling.

Drill bit specifications	Drill parameters
Drill diameter	Drill speed
Drill point:	Feed-rate
Point angle	Drilling energy
Chisel edge	
Cutting face	Cooling
Rake angle	Internal cooling (open/closed system)
Clearance angle	External cooling
Drill material and wearing	Drilling depth
Flutes and helix angle	Predrilling
	Bone thickness

#### ❖ *Drill bit specifications*

The drill bit geometry is a very important aspect on the bone drilling. Its main function is to remove the material during the drilling in the desired direction and produce a uniform and regular hole. As the drill progresses, there is the chip formation, which tend to follow the spiral path formed by the drill flutes.

Several types of surgical drill bits are available in a broadly variety of configurations and sizes with different diameters. However, any drill bit is mainly characterized by its diameter, cutting face, helix angle and drill point, as show in Figure 9.

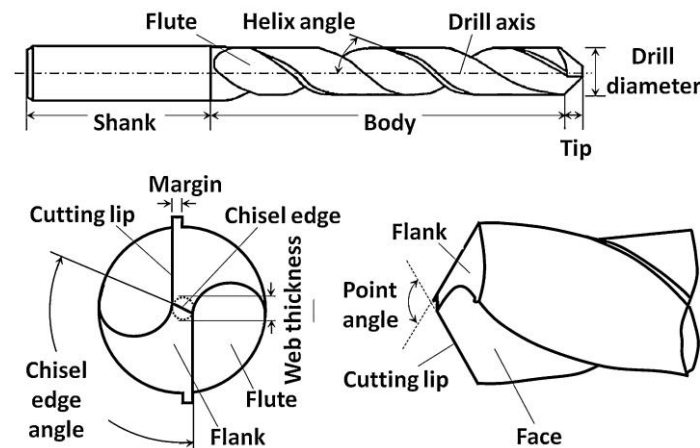


**Figure 9.** Geometry of a twist drill bit and its drill bit tip. (Adapted from [98])

The selection of an optimal drill bit requires knowledge of the material being drilled as well as cutting parameters (applied force, feed-rate and drill speed) in order to match this to the physical characteristics of the drill bit [3].

Some authors have been compared the surgical drills with other drill bit designs commercially available for engineering applications. Natali et al. [99] studied various drill bits available for engineering purposes, and compared them with standard orthopaedic drill bits, while drilled fresh cadaver human tibia. They found that some commercially available drill bits performed better than their orthopaedic equivalents, producing significantly less thermal injury to the bone and having the force required for cortical penetration.

The use of drill bits that minimize the heat generated during drilling is crucial to the success of bone surgeries. Researches have shown that many features of drill are responsible for increase in thermal injury to the bone [52, 98-100]. In addition, the design of the drill bit point and the cutting edges dictates the cutting forces for given drilling conditions [98]. Following points reviews each drill bit specification individually. The most important published studies and their conclusions are discussed and explored.

**Drill diameter:** The influence of drill diameter has been the subject of considerable attention in the literature. Many researchers carried out drilling tests to determine the effect of drill diameter on the temperature rise during drilling [98, 101-103]. Higher drill diameters means that the contact surface between the cutting tool and bone tissue will increase, which in turn increases the friction and also the bone temperature.

In 2004, Kalidindi studied the temperatures produced while drilling an acrylic bone cement with three different drill diameters (2, 3.5 and 4.3 mm). He found that the temperature increases exponentially with increasing drill diameter [104]. Augustin et al. reported similar results in its studies with porcine bones [103]. Karaca et al. [101] performed an *in vitro* study using bovine tibia and analysed five different drill diameters (1.5, 2.7, 3.2, 4.5 and 6.0 mm) but did not mentioned influence of diameter on the increase in bone temperature. Two years later, Karaca and Aksakal carried out an *in vitro* study by using fresh calf cortical bones with the same five drill diameters used in the previous study. They recorded the temperatures at the drilling sites with high accuracy using multi-thermocouples mounted around the tibial diaphyseal cortex and showed that the temperatures increased with larger drill diameters [102].

Strbac et al. showed through their studies that the heat increased is inversely proportional to the drill diameter [105-107]. They evaluated the temperature changes during implant osteotomies with surgical twist and conical drills from 2 to 5 mm diameter at various drilling depths. They verified significant differences on the temperature increase with different drill diameters [105, 106].

In another study they investigated the temperature changes in the shearing and withdrawing processes during osteotomies. They used an overall 160 automated intermittent osteotomies with 2 mm diameter twist drills and 3.5 mm diameter conical drills on standardized bone specimens. Real-time recording showed that a 2 mm diameter twist drills caused higher temperatures compared with 3.5 mm diameter conical implant drills [107].

According to the authors Augustin, Zigman et al. [55], there are an advantage in larger drill due its larger flutes, which contribute to better elimination of heated bone fragments resulting in a more efficient drilling with lesser increase in bone temperature. However, this phenomenon is not sufficient to decrease the total bone temperature generated due to poor thermal capacity of the bone tissue.

Another problem found on the larger drill holes is that larger holes reduce the strength of the bone, which leads to increase of time recovery. According to the author Bechtol et al. [108], drill holes of 20% of the bone diameter reduces the strength of the bone by 40% of its original strength. Burstein et al. [109], studied the postoperative behaviour of femoral diaphysis of dogs with screws and concluded that the drill holes are present up to 12 weeks, which increases the fracture risk or refractory due to decrease in bone strength. Hufner et al. [110] carried out investigations to see the effect of drill diameter and length on the deviation of the actual to the planned target point during bone drilling. They used twelve drills of varying lengths and diameters. The results suggest that drill bit deflection interferes directly with the precision. The precision is decreased when using small diameter and longer drill bits.

**Drill point:** The main aspects of the drill point is the angle formed by the projection of the cutting edges on to a plane passing through the longitudinal axis of the tool; and the chisel edge defined at the end of the web that connects the cutting lips (Figure 9) [36].

Point angle of the cutting tool allows to the operator to drill at the desired site without significant deviations. The improvement of this parameter leads to an increase the performance drilling. According to the authors Augustin et al. [55] and Pandey and Panda [36], the smaller or sharper ( $\leq 90^\circ$ ) point angle produces more acute tip which can easily stab in the material preventing the walking of the drill. However, using a sharper point angle, less portion of cutting lip is involved in the drilling action in the first moments of drilling, which leads to higher rise in the temperature. Drill bits with a larger ( $> 90^\circ$ ) point angle provide full contact of the cutting lip with the bone tissue as soon as drilling starts.



According to the authors Karmani and Lam, drills with larger point angle are more suitable for hard materials and drills with smaller point angle for soft materials, such as bone tissue [74]. According to these authors, a range of  $110^{\circ}$ - $118^{\circ}$  point angles are recommended for the design of orthopaedic drill.

Other important aspect is the axial drilling force. The drill point angle has significant influence on the axial force. The sharper the drill point angle, the lower is the axial drilling force [55]. According to the authors Augustin et al. [52] drill point angles below of  $80^{\circ}$  are not desirable. They studied different drill point angles ( $60^{\circ}$ ,  $80^{\circ}$ ,  $100^{\circ}$  and  $120^{\circ}$ ) and found that the point angle equal to  $60^{\circ}$  causes drill holes ellipsoidal and not circular. They also reported that the drill point angle of  $80^{\circ}$ ,  $100^{\circ}$  and  $120^{\circ}$  did not show significant difference on the increase in bone temperature during drilling. Davidson and James [111] developed thermo-mechanical equations to predict the heat generation on drilling process and also reported that the point angle did not have significant influence. On the other hand, Wiggins and Malkin [72] investigated three different drill bits (surgical twist drill, general purpose twist drill and a spade drill) with different point angles and observed that the drill bit with a point angle of  $118^{\circ}$  generates much lower torque and energy as compared to the other two. Also, Saha et al. [100] and Natali et al. [99] studied different drill bits with different point angles and reported that a split-point drill bit with a point angle of  $118^{\circ}$  presents an improved performance, reducing the force required (the time of surgery and consequently the time for heat generation), and therefore causing less thermal damage than a standard orthopaedic drill. Hillery and Shuaib [112] studied the heat generated while drilling bovine tibia and cadaveric human bone using different drill point angles ( $70^{\circ}$ ,  $80^{\circ}$  and  $90^{\circ}$ ) and did not find significant difference in the temperatures produced. Recently, Lee et al. [98] showed that the maximum temperature increases with increasing point angle. Paszenda and Basiaga [113] developed an analysis of surgical drill during bone drilling with the use of finite element method. They determined the strains and stresses in working part of the drill bit, without correlation of drill point angle influence on bone temperature elevation. They found that the drill point angle of  $90^{\circ}$  presents strains and stresses lesser than drill bit with point angle equal to  $120^{\circ}$ .

Several researchers have developed its studies in order to find the influence of drill point angle on bone drilling. It has been suggested in the literature that the overall effect of point angle is negligibly small. However, there is no general agreement on the optimum drill point angle and further improvements are still needed.

The chisel edge of a conventional twist drill bit has a significant effect on its locating ability and the drilling thrust force [36]. Furthermore, the chisel edge causes severe deformation of the work material. As a result, chisel edge represent more than 50% of the total thrust force and the increase in the heat generated, regardless of the work material [114]. However, Bertollo and Walsh [53] reported that the chisel edge contributes little to cutting and significantly to the axial thrust force, due to a relatively slow drilling velocity and a large negative rake angle. Also according to the authors, the extent of the contribution made by the chisel edge to the axial thrust force depends on the length ratio between the chisel and cutting edges. Saha et al. [100] reported through their studies, that the presence of the chisel edge was mainly responsible for increasing the thrust force and the heat generated. They suggested that the width of the chisel edge can be reduced by grinding to improve the cutting efficiency. However, the maximum amount of web thinning is limited by minimum strength of the web necessary to avoid the breakage of the drill due to the cutting force [36]. Natali et al. [99] suggested that an optimal drill bit for orthopaedic purposes should have a split point because reduces the chisel edge to almost a tip. Consequently the extrusion effect of the chisel edge is transformed to the cutting action by imparting positive rake angle at the chisel edge zone. Also this new drill bit design facilitates the breaking of the fragments into smaller pieces causing their easy ejection through the flutes. Although it not much reported in the literature, it is evident that the reduction of the chisel edge contributes significantly to the reduction of the thrust forces during bone drilling and increases the accuracy of the hole position.

**Cutting face:** The cutting face is divided into rake angle and clearance angle. The rake angle is defined as the angle between the cutting edge and the plane perpendicular to the workpiece [36]. According to several researches, this drill bit specification has an important role in the cutting forces during drilling. Broad agreement exists on the results obtained by Jacob et al [115] that, as the rake angle increases the bone drilling forces decreases for a single edge cutting tool. Saha et al. [100] also observed the combined effect of the helix and the point angles on the rake angle. They concluded that the higher rake angle increases the cutting efficiency of the drill. Hillery and Shuaib [8] recommended an optimum rake angle between 20° and 30°, as appropriate for clean the bone fragments and generates lower thrust force.

Clearance angle is the space provided to avoid undesirable contact of the flank with the workpiece, and is the angle whereby the flank of the drill clears the material during drilling [99].

The flank is the flat part of the drill when viewed end on and represents a large surface area for friction during drilling [36]. Studies have been shown that the large surface of the flank provided by clearance angle, results in high friction with workpiece. This causes the increased frictional heat and hence the temperature during drilling. Farnworth and Burton [77] suggested a clearance angle of  $15^\circ$  for better cutting efficiency during bone drilling. Saha et al. [100] concluded that a clearance angle of  $15^\circ$  at the periphery, and  $18^\circ$  towards the centre for a 6.35 mm drill bit to be ideal for bone tissue. Natali et al. [99] reported that the effect of friction caused by the flank of the drill can be reduced by increasing the clearance angle halfway along the surface termed as split point. Split point causes reduction of the friction of the flank with workpiece so less heat is generated. Karmani and Lam [74] demonstrated that the optimal clearance angle of the drill bit for soft materials such as plastics with hardness similar to cortical bone tissue, lies in the range of  $12^\circ$ - $15^\circ$ .

**Drill material and wear:** several authors have been studying the effect of drills made of different materials and also its wear due to over-frequent use. Considering the drill material, Sumer et al. [116] studied the heat generated by stainless steel and ceramic drill bits at different depths. They reported that although more heat was generated in the superficial part of the drilling cavity with the ceramic drill, heat modifications did not correlate with the drill material in the deep aspect of the cavity.

Recently, Koo et al. [117] confirmed the same results. They analysed the effect of three types of drill bits (titanium nitride-coated metal, tungsten carbide carbon-coated metal and zirconia ceramic) during osteotomy preparation and compared the heat production between them. The authors did not find significant differences between drill materials. On the other hand, other authors have found significant changes between different materials.

Karaca et al. [101] reported that the TiBN coated drills caused higher temperatures than uncoated ones but without detailed discussion of its cause. Oliveira et al. [118] used two types of drill bits (twisted stainless steel and ceramic) to assess thermal changes in bovine tissue. They found higher bone temperatures in the drills of stainless steel than ceramic materials.

Harder et al. [119] evaluated the intrabony friction heat produced by implant drills, using different materials and methods of cooling. They found that differences in the heat generated by different drill materials were not significant.

Considering the drill wear, this is a subject focused in recent researches. The drill wear is common during drilling and is directly related to the frequency of use, applied force, sterilisation technique, bone tissue density, material construction, and surface treatment [120]. Repeated use of the drill bit produces wear on the cutting edges due to the mechanical and thermal load during drilling. According to the authors Matthews and Hirsch [121] the bone temperature increases with the multiple use of the drill bit. The wear of the drill bit also increases the surface roughness of cutting lips resulting in the increase of axial thrust force, temperature and cutting vibrations [36]. Until now, scanning electron microscopy (SEM) and light microscope have been used to analyse wear of the drill bit. In 2000, Jochum and Reichart studied the surgical trauma due to multiple use of Timedur®-titanium cannon drills for 51 times in an *in vitro* experimental setting using pig mandibles. They concluded that the use of drill more than 40 times causes significant wear and increase in temperature [122]. Allan et al. [123] devised an *in vitro* experiment to simulate preparation for osteosynthesis by using drills with different degrees of wear: one was new, one had drilled 600 holes, and the third drill bit had been used for several month.

They found a highly significant difference in the temperatures generated by the three drills, and reported that the change in temperature was due to the amount of wear. Chacon et al. [124] measured the generated heat in bone tissue by three implant drill systems after repeated drilling and sterilization. They used the light microscope to evaluate drill wear and found that the temperature increased with multiple uses of drill (after 25 uses). Misir et al. [83], demonstrated that after 35 uses, implant drills tend to generate more heat. In opposite to the previous studies, Oliveira et al. [118] found a positive correlation between temperatures generated and the number of uses of drill bit. They reported that drills can be used up to 50 times without producing harmful temperatures to bone tissue or severe signs of wear and deformation.

In summary, the majority of studies suggest that the drill bit wear and the heat generated during bone drilling increase with the number of times that the drill is used. However, there exist no suggestions of a specific number of times that is possible to use the drill bit before it becomes blunt and ineffective, producing a significant increase in temperature.

**Flutes and helix angle:** Flutes are helical or straight grooves cut that usually revolve around the drill bit to provide cutting lips, removal of chips and allow that the cutting fluid reaches the cutting lip.

Drill bits can be constructed with two or three flutes with different sizes and various helix angles [36]. The common tool used is a twist drill with two helical flutes [55].

Bertollo et al. [125] studied the differences between 2-fluted and 3-fluted surgical drills and showed that the 3-fluted drill offers a significant improvement than the 2-fluted, not only in targeting ability but also in the range of permissible approach angles and has superior bending stiffness. They also reported that acute point-angle and the increase flexural stiffness of 3-fluted drills, in certain clinical scenarios, can increase the surgeon ability to accurately position a hole. Also to avoid the difference in position of the intended hole or damage to the surrounding tissues. After two years, Bertollo et al. [126] observed that the increase in cutting efficiency of the 3-fluted drills tested did not translate into a reduction in generation heat or improvement in bone healing or screw fixation. According to the authors Pandey and Panda [36], despite the theoretical advantage of 3-fluted drills in comparison with the 2-fluted, there is a lack of evidences in the literature to support of their use.

The helix angle of the drill bit is defined as the angle formed by the edge of the flute with the parallel line to drill centre line. A slow or low helix has elongated drill flutes whereas high or quick helix drills have compact flutes i.e. number of turns is higher in quick helix than in slow helix [36]. According to some contributors, the optimal helix angle for short chipping materials, such as dry bone, is the small or slow helix because the debris generated are small particles that are easily cleared by the drill bit [36, 55]. High or quick helix is recommended to the materials in which the chips get clogged, such as bone fragments during a surgery which the bone debris are mixed with blood and marrow fat, and in this wet state it flows differently and tends to clog slow helix flutes [99]. For surgical drill, the range of 13°-35° helix angle are usually employed depending upon the drill diameter [100]. Fuchsberger [127] suggested through its studies, a helix angle of 12° to 14° for effective bone drilling. Davidson and James [35] concluded that the temperature decreases uniformly with increasing helix angle.

#### ❖ *Drill parameters*

Cutting parameters play a fundamental role in the drilling quality and precision. Parameters associated within the setup of hand drills are the machining parameters, such as drill speed, feed rate, drilling depth and the bone density. The improvement of these parameters and all involved variables are essential to improve the bone drilling processes and to minimize the bone injuries.

From last few decades many studies have focused on this aspect in order to minimize the chances of bone damage during the drilling procedures.

**Drilling speed:** Many researches have been carried out to determine the optimal drilling speed for bone perforation [51, 52, 112, 128, 129]. However, the review of the literature on the drilling speed showed no consistent trend. For many years, researchers focused on low speed drillings (up to 3000 rpm) and concluded that increase of drilling speed increases bone temperature. Vaughan and Peyton [130] observed the influence of drill speed during cavity preparation and concluded that increase of this parameter produces increase on the heat generated during drilling. Also, Thompson [70] studied the influence of drill speed and found that the temperature increases with increasing speed from 125 rpm to 2000 rpm during skeletal pin insertion *in vivo*. However, Matthews and Hirsch [121] investigated the drill speed range of 345 rpm to 2900 rpm on the drilling of human cadaveric femora and not found any significant change in temperature. Eriksson and Adell [131] suggested that the ideal instruments for preparation of an implant site were considered low speed (1500-2000 rpm) handpieces. Brisman [132] measured the temperatures while drilling bovine cortical bone and found that the increase of drill speed and load together allow an efficient cutting with no significant increase in temperature. In 1999, Hillery and Shuaib [112] observed a significant decrease in the heat generated during bone drilling with increasing drill speed from 400 rpm to 2000 rpm with a drill diameter of 3.2 mm. They also suggested that the drill speeds of 800-1400 rpm with a drill diameter of 3.2 mm provide the best drilling conditions and maintaining temperatures at a controllable level. Sharawy et al. [133] conducted experiments to measure the generated heat for drill speeds from 1225 rpm to 2500 rpm and found that the heat decreases with the increases of drill speed. Nam et al. [134] conducted its their studies on bovine ribs and established four drilling conditions, combining two speeds and two pressure loads. They found that the increase either the speed or the pressure resulted in a temperature rise. In 2008, Augustin et al. [52] studied different drill speeds (188, 462, 1140 and 1820 rpm) on porcine cortical femora and found that the temperature increases with increases of drill speed for a constant drill diameter. Karaca et al. [101] conducted their studies for a drill speed range of 200 to 1180 rpm and suggested that high drill speeds would not be appropriated for the orthopaedic surgery. Tu et al. [135] used a dynamic elastic-plastic finite element model to simulate the bone temperature rise during drilling process. Based on the numerical results they concluded that the temperature generated during drilling decreases with an increase in drilling speed or the applied force.

Lee et al. [64] studied three different drill speeds (800, 2800 and 3800 rpm) and observed that the maximum temperature increase with the increasing of drill speed. Also, Sezek et al. [136] analysed the temperature changes during cortical bone drilling for different parameters with the finite element method. Through its experiments with five different drill speeds (230, 370, 570, 1080 and 1220), concluded that the temperature increased with increasing drill speed and falls below necrosis area at drill speeds lower than 570 rpm. More recently, Alam et al. [137] have measured the bone temperature by experimental and numerical methods using different parameters. The drill speed were changed from 1000 rpm to 3000 rpm. They concluded that the maximum bone temperature was directly proportional to the drill speed. Same results were obtained by Alam in other publication where he performed experimental tests on cortical specimens of cow and measured the temperature changes with thermocouples at different drill speeds [86].

There is a difficulty in defining an optimum value of the speed on bone drilling and depends on the surgery type. Dental burs operate at speeds of 3600–7500 rpm compared to orthopedic drills at 60-800 rpm [34]. In neurosurgery high speed drilling is more affiliated. The comparison of drill speed on different medicine fields is not straightforward.

The doubt of optimum value of the speed on bone drilling continues to be target of the study. Some authors suggest low drilling speeds while others suggest a decrease of temperature for high drill speeds. It is important to keep the investigations on this subject and to find a consensus.

**Feed-rate and applied drill force:** the feed-rate is the speed of insertion of the drilling tool inside the bone tissue i.e., with the increase of the feed-rate shorter is the drilling time and thereby lesser heat transfer to the bone. On the other hand, the applied axial force during drilling on the bone is directly related to the feed-rate. With higher axial force increases friction between the bone and the tool, which could lead to temperature increase and drill failure [55]. The great challenge for the researchers is to find an optimal relation between the feed-rate and the axial drilling force, which the force is not excessive and the drilling time as short as possible to minimize the duration of friction between the drill and the bone tissue. Available data is insufficient but most agree that the drilling axial force in conjunction with the feed-rate can significantly contribute to the reduction of the drilling time and subsequently the heat production [55, 138].

Matthews and Hirsch [121] investigated the applied force effect (19.6 N to 117.6 N) and reported that this parameter is much more important than drilling speed as a factor in both the magnitude and duration of cortical temperature rises. They verified that increases in the applied force was associated with decreases in the maximum temperatures and the durations of temperature elevation. These results are also shown by Augustin et al. [52] who concluded that the peak temperature during drilling decreases as the feed-rate increases. Bachus et al. [139] determined how differences in applied drilling forces affect the temperature of fresh frozen human cadaver femora and found that the duration and magnitude of maximum temperature decreases with increasing axial thrust force at 820 rpm. Kalidindi [104] concluded that the increase of the axial force and feed-rate decreases drilling time with a constant drilling depth. Nam et al. [134] reported through its studies that the temperature rise relies significantly of the applied force. For them, the increasing of the pressure resulted in a temperature increase. Augustin et al. [52] reported that higher feed-rate causes lower increase in bone temperature, but for the delivered combination of parameters that are used in orthopedics or traumatology it is not clinically important as an isolated parameter. Tu et al. [140] simulated the Kirschner pin and bone thermal contact during drilling process through finite element model. Based on the numerical results they concluded that a larger applied force can reduce the temperature rise effectively.

Sezek et al. [136] mentioned in its studies that the applied drill force should not be evaluated as a single parameter. The changes in drill forces also change the feed-rate. According to these authors, the temperature is inversely proportional with feed-rate and applied drill force. Lee et al. [64] also concluded that the maximum temperature decreases with the increasing of feed-rate. Alam et al. [137] changed the feed-rate from 30 mm/min to 70 mm/min and fixed the drill speed at 2000 rpm to find the effect of feed-rate on maximum bone temperature. They observed that the heat generated on bone tissue increases with the increase of the feed-rate. The same behaviour of the feed rate were found in others studies [141].

Although there is no clear indication about the optimum bone drilling speed and axial drilling force, the most of above publications recommend high drill speed with larger force or feed-rate for minimum temperature generation during bone drilling and, consequently, lesser bone damage.

**Drilling energy:** the vast majority of papers found in the literature about drilling energy are directed to the metal machining and generally these are not applicable in bone drilling.



Drilling energy associated with bone perforation can be defined as the energy expended per unit volume of bone removal and is directly related with the amount of heat generated during the process [72]. The amount of energy necessary to drill a hole in a specific time is call of power. Power is calculated as a product of drilling speed (in rpm) and torque [55]. In most researches on drilling energy, lower energy is associated with less mechanical and thermal damage (cracking and bone necrosis), because higher consumed energy implies higher generated of heat leading to higher rise in temperature [36].

Jacob et al. [68] measured the axial force and torque during drilling of bovine tibia with different drill speeds and feed-rates. They concluded that at lower drill speeds the forces are much higher as compared to the higher speeds and, as the feed-rate is increased the forces increases. However, higher forces means more energy delivered during drilling and consequently more heat to the bone tissue. The problem is that in the surgical procedure the thrust is varied by the sensibility of the surgeon, and higher feed-rate is desired. Wiggins and Malkin [72] carried out an experimental method on bone drilling using different types of drill bits and diameters. They measured the feed-rate, torque and specific energy for a constant axial force. It was verified that the clogging of drill flutes is a serious problem which causes increased torque and drilling energy. They also described dependence of torque and specific drilling energy on feed-rate, and showed that both are higher at smaller feed-rates, meaning more generated heat.

Abouzgia and James [71] investigated the effect of axial forces between 1.5 and 9.0 N on the drill speed and measured the energy consumed during the drilling process. The measurements showed that the total drilling energy consumed generally decreases with increasing drill speed and axial force due the decrease in drilling time. They suggested that high drill speed with a large force is desirable because bone temperature is reduced. Bachus et al. [139] reported that for the same drilling conditions higher thrust produces less heat. This is accomplished by reaching maximum feed-rate and minimum drilling time. Karmani and Lam [74] studied the effect of rake angle on the drilling efficiency. They showed that an optimum rake angle facilitates the drilling, decreases deformation of material cut by the tool, improves fragments flow and reduces specific drilling energy. Increasing the positive rake angle decreases the drilling force for bone drills, increasing their drilling efficiency. Ercoli et al. [142] evaluated the drilling efficiency, durability, heat production and wear of implant drills. They showed that the drill design, material and mechanical properties significantly affect drilling efficiency and durability.

The 2 mm twist drill design with a low hardness exhibited plastic deformation at the cutting edge, loss of cutting efficiency and drill fracture.

**Cooling:** the effect of cooling systems on bone drilling is one of the most discussed parameters on the literatures. Currently it is known that the use of cooling keeps the drilling site at safe temperatures [143]. The doubt that still prevails among the different studies is which cooling system is better for the different types of surgeries. Two main types of cooling have been mentioned by the authors: external and internal cooling system (Figure 10). The last one is divided into closed and open type.

External cooling is not attached to the drill bit and directly supplies the coolant (through pressurized air or fluid) to the surface of the drill at the entry point. Usually, the cooling fluid is a saline solution (sterile NaCl) [3]. Internal cooling involves the circulation of pressurized air or cooling fluid inside the drill bit through the tubules in the drill shaft. The closed type is when the coolant circulated in a closed circuit and does not come directly in contact with the bone tissue undergoing drilling. The cooling is reached only by heat transfer from the drill bit to the coolant flowing through tunnels. This system helps to cool the drill bit but there are chances of bone tissue being heated up [3]. Open type on the other hand has the coolant coming out of the drill tip to the operational field keeping a direct contact with the bone tissue.

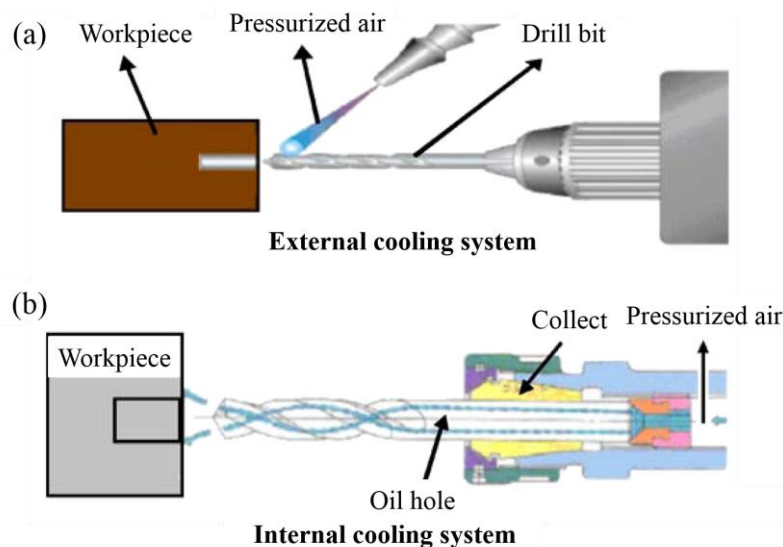


**Figure 10.** Cooling systems: (a) external and (b) internal cooling. (Adapted from [144])

All systems could be achieved either with automated systems with continuous cooling (where flow can be regulated) or manually [36].

The main functions of the cooling systems are not only the cooling but also provides lubrication and irrigation (excluding closed internal cooling system) [55]. Lubrication reduces the friction between the drill bit and, in turn, reduce the heat generated. Irrigation is important in the elimination of bone debris and fragments, since that can prevent the clogging of flutes during bone drilling and indirectly to reduce the friction and the heat generated. Despite continued improvement of the cooling systems, there are still limitations. As already mentioned, both irrigation and lubrication cannot be achieved using closed internal coolant systems. In its turn, the infiltration depth of cooling fluid is unknown in external system, as well as the possible complications to the soft and hard tissues. Further, the contact zones that cause the friction are not lubricated therefore this is also ineffective in lowering the friction. External cooling is partly efficient in prevention and elimination of clogging of drill bit flutes [55].

Over the years, cooling systems have been investigated for drilling operation in an extensive manner. Matthews and Hirsch [121] evaluated the use of external cooling during drilling of human cortical bone using water at room temperature at flow rates of 300, 500 and 1000 ml/min. They found that increasing of irrigation rate decreases the heat generated on bone tissue, and the temperature never increases beyond 50 °C for the irrigation rate of 500 ml/min or above. Lavelle and Wedgwood [145] performed an *in vitro* study using two drill bit tools at low drill speeds to prepare experimental cavities to varying depths.

They reported that the frictional heat during bone drilling was reduced by internal irrigation compared with external or no irrigation. Haider et al. [146] have compared the internal drill cooling with manual external cooling on the diaphysis (cortical bone) and metaphysis (trabecular bone) of the left distal tibia in each of six sheep. They concluded that external cooling is better at all surface drill hole levels in cortical and in all trabecular bone beds, while internal cooling was only better at the deeper drill hole levels in compact bone. However, Benington et al. [147] observed in the preparation of osseointegrated dental implant sites, that there is no substantial difference in the generated heat at implant sites between internal or external cooling system. They concluded that there is no benefit of expensive internal irrigation system over the external irrigation. Sharawy et al. [133] concluded that heat generation decreases with drill speed, regardless the cooling system used. Kalidindi [104] compared the use of external cooling and no cooling system, and observed significant temperature rise without cooling.

Augustin et al. [52] used external irrigation with water of 26 °C on drilling of porcine femora and concluded that the external irrigation is the most important cooling factor in maintained the bone temperature below 47 °C. Sener et al. [148] performed an *in vitro* study to simulate the clinical conditions involved in implant bed osteotomy. They used fresh bovine mandibles and investigated the effects of external cooling with saline at 25 °C and 10 °C respectively. They suggested that the external irrigation at room temperature can provide sufficient cooling during drilling. Lower temperature saline was more effective in cooling the bone, and irrigation of the site should be continued between the drilling steps. These results are similar to results obtained by Al-Dabag and Sultan [149], using the external irrigation at 5 °C and 25 °C. Augustin et al. [103] performed several experiments using an internally cooled drill with and without cooling water of 24 °C. They found that in all parameters combinations with internal cooling produces bone temperatures below the critical 47 °C. More recently, Harder et al. [119] investigated the heat produced at different depths and found significant differences between internal and external cooling systems. They reported that the steel drill bits with internal cooling generated significantly less intrabony heat than those in which an external cooling supply was used. Strbac et al. [105] investigated the thermal effects of different irrigation methods during intermittent and graduated drilling. They combined internal, external and without irrigation, with constant 50ml/min isotonic saline solution. According this authors, the saline irrigation is indispensable during drilling to avoid the harmful temperature threshold of 47°C.

The internal and combined irrigation is more favourable compared with external cooling during an intermittent and graduated drilling procedure.

From the literature review under this section it is clear that there is still a lot of work to be done in order to determine which cooling system is better for bone drilling. Few researchers had carried out the investigations for the comparison of internal and external cooling and there is not always consistency between the authors. In general, cooling systems clearly help to bring down the temperature to safe level during drilling for same set of parameters and same drill bits used.

**Drilling depth:** the effect of drilling depth on bone tissue has a total concordance between the authors. Broad agreement exists that with greater drilling depth, the higher bone temperature. Wiggins and Malkin [72] found that the produced temperature is directly proportional to the drilling depth.

Cordioli and Majzoub [150] performed an *in vitro* study on blocks of bovine cortical femur bone and measured the thermal changes during drilling procedures used in site preparation. They reported a significant increase in temperature at depths of 8 mm versus 4 mm, regardless of the diameter of the used drill and regardless of the presence of cooling. Kalidindi [104] concluded that increase of drilling depth increases the generated heat during bone drilling due to increase the contact time between the bone tissue and drill bit. This leads to an increase of the overall friction and consequently a higher heat is produced. Others authors, such as authors Oliveira et al. [118] and Lee et al. [51] also reported that depth is the predominant factor influencing the temperature induced during bone drilling. However, it is known that the heat generated along the depth of the samples was dependant on drill design and other parameters. Some authors emphasized that when using open type of internal cooling, influence of the drilling depth on temperature rise is not an important factor [151].

In all studies there are a positively correlated between drilling depth and heat generated during bone drilling.

**Predrilling:** drilling of bone tissue can be done either in single step or in multistep. In the single step only one drill bit of required diameter is used to produce the desired hole, while for multistep the drilling diameter increase gradually using a series of drill bits. The main purpose of the multistep is to gradually enlarge the drilling hole, decrease the bone fragments which expel during drilling, and thus enhance the heat dissipation. However, there are many controversies about the predrilling. In multistep, the total time of drilling is increased, which means greater exposure time for bone tissue.

On the other hand, drilling with hand operated drills can involve complications with maintaining the same direction of predrilled hole [55].

Predrilling was described for many researchers during years. In 1983, Itay and Tsur suggested that a proper technique, including predrilling or hand drills, can effectively lessen the temperature during bone drilling [152]. Also, Matthews et al. [153] studied the effect of predrilling and measured the maximum temperatures on human cadaveric cortical bone during experimental insertion of five types of external skeletal-immobilization pins. They concluded that the predrilling was highly effective as a method of minimizing temperature elevation. By contrast, Reingewirtz et al. [154] studied the influence of various parameters on bone heating during drilling on bovine cortical femur model. They concluded that the predrilling did not affect temperature elevation but decreased drilling time with final diameter drill.

Kalidindi [104] confirmed that the maximum obtained temperature during predrilling is far less than drilling a large diameter hole at a single stretch. According to the author, this may be due to the time gap between the changes of drills during incremental drilling that allows the material cools. In addition, the new drill bit will be cooler than the previous drill. Recently, Augustin et al. [103] conducted its experiments with a step drill. They did not find any differences in the maximum bone temperature with two-step drill as compared to the standard drill of the same diameter.

Although there are many studies which recommend the multistep, predrilling is not used routinely in clinical settings [55].

**Bone thickness:** the bone thickness is another aspect that influence the temperature during bone drilling and is positively correlated. As previously indicated, bone is composed of cortical and trabecular part. However, the most critical part to the higher temperatures is the cortical tissue. It is known that the duration of bone drilling depends on the cortical thickness due the frictional resistance offered by the bone to the drill bit and consequently causes increase in temperature.

Eriksson et al. [155] measured the temperature generated during *in vivo* drilling tests with rabbit, dog and human bones under similar conditions. They reported that the difference in temperature between the animal and clinical studies was mainly attributed to the difference in cortical thickness between the species. Its results indicated that the temperatures generated is highest in humans followed by dog and then in rabbits. Hillery and Shuaib [112] performed its study on bovine and human bones and found that the temperature generated when drilling bovine bone was higher than that produced when drilling human bone. They explained that the bovine bone is much harder and the depth of the cortical bone tissue is greater than human bone. The cortical specimen thickness for the bovine bone was 7-9 mm and the human ulna was 3-5 mm.

Although there are concordance on this subject, there is still many topics about bone tissues that need to be done, such as the differences on bone damage, not only thermal but also mechanical damage; to assess different bones in the same species, different stages of age, among others.

### 2.2.3 Temperature measurement in bone drilling

Temperature monitoring is a crucial requirement to determine the exact effect of drilling parameters. The methods used to record temperature rise in real time include either direct

recording by thermocouple instruments or indirect estimating by infrared thermography, mathematic calculation or by measuring the electrical power supplied to the drill.

The thermocouples have been used for many years and is the most popular method to measure the temperature changes in both *in vivo* and *ex vivo* experiments. However, the results from thermocouples are usually governed by numerous factors that may render future comparison somewhat questionable. The use of thermographic camera has increased for the determination of the bone temperature during drilling due to its ease in measuring the temperature at any desired location. This technique is limited for clinical use due its high cost and the camera cannot be used in conjunction with irrigation systems. Few studies compare both methods, making it difficult to know which of them is better to use during bone drilling.

#### ❖ *Thermocouples*

Thermocouples are the sensors based on two different conductors (usually metal alloys). As the temperature changes between ends of both the conductors, there is a proportional change in the voltage between them [3]. Currently, there are a range of thermocouples available on the market. The difference between them depends upon composing metals which dictate a temperature range and sensitivity. The thermocouples with low sensitivities (B, R, and S types) have lower resolutions and thermocouples with high sensitivities (E, J, K and T types) have higher resolutions. There are also thermocouples intended for a higher and lower range of temperatures. The use of thermocouples in medicine were first reported in dentistry by Horch and Keiditsch [156].

These sensors can be placed inside of drill bit with its leads glued along the drill barrel, thus allowing that temperature could be monitored with the movement of the tool [86, 112]. Other methods place several thermocouples at different positions on the surface or at the depth of bone tissue [86, 148, 157]. This allows to capture extent of effect of temperature rise based on anisotropic bone nature [3, 112]. In the literature has been reported that the thermocouples are normally placed at increasing radial distances of 0.5 mm, 1 mm and 3 mm from the drilling site which is suitable for comparing results. There are, however, numerous published studies using different thermocouples at different distances, bone models, etc. For easier reading were selected some articles published between the years 2000 and 2015, that use thermocouples to assess the amount of heat generated in real time (Table 6).

**Table 6.** Some experimental studies of heat measured using thermocouples.

Bone model	Sensor	Thermocouple		Distance to the hole (mm)	Depth (mm)	Ref.
		No	Size			
Porcine jaw	K type	4	0.15	1.0	8	[133]
PMMA	K type	2	0.9	6.0	6, 12	[104]
Porcine jaw	K type	1	0.75	-	5	[123]
Bovine femur	K type	1	2.3	0.5	15	[124]
Porcine femur	unitest therm 100	-	-	0.5	3	[52]
Bovine jaw	W type	3	-	0.5	3, 7, 12	[148]
Bovine femur	K type	3	1.0	-	3, 6, 9	[116]
Bovine femur	several types	-	-	0.5	1, 3, 5	[51]
Bovine rib	K type	-	1.0	1.5	8	[118]
Bovine femur	K type	2	0.8	1.0	8	[89]
Bovine rib	T type	3	0.2	0.5	4	[119]
Bovine tibia	T type	3	-	0.5	superficial	[102]
Bovine femur	K type	4	-	5, 10	2	[158]
Bovine femur	J type	16	1.6	0.3	-	[159]
Artificial bone	Multichannel	2	1.5	1, 2	2, 4, 8, 10, 11, 13, 16	[106]
	SHT, 7 NTC type	1	1.5	1		[107]
Sheep cervical vertebrae	K type	2	-	-	2	[87]
Human cadaveric tibia	K type	4	-	3	2	[160]
Cortical femur	K type	1	0.13	1	4	[137]

The review of the literature shown in Table 6 suggests that the thermocouples chosen for bone models are normally of the K type. Most of them use two or more thermocouples and placed on bone specimen at radial distances of 0.5 mm and 1 mm. Very few of the studies have been carried out on longer distances.

Although thermocouple technology is well established, studies on its use are still not uniform and there are variations in the distance to the final hole (between 0.5 and 10 mm), depths and numbers in the vertical dimension (monochannel and multichannel). The authors have been demonstrating other problems associated to the use of thermocouples. There have been concerns regarding thermocouple ability to detect only spot temperature and the technology does not to allow production of an overall thermal profile or measurement of heat that has leaked through the holes [91].

Another limitation is the technical difficulty frequently encountered during insertion of the elements very close to the drill [161]. Pandey and Panda [36] mentioned that the temperature measurement by thermocouple is not a reasonable method because of poor thermal conductivity and inconsistent properties of bone. Also, the large number of pilot holes needs to be prepared for thermocouple insertion during experiments.



To overcome these difficulties, infrared technology has been employed. Some authors describe this technique as being the most accurate with a lower probability of error [162].

#### ❖ *Infrared thermography*

The infrared thermography is based on the detection of energy emitted by electromagnetic radiation. As this energy is dependent on the temperature of the body examined, accurate determination of the temperature could be made [161]. The signals acquired are used for constructing the two-dimensional (2D) thermal image. Combining two or more cameras, a 3D surface can be reconstructed [3].

According the author Möhlhenrich et al. [91], the use of this technology in medicine was introduced by D'Hodet et al. [163]. As mentioned above, recently some authors have been suggesting the use of thermography as more accurate method than thermocouples because of their overall assessment of the heat. Moreover, this method does not require physical contact and thus is more feasible during *in vivo* studies or actual surgeries. A complete heat map generated gives the spatial distribution of the heat and spread of the affected areas [3, 162, 164].

Many studies have been used the thermography technique to assess the amount heat generated in real time. As was done to the thermocouple studies, Table 7 summarizes the studies that use infrared camera since 2000 until the present day.

**Table 7.** Some experimental studies of heat measured using infrared thermography.

Bone model	Thermal imaging system	No. of cameras	Distance to the hole (m)	Ref.
Bovine jaw	Agema Thermovision 900 system	1	0.05	[147]
Porcine femur	ThermaCAM PM695®, FLIR System	1	0.5	[88]
Porcine rib	IRI 1001 system, Infrared Integrated Systems Ltd	1	-	[165]
Ovine tibia	Digicam-IR, Ircon, Niles, IL, USA	1	-	[126]
Bovine femur	FLIR SC3000 QWIP, FLIR Systems, Daderyd, Sweden	1	0.5	[162]
Bovine femur	Fluke 62 Mini IR Thermometer	1	-	[89]
Artificial bone	IRI 1001 (E Irisys, Northampton, UK)	1	0.8	[166]
Bovine femur	Therma Cam Flir E300	1	-	[158]

Most of the studies uses only one camera. However, as stated above, the use of two or more cameras may reconstruct 3D images but still shows the surface temperature, although it is a 3D surface [88]. Other studies described the use of thermographic camera as a template for the placement of the thermocouple [104].

In spite of all its advantages, the infrared thermography also has some limitations imposed either by lack of data of thermal properties of the bone tissue or by the technique itself. Through this technique is only possible detect the surface temperature, that renders it impossible to determine the extent of depth of necrotic regions.

Both methods have disadvantages. To get an overall idea of temperature profile, infrared thermography should be used in simultaneous with thermocouples [104].

In spite of all efforts to determine the optimal drilling parameters, there are still controversies in the literature over its effect on bone tissue. The complexity of drilling processes associated to the wide range of parameters and physical phenomenon makes it difficult to draw stable conclusions. On the other hand, bone tissue is a multicomponent, multi-composition, and hierarchical material that in turn makes its mechanical and thermal interaction with a cutting tool very complicated. Analyse and understand key aspects involved in bone drilling are essential in the control of this processes and reach the desired outcome. The use of experimental techniques, as unique method, is not sufficient to ensure accurate results. Optimization of bone drilling process based on computational models may be help in predicting bone damage during drilling and help to choose the right parameters for the machining operations. The field of numerical modelling related to bone drilling has been explored in the following section.

#### **2.2.4 Numerical modelling in bone drilling**

Finite element analysis (FEA) has been widely used in human medicine, namely in the biomechanical evaluation of tissues, design and manufacture of medical devices and simulation of different surgical procedures as possible substitute for complex experimental work and validation of analytical and experimental results.

In bone drilling, FEA is an essential tool to reproduce the factors influencing the output variables and thus to help achieve a better understanding of the drilling processes. A review of the literature revealed lack of efforts on computational modelling of bone drilling processes. A recent study reviewed the bibliography of the main contributions in modelling of bone cutting including bone drilling and reported that the extensive number of variables involved complicates the statement of concluding remarks and corroborates

the interest in developing predictive tools for bone drilling [167]. According to this study, the numerical models on bone drilling has been poorly developed. The few available works were focused on heat transfer and mechanical behaviour of bone. Following sub-sections cover the most important numerical models.

#### ❖ *Thermal models*

Prediction of temperature gradient during bone drilling helps in optimization of the process intended to minimize the damage by osteonecrosis. Recently, studies have been carried out on the development of thermal models applied to drilling processes. The pioneer study in this field was conducted by Davidson [168]. The author used a numerical simulation to perform a parametric analysis of the thermal impact of bone drilling operations. In 2003, Davidson and James [111] developed thermo-mechanical equations to predict the heat involved in drilling processes. The equations were coupled with a numerical model of heat transfer based on finite element method (FEM) to predict the temperature rise and thermal injury in bone drilling. The authors evaluated a set of drilling parameters (drill speed, feed-rate, drill geometry and bone material properties) to determine the importance of each on temperature rise. They observed consistent trend between numerical and experimental results for low or moderate drill speeds, but it didn't happen for higher drill speeds. According to Marco et al. [167] the most probable cause is improper modelling of bone failure at high speeds. Lee et al. [98] developed a thermal model for bone drilling with applications to orthopaedic surgery. The model combined a unique heat-balance equation for the system of the drill bit and the chip stream, an ordinary heat diffusion equation for the bone tissue, and heat generation at the drill bit tip. The thermal model was solved numerically using a tailor-made finite-difference scheme for the drill bit-chip stream system, coupled with a classic finite difference method for the bone tissue. Also this study analysed different drilling parameters on the heat generated during drilling. Unlike the Davidson and James [111], Lee et al. [98] observed that the higher drill speeds lead to the highest maximum temperatures. Sezek et al. [136] also developed a 3D numerical model to analyse the temperature changes during cortical bone drilling (bovine tibia) for different parameters, including the effect of gender on bone temperature rise. The numerical model was validated through *in vitro* experiments using fresh calf cortical bones. The authors concluded that not only drilling parameters influenced the maximum temperature, but also bone density has a significant effect. Tu et al. [169] utilized a 3D elastic-plastic temperature-displacement coupled FEM

to simulate the thermomechanical behavior of the contact region between the drill bit and bone. The dynamic simulations were performed through the commercial ABAQUS/Explicit code and used a failure criterion to control the element removal during the drilling operation. They concluded that higher drill speed can cause a noticeable increase in bone temperature as well as the size of the thermally affected zone. The numerical model was verified by experiments and was used to propose an empirical equation to estimate the peak bone temperature, considering different drill speeds. They also reported that the maximum difference between the peak bone temperatures predicted by the proposed equation and those obtained from the numerical model is less than 3.5%. Alam et al. [141] predicted an increase in the necrosis penetration depth as function of drilling speed based on a fully thermo-mechanically coupled FEM for various cooling conditions. The FE model was developed using the MSC. Marc general FE code; and the Johnson-Cook (JC) constitutive equation was applied to represent the bone behaviour. Wang et al. [170] investigated the cutting heat in the vibrational drilling of fresh bovine bones compared with conventional drilling through experimental and finite element approach. In this case, a 2D FE model was developed by the pre-processing software GAMBIT along with the CFD software FLUENT to simulate the cutting heat conduction. Their experimental results showed that vibrational drilling could significantly reduce the temperature in drilling of cortical bone and the FEA results also showed that the vibrational amplitude holds a significant effect on the cutting heat conduction. Thermal FE models are a good tool in predicting the heat generated during drilling processes. Besides the thermal effect, mechanical loading also determines the drilling characteristics as well as induces effects such as surface damage and roughness. Computational efforts related to mechanical loading based FE models were also reviewed.

#### ❖ *Mechanical models*

During bone drilling operations there are chip formation. This happens because the shear force exceeds the fracture strength of the material. Along with shear, these forces can be solved into various components such as gravity, normal, and shear components [3]. The reproduction of the hole formation during drilling with all dynamic characteristics involved in this process requires the development of 3D FE approaches with element removal. According to Marco et al. [167] the major drawback of the 3D models is the elevated computational cost, because this simulation requires a great number of small

elements to reproduce accurate results. The researches have been trying to improve these models, aiming to approach as close as possible to realistic surgeries.

Lughmani et al. [79, 80] published their first results related to the numerical modelling of bone drilling in the year of 2013. They have developed a 3D FE model for thrust force experienced during drilling of cortical bone (bovine femur). The model was developed in the commercial code ABAQUS/Explicit and incorporates the dynamic characteristics involved in the process along with the accurate geometrical considerations. Element removal scheme was applied in order to depict chip formation through the simple erosion criterion. In this criterion was defined the maximum level of the equivalent plastic strain above which mesh elements were removed. Cortical bone was considered as a transversely isotropic material and an elastic–plastic law was used for the material constitutive model. The average thrust forces and torques obtained using FE analysis were compared with the experimental results and showed good agreement. They suggested that the thrust force and torque may be reduced using a combination of low feed rate and high rotational speed when drilling in cortical bone. Sezek et al. [136] also optimised the drill force via FEM analysis and experiments. Drill forces from 20 N to 140 N were applied throughout the drilling procedures, using a specially designed drilling rig enabling to apply various speeds between 230 and 1220 rpm. According to them, the applied drill force increased as bone density increased and the optimum drill force was found to be 140 N.

Mechanical bone behaviour based modelling approach has been applied extensively in other cases of orthogonal cutting [44, 78, 171, 172].

Numerical models based on drilling approach have been discussed from thermal and mechanics point of view. It was clear from the literature review that the modelling of bone drilling is difficult and few works showed complete models with material removal capable of predicting drilling forces, temperature and mechanical damage. Most of the studies only developed thermal models focused on temperature prediction but unable to predict the mechanical damage. The implementation of bone drilling models is a challenge, probably due to the complexity of the simulation tools and the computational time required. However, it is clear that numerical modelling could help to determine the suitable drilling parameters so as to perform the drilling processes in most efficient and least damaging way. Seen in these terms, the present work intends to be a pioneer, including in this field new dynamic models capable to predict the temperatures, strains and stresses during bone drilling for different drilling parameters.

The development of accurate models and its integration with the surgical procedures require an exchange of views with active collaboration between professionals from medical and engineering fields. This is the only way to achieve success.

## References

1. Jee WSS (2001) Integrated bone tissue physiology: anatomy and physiology. In: Cowin SC (Eds), *Bone Mechanics Handbook*. Second Edition, New York: CRC Press, pp. 1-34.
2. Fazzalari NL (2011) Bone fracture and bone fracture repair. *Osteoporos Int* 22(6):2003-2006.
3. Dahotre N, Joshi S (2016) Machining of bone and hard tissues. Springer International Publishing, Switzerland, pag.12. ISBN: 978-3-319-39158-8 (e-Book).
4. Clarke B (2008) Normal Bone Anatomy and Physiology. *Clin J Am Soc Nephrol* 3(Suppl 3): S131–S139.
5. Weiner S, Wagner HD (1998) The material bone: structure-mechanical function relations. *Annu Rev Mater Sci* 28(1):271-98.
6. Bone tissue and the skeletal system. In: *Anatomy & Physiology*, pp. 203-238, OpenStax Publisher, 2013. ISBN-10: 1938168135; ISBN-13: 978-1-938168-13-0.
7. Downey PA, Siegel MI (2006) Bone biology and the clinical implications for osteoporosis. *Phys Ther* 86(1):77-91.
8. Sambrook P (2010) Bone structure and function in normal and disease states. In Sambrook P et al. (Eds), *The Musculoskeletal System: Systems of the Body Series*, Second Edition, Churchill Livingstone, pp. 68-84.
9. Blausen.com staff. Blausen gallery 2014. *Wikiversity Journal of Medicine* 1(2). doi:10.15347/wjm/2014.010. ISSN 20018762.
10. Rho JY, Kuhn-Spearing L, Zioupos P (1998) Mechanical properties and the hierarchical structure of bone. *Med Eng Phys* 20(2):92-102.
11. Sato M, Grese TA, Dodge JA, Bryant HU, Turner CH (1999) Emerging therapies for the prevention or treatment of postmenopausal osteoporosis. *J Med Chem* 42(1):1-24.
12. Cole JH, van der Meulen MC (2011) Whole bone mechanics and bone quality. *Clin Orthop Relat Res* 469(8):2139-49.

13. An YH (2000) Mechanical properties of bone. In: An YH and Draughn RA (Eds), *Mechanical Testing of Bone and the Bone-Implant Interface*. Boca Raton, CRC press, pp.41-58
14. Guo XE (2001) Mechanical Properties of Cortical Bone and Cancellous Bone Tissue. In: Cowin SC (Eds), *Bone Mechanics Handbook*. Second Edition, New York: CRC Press, pp. 10-1-10-18.
15. Wu Z, Ovaert TC, Niebur GL (2012) Viscoelastic properties of human cortical bone tissue depend on gender and elastic modulus. *J Orthop Res* 30(5):693-699.
16. Reilly DT, Burstein AH, Frankel VH (1974) The elastic modulus for bone. *J Biomech* 7(3):271-5.
17. Burstein AH, Reilly DT, Martens M (1976) Aging of bone tissue: mechanical properties. *J Bone Joint Surg Am* 58(1):82-6.
18. Cezayirlioglu H, Bahniuk E, Davy DT, Heiple KG (1985) Anisotropic yield behavior of bone under combined axial force and torque. *J Biomech* 18(1):61-9.
19. Keller TS, Mao Z, Spengler DM (1990) Young's modulus, bending strength, and tissue physical properties of human compact bone. *J Orthop Res* 8(4):592-603.
20. Currey JD (1988) The effects of drying and re-wetting on some mechanical properties of cortical bone. *J Biomech* 21(5):439-441.
21. Huiskes R (1980) Some fundamental aspects of human joint replacement. Analyses of stresses and heat conduction in bone-prosthesis structures. *Acta Orthop Scand Suppl* 185:1-208.
22. Spatz HC, O'Leary EJ, Vincent JF (1996) Young's moduli and shear moduli in cortical bone. *Proc Biol Sci* 263(1368):287-94.
23. Morgan EF, Bouxsein ML (2008) Biomechanics of Bone and Age-Related Fractures. In: Bilezikian JP, Raisz LG, Martin TJ (Eds), *Principles of Bone Biology*. Third Edition, Elsevier Inc., pp. 29-51.
24. Kaplan SJ, Hayes WC, Stone JL, Beaupré GS (1985) Tensile strength of bovine trabecular bone. *J Biomech* 18(9):723-7.
25. Keaveny TM, Wachtel EF, Ford CM, Hayes WC (1994) Differences between the tensile and compressive strengths of bovine tibial trabecular bone depend on modulus. *J Biomech* 27(9):1137-46.
26. Kuhn JL, Goldstein SA, Ciarelli MJ, Matthews LS (1989) The limitations of canine trabecular bone as a model for human: a biomechanical study. *J Biomech* 22(2):95-107.

27. Martens M, Van Audekercke R, Delpont P, De Meester P, Mulier JC (1983) The mechanical characteristics of cancellous bone at the upper femoral region. *J Biomech* 16(12):971-83.
28. Poumarat G, Squire P (1993) Comparison of mechanical properties of human, bovine bone and a new processed bone xenograft. *Biomaterials* 14(5):337-40.
29. Vahey JW, Lewis JL, Vanderby R Jr (1987) Elastic moduli, yield stress, and ultimate stress of cancellous bone in the canine proximal femur. *J Biomech* 20(1):29-33.
30. Mosekilde L, Kragstrup J, Richards A (1987) Compressive strength, ash weight, and volume of vertebral trabecular bone in experimental fluorosis in pigs. *Calcif Tissue Int* 40(6):318-22.
31. Rho JY, Flaitz D, Swarnakar V, Acharya RS (1997) The characterization of broadband ultrasound attenuation and fractal analysis by biomechanical properties. *Bone* 20(5):497-504.
32. Natali AN, Hart RT, Pavan PG, Knets I (2003) Mechanics of bone tissue. In: Natali AN (Eds.) *Dental Biomechanics*. CRC Press: Taylor & Francis Group, pp. 1-19.
33. Zelenov ES (1985) Experimental investigation of the thermophysical properties of compact bone. *Mech Compos Mater* 21(6):1092-1095.
34. Karmani S (2006) The Thermal properties of bone and the effects of surgical intervention. *Curr Orthop* 52:20-58.
35. Davidson SR, James DF (2000) Measurement of thermal conductivity of bovine cortical bone. *Med Eng Phys* 22(10):741-7.
36. Pandey RK, Panda SS (2013) Drilling of bone: A comprehensive review. *J Clin Orthop Trauma* 4:15-30.
37. Eriksson AR, Albrektsson T (1983) Temperature threshold levels for heat induced bone tissue injury. A vital-microscopic study in the rabbit. *J Prosthet Dent* 50:101-107.
38. Lundskog J (1972) Heat and bone tissue. An experimental investigation of the thermal properties of bone and threshold levels from thermal injury. *Scand J Plast Reconstr Surg* 6:5-75.
39. Henschel CJ (1943) Heat Impact of Revolving Instruments on Vital dentin Tubules. *Journal of Dental Research* 22(4): 323.
40. Huiskes R (1980) Some fundamental aspects of human joint replacement. *Acta Orthop Scand Suppl* 1851-208.



41. Clattenburg R, Cohen J, Conner S, Cook N (1975) Thermal properties of cancellous bone. *J Biomed Mater Res* 9(2):169-82.
42. Fukushima H, Hashimoto Y, Yoshiya S, Kurosaka M, Matsuda M, Kawamura S, Iwatsubo T (2002) Conduction analysis of cement interface temperature in total knee arthroplasty. *Kobe J Med Sci* 48(1-2):63-72.
43. Abayazid M (2010) *Modelling heat generation and temperature distribution during dental surgical drilling*. M.Sc. Thesis, Delft University of Technology, Netherlands.
44. Santiuste C, Rodríguez-Millán M, Giner E, Miguélez H (2014) The influence of anisotropy in numerical modeling of orthogonal cutting of cortical bone. *Composite Structures* 116:423-431.
45. Biyikli S, Modest MF, Tarr R (1986) Measurements of thermal properties for human femora. *J Biomed Mater Res* 20(9):1335-45.
46. Zhang Y, Gan M, Tomar V (2014) Raman Thermometry Based Thermal Conductivity Measurement of Bovine Cortical Bone as a Function of Compressive Stress. *J Nanotechnol Eng Med* 5(2):021003-11.
47. Chato JC (1965) A survey of thermal conductivity and diffusivity data on biological materials. In: *5th Conference on Thermal Conductivity* Vol. 2, Sessions IV-VI. Denver, Colorado.
48. Vachon RI, Walker FJ, Walker DF, Nix GH (1967) In vivo determination of thermal conductivity of bone using the thermal comparator technique. In: *7th International Conference on Medical and Biological Engineering*, Stockholm, Sweden.
49. Kirkland, R (1967) In vivo thermal conductivity values for bovine and caprine osseous tissue. In: *Proceedings of Annual Conference on Engineering in Medicine and Biology*, Boston, MA.
50. Moses WM, Witthaus FW, Hogan HA, Laster WR (1995) Measurement of the thermal conductivity of cortical bone by an inverse technique. *Exp Therm Fluid Sci* 11(1):34-39.
51. Lee J, Ozdoganlar B, Rabin Y (2012) An experimental investigation on thermal exposure during bone drilling. *Med Eng Phys* 34:1510-1520.
52. Augustin G, Davila S, Mihoci K, Udiljak T, Vedrina DS, Antabak A (2008) Thermal osteonecrosis and bone drilling parameters revisited. *Arch Orthop Trauma Surg* 128:71-77.

53. Bertollo N, Walsh WR (2011) Drilling of bone: practicality, limitations and complications associated with surgical drill bits. In: Vaclav Klika (Ed.), *Biomechanics in Applications*. InTech.
54. Lutz W, Sanderson W, Scherbov S. (2008) The coming acceleration of global population ageing. *Nature* 451(7179):716-719.
55. Augustin G, Zigman T, Davila S, Udilljak T, Brezak D, Babic S (2012) Cortical bone drilling and thermal osteonecrosis. *Clin Biomech* 27:3313-325.
56. Tsai MD1, Hsieh MS, Tsai CH (2007) Bone drilling haptic interaction for orthopedic surgical simulator. *Comput Biol Med* 37(12):1709-18.
57. Li S, Wahab AA, Demirci E, Silberschmidt VV (2014) Penetration of cutting tool into cortical bone: Experimental and numerical investigation of anisotropic mechanical behaviour. *J Biomech* 47:1117-1126.
58. Ebacher V, Guy P, Oxland TR, Wang R (2012) Sub-lamellar microcracking and roles of canaliculi in human cortical bone. *Acta Biomater* 8:1093-1100.
59. Kasiri S, Reilly G, Taylor D (2010) Wedge indentation fracture of cortical bone: experimental data and predictions. *J Biomech Eng* 132(8):081009.
60. Soriano J, Garay A, Aristimuño P, Iriarte LM, Eguren JA, Arrazola PJ (2013) Effects of rotational speed, feed rate and tool type on temperatures and cutting forces when drilling bovine cortical bone. *Mach Sci Technol: An Int J* 17:611-636.
61. Fonseca EMM, Magalhães K, Fernandes MGA, Barbosa MP, Sousa G (2014) Numerical Model of Thermal Necrosis due a Dental Drilling Process. In: R Natal, et al (Eds) *Biodental Engineering II*, London: Taylor & Francis Group, CRC Press 2013, pp.69-73.
62. Boyan BD, Sylvia VL, Liu Y, Sagun R, Cochran DL, Lohmann CH, Dean DD, Schwartz Z (1999) Surface roughness mediates its effects on osteoblasts via protein kinase A and phospholipase A2. *Biomaterials* 20(23-24):2305-10.
63. Donnelly E, Baker SP, Boskey AL, van der Meulen MC (2006) Effects of surface roughness and maximum load on the mechanical properties of cancellous bone measured by nanoindentation. *J Biomed Mater Res A* 77(2):426-35.
64. Lee J, Gozen BA, Ozdoganlar OB (2012) Modeling and experimentation of bone drilling forces. *J Biomech* 45(6):1076-83.
65. Ong FR, Bouazza-Marouf K (1999) The detection of drill-bit break-through for the enhancement of safety in mechatronic assisted orthopaedic drilling. *Mechatronics* 9(6):565–588.

66. Brett PN, Baker DA, Taylor R, Griffiths MV (2004) Controlling the penetration of flexible bone tissue using the stapedotomy microdrill. *Proc IMechE Part I: J Systems and Control Engineering* 218(5):343-351.
67. Kendoff D, Citak M, Gardner MJ, Stübig T, Krettek C, Hüfner T (2007) Improved accuracy of navigated drilling using a drill alignment device. *J Orthop Res* 25(7):951-7.
68. Jacob CH, Berry JT, Pope MH, Hoagland FT (1976) A study of bone machining process. *J Biomech Eng* 9:343-349.
69. Albrektsson T (1995) Measurements of shaft speed while drilling through bone. *J Oral Maxillofac Surg* 53:1315-1316
70. Thompson HC (1958) Effect of drilling into bone. *J Oral Surg (Chic)* 16(1):22-30.
71. Abouzgia MB, James DF (1995) Measurements of shaft speed while drilling through bone. *J Oral Maxillofac Surg* 53(11):1308-15.
72. Wiggins KL, Malkin S (1976) Drilling of bone. *J Biomech* 9(9):553-554.
73. Krause WR (1987) Orthogonal bone cutting: saw design and operating characteristics. *J Biomech* 109(3):263-71.
74. Karmani S, Lam F (2004) The design and function of surgical drills and K-wires. *Current Orthopaedics* 18(6):484-490.
75. Franssen BB, van Diest PJ, Schuurman AH, Kon M (2008) Keeping osteocytes alive: a comparison of drilling and hammering k-wires into bone. *J Hand Surg Eur* 33(3):363-8.
76. Hobkirk JA, Rusiniak K (1977) Investigation of variable factors in drilling bone. *J Oral Surg* 35(12):968-73.
77. Farnworth GH, Burton JA (1974) Optimization of drill geometry for orthopaedic surgery. In: *Proceedings of the 14th International Conference on Machine Tool Design and Research Conference*, Manchester, England.
78. Alam K, Mitrofanov AV, Silberschmidt VV (2009) Finite element analysis of forces of plane cutting of cortical bone. *Comp Mater Sci* 46:738-743.
79. Lughmani WA, Bouazza-Marouf K, Ashcroft I (2013) Finite element modelling and experimentation of bone drilling forces. *J Phys Conf Ser*, p. 451.
80. Lughmani WA, Marouf KB, Ashcroft I (2015) Drilling in cortical bone: a finite element model and experimental investigations. *J Mech Behav Biomed Mater* 42:32-42.

81. Anderson R, Finlayson BL (1943) Sequele of transfixation of bone. *Surgery* 13:46–54.
82. Rafel SS (1962) Temperature changes during high-speed drilling on bone. *J Oral Surg Anesth Hosp Dent Serv* 20:475-7.
83. Misir AF, Sumer M, Yenisey M, Ergioglu E (2009) Effect of surgical drill guide on heat generated from implant drilling. *J Oral Maxillofac Surg* 67(12):2663-8.
84. Marković A, Mišić T, Miličić B, Calvo-Guirado JL, Aleksić Z, Đinić A (2013) Heat generation during implant placement in low-density bone: effect of surgical technique, insertion torque and implant macro design. *Clin Oral Implants Res* 24(7):798-805.
85. Stelzle F, Frenkel C, Riemann M, Knipfer C, Stockmann P, Nkenke E (2014) The effect of load on heat production, thermal effects and expenditure of time during implant site preparation - an experimental ex vivo comparison between piezosurgery and conventional drilling. *Clin Oral Implants Res* 25(2):e140-8.
86. Alam K (2015) Experimental measurements of temperatures in drilling cortical bone using thermocouples. *Scientia Iranica B* 22:487-492.
87. Livingston A, Wang T, Christou C, Pelletier MH, Walsh WR (2015) The Effect of Saline Coolant on Temperature Levels during Decortication with a Midas Rex: An in Vitro Model Using Sheep Cervical Vertebrae. *Front Surg* 2:37.
88. Augustin G, Davila S, Udiljak T, Vedrina DS, Bagatin D (2009) Determination of spatial distribution of increase in bone temperature during drilling by infrared thermography: preliminary report. *Arch Orthop Trauma Surg* 129:703-709.
89. Bulloch SE, Olsen RG, Bulloch B (2012) Comparison of Heat Generation Between Internally Guided (Cannulated) Single Drill and Traditional Sequential Drilling With and Without a Drill Guide for Dental Implants. *Int J Oral Maxillofac Implants* 27(6):1456-1460.
90. Alam K, Silberschmidt VV (2014) Analysis of temperature in conventional and ultrasonically-assisted drilling of cortical bone with infrared thermography. *Technol Health Care* 22(2):243-52.
91. Möhlhenrich SC, Modabber A, Steiner T, Mitchell DA, Hölzle F (2015) Heat generation and drill wear during dental implant site preparation: systematic review. *Br J Oral Maxillofac Surg* 53(8):679-89.
92. Fondi C, Franchi A (2007) Definition of bone necrosis by the pathologist. *Clin Cases Miner Bone Metab* 4(1):21-6.

93. Beaulé PE, Amstutz HC (2004) Management of Ficat stage III and IV osteonecrosis of the hip. *J Am Acad Orthop Surg* 12(2):96-105.
94. Moritz AR, Henriques FC (1947) Studies of Thermal Injury: II. The Relative Importance of Time and Surface Temperature in the Causation of Cutaneous Burns. *Am J Pathol* 23(5):695-720.
95. Bonfield W, Li CH (1968) The temperature dependence of the deformation of bone. *J Biomech* 1(4):323-9.
96. Eriksson RA, Albrektsson T, Magnusson B (1984) Assessment of bone viability after heat trauma. A histological, histochemical and vital microscopic study in the rabbit. *Scand J Plast Reconstr Surg* 18(3):261-8.
97. Eriksson AR, Albrektsson T (1984) The effect of heat on bone regeneration: An experimental study in the rabbit using the bone growth chamber. *J Oral Maxillofac Surg* 42:705-711.
98. Lee J, Rabin Y, Ozdoganlar OB (2011) A new thermal model for bone drilling with applications to orthopaedics surgery. *Med Eng Phys* 33:1234-1244.
99. Natali C, Ingle P, Dowell J (1996) Orthopaedic bone drills-can they be improved? Temperature changes near the drilling face. *J Bone Joint Surg Br* 78(3):357-62.
100. Saha S, Pal S, Albright JA (1982) Surgical drilling: design and performance of an improved drill. *J Biomech Eng* 104(3):245-52.
101. Karaca F, Aksakal B, Kom M (2011) Influence of orthopaedic drilling parameters on temperature and histopathology of bovine tibia: An in vitro study. *Med Eng Phys* 33:1221-1227.
102. Karaca F, Aksakal B (2013) Effects of various drilling parameters on bone during implantology: An in vitro experimental study. *Acta Bioeng Biomech* 15(4):25-32.
103. Augustin G, Davila S, Udiljak T, Staroveski T, Brezak D, Babic S (2012) Temperature changes during cortical bone drilling with a newly designed step drill and an internally cooled drill. *Int Orthop* 36:1449-1456.
104. Kalidindi V (2004) *Optimization of drill design and coolant systems during dental implant surgery*. PhD thesis, University of Kentucky.
105. Strbac GD, Giannis K, Unger E, Mittlböck M, Watzek G, Zechner W (2014) A novel standardized bone model for thermal evaluation of bone osteotomies with various irrigation methods. *Clin Oral Implants Res* 25(5):622-31.

106. Strbac GD, Unger E, Donner R, Bijak M, Watzek G, Zechner W (2014) Thermal effects of a combined irrigation method during implant site drilling. A standardized in vitro study using a bovine rib model. *Clin Oral Implants Res* 25(6):665-74.
107. Strbac GD, Giannis K, Unger E, Mittlböck M, Vasak C, Watzek G, Zechner W (2015) Drilling- and withdrawing-related thermal changes during implant site osteotomies. *Clin Implant Dent Relat Res* 17(1):32-43.
108. Bechtol CO, Ferguson AB, Laing PG (1959) Metals and Engineering in Bone and Joint Surgery. *Calif Med* 91(5):303–304.
109. Burstein A, Currey J, Frankel V, Heiple K, Lunseth P, Vessely J (1972) Bone strength, the effect of screw holes. *J Bone Joint Surg Am* 54(6):1143-56.
110. Hufner T, Geerling J, Oldag G, Richter M, Kfuri M, Pohlemann T (2005) Accuracy study of computer-assisted drilling: the effect of bone density, drill bit characteristics and use of a mechanical guide. *J Orthop Trauma* 19(5):317-22.
111. Davidson SR, James DF (2003) Drilling in bone: modelling heat generation and temperature distribution. *J Biomech Eng* 125(3):305-314.
112. Hillery MT, Shuaib I (1999) Temperature effects in the drilling of human and bovine bone. *J Mater Process Technol* 92-93:302-308.
113. Paszenda, Basiaga M (2009) FEM analysis of drills used in bone surgery. *Archives of Materials Science and Engineering* 36:103-109.
114. Ong FR(1998) *Analysis of bone drilling characteristics for the enhancement of safety and the evaluation of bone strength*. PhD Thesis, Loughborough University.
115. Jacobs CH, Pope MH, Berry JT, Hoaglund F (1974) A study of the bone machining process-orthogonal cutting. *J Biomech* 7(2):131-6.
116. Sumer M, Misir AF, Telcioglu NT, Guler AU, Yenisey M (2011) Comparison of heat generation during implant drilling using stainless steel and ceramic drills. *J Oral Maxillofac Surg* 69(5):1350-4.
117. Koo KT, Kim MH, Kim HY, Wikesjö UM, Yang JH, Yeo IS (2015) Effects of implant drill wear, irrigation, and drill materials on heat generation in osteotomy sites. *J Oral Implantol* 41(2):e19-23.
118. Oliveira N, Alaejos-Algarra F, Mareque-Bueno J, Ferrés-Padró E, Hernández-Alfaro F (2012) Thermal changes and drill wear in bovine bone during implant site preparation. A comparative in vitro study: twisted stainless steel and ceramic drills. *Clin Oral Implants Res* 23(8):963-9.

119. Harder S, Egert C, Wenz HJ, Jochens A, Kern M (2013) Influence of the drill material and method of cooling on the development of intrabony temperature during preparation of the site of an implant. *Br J Oral Maxillofac Surg* 51(1):74-8.
120. Möhlhenrich SC, Modabber A, Steiner T, Mitchell DA, Hölzle F. Heat generation and drill wear during dental implant site preparation: systematic review. *Br J Oral Maxillofac Surg* 53(8):679-89.
121. Matthews LS, Hirsch C (1972) Temperatures measured in human cortical bone when drilling. *J Bone Joint Surg Am* 54(2):297-308.
122. Jochum RM, Reichart PA (2000) Influence of multiple use of Timedur-titanium cannon drills: thermal response and scanning electron microscopic findings. *Clin Oral Implants Res* 11(2):139-43.
123. Allan W, Williams ED, Kerawala CJ (2005) Effects of repeated drill use on temperature of bone during preparation for osteosynthesis self-tapping screws. *Br J Oral Maxillofac Surg* 43(4):314-9.
124. Chacon GE, Bower DL, Larsen PE, McGlumphy EA, Beck FM (2006) Heat production by 3 implant drill systems after repeated drilling and sterilization. *J Oral Maxillofac Surg* 64:265-269.
125. Bertollo N, Gothelf TK, Walsh WR (2008) 3-Fluted orthopaedic drills exhibit superior bending stiffness to their 2-fluted rivals: clinical implications for targeting ability and the incidence of drill-bit failure. *Injury* 39(7):734-41.
126. Bertollo N, Milne HR, Ellis LP, Stephens PC, Gillies RM, Walsh WR (2010) A comparison of the thermal properties of 2- and 3-fluted drills and the effects on bone cell viability and screw pull-out strength in an ovine model. *Clin Biomech (Bristol, Avon)* 25(6):613-7.
127. Fuchsberger A (1988) Damaging temperature during the machining of bone. *Unfallchirurgie* 14(4):173-83.
128. Udiljak T, Ciglar D, Skoric S (2007) Investigation into bone drilling and thermal bone necrosis. *Adv Prod Eng Manag* 2:103–112.
129. Shakouri E, Sadeghi MH, Maerefat M, Shajari S (2014) Experimental and analytical investigation of the thermal necrosis in high-speed drilling of bone. *Proc Inst Mech Eng H* 228(4):330-41.
130. Vaughan RC, Peyton FA (1951) The influence of rotational speed on temperature rise during cavity preparation. *J Dent Res* 30(5):737-744.

131. Eriksson RA, Adell R (1986) Temperatures during drilling for the placement of implants using the osseointegration technique. *J Oral Maxillofac Surg* 44(1):4-7.
132. Brisman DL (1996) The effect of speed, pressure, and time on bone temperature during the drilling of implant sites. *Int J Oral Maxillofac Implants* 11(1):35-7.
133. Sharawy M, Misch CE, Weller N, Tehemar S (2002) Heat generation during implant drilling: the significance of motor speed. *J Oral Maxillofac Surg* 60(10):1160-9.
134. Nam O, Yu W, Choi MY, Kyung HM (2006) Monitoring of Bone Temperature during Osseous Preparation for Orthodontic Micro-Screw Implants: Effect of Motor Speed and pressure. *Key Eng Mater* 321-323:1044-1047.
135. Tu Yuan-Kun, Chen Li-Wen, Chiang Chun-Hui, Chen Yung-Chuan, Lu Wei-Hua, Tsai Hsun-Heng (2010) Thermal Contact Simulation of the Drill Bit and Bone During Drilling. Doi:10.1109/ICBBE.2010.5517275. IEEE.
136. Sezek S, Aksakal B, Karaca F (2012) Influence of drill parameters on bone temperature and necrosis: A FEM modelling and in vitro experiments. *Comp Mater Sci* 60:13-18.
137. Alam K, Khan M, Muhammad R, Qamar SZ, Silberschmidt VV (2015) In-vitro experimental analysis and numerical study of temperature in bone drilling. *Technol Health Care* 23(6):775-83.
138. Udiljak T, Ciglar D, Mihoci K (2003) Influencing parameters in bone drilling. *9th International Scientific Conference on Production Engineering CIM*, Lumbarda, Korčula, I133-I142.
139. Bachus KN, Rondina MT, Hutchinson DT (2000) The effects of drilling force on cortical temperatures and their duration: an in vitro study. *Med Eng Phys* 22(10):685-91.
140. Tu YK, Hong Y, Chen YC (2009) Finite element modeling of kirschner pin and bone thermal. *Life Science Journal* 6(4): 23-27.
141. Alam K, Khan M, Silberschmidt VV (2014) 3D Finite-Element Modelling of Drilling Cortical Bone: Temperature Analysis. *Journal of Medical and Biological Engineering* 34(6):618-623.
142. Ercoli C, Funkenbusch PD, Lee HJ, Moss ME, Graser GN (2004) The influence of drill wear on cutting efficiency and heat production during osteotomy preparation for dental implants: a study of drill durability. *Int J Oral Maxillofac Implants* 19(3):335-49.



143. Kondo S, Okada Y, Iseki H, Hori T, Takakura K, Kobayashi A, Nagata H (2000) Thermological study of drilling bone tissue with a high-speed drill. *Neurosurgery* 46(5):1162-8.
144. Bagci E, Ozcelik B (2007) Effects of different cooling conditions on twist drill temperature. *Int J Adv Manuf Technol* 34(9):867-877.
145. Lavelle C, Wedgwood D (1980) Effect of internal irrigation on frictional heat generated from bone drilling. *J Oral Surg* 38(7):499-503.
146. Haider R, Watzek G, Plenck H (1993) Effects of drill cooling and bone structure on IMZ implant fixation. *Int J Oral Maxillofac Implants* 8(1):83-91.
147. Benington IC, Biagioni PA, Briggs J, Sheridan S, Lamey PJ (2002) Thermal changes observed at implant sites during internal and external irrigation. *Clin Oral Implants* 13(3):293-7.
148. Sener BC, Dergin G, Gursoy B, Kelesoglu E, Slih I (2009) Effects of irrigation temperature on heat control in vitro at different drilling depths. *Clin Oral Implants Res* 20(3):294-8.
149. Al-Dabag AN, Sultan AA (2010) Effect of cooling an irrigation solution during preparation of implant site on heat generation using Elite system for implant. *Al-Rafidain Dent J* 10(2):260–264.
150. Cordioli G, Majzoub Z ( ) Heat generation during implant site preparation: an in vitro study. *Int J Oral Maxillofac Implants* 12(2):186-93.
151. Tehemar SH (1999) Factors affecting heat generation during implant site preparation: a review of biologic observations and future considerations. *Int J Oral Maxillofac Implants* 14(1):127-36.
152. Itay S, Tsur H (1983) Thermal osteonecrosis complicating Steinmann pin insertion in plastic surgery. *Plast Reconstr Surg* 72(4):557-61.
153. Matthews LS, Green CA, Goldstein SA (1984) The thermal effects of skeletal fixation-pin insertion in bone. *J Bone Joint Surg Am* 66(7):1077-83.
154. Reingewirtz Y, Szmukler-Moncler S, Senger B (1997) Influence of different parameters on bone heating and drilling time in implantology. *Clin Oral Implants Res* 8(3):189-97.
155. Eriksson AR, Albrektsson T, Albrektsson B (1984) Heat caused by drilling cortical bone. Temperature measured in vivo in patients and animals. *Acta Orthop Scand* 55(6):629-31.

156. Horch HH, Keiditsch E (1980) Morphological findings on the tissue lesion and bone regeneration after laser osteotomy. *Dtsch Zahnärztl Z* 35(1):22-4.
157. Tai BL, Zhang L, Wang AC, Sullivan S, Wang G, Shih AJ (2013) Temperature prediction in high speed bone grinding using motor PWM signal. *Med Eng Phys* 35(10):1545-9.
158. Roseiro L, Veiga C, Maranhã V, Neto A, Laraqi N, Baïri A, Alilat N (2014) Induced Bone Tissue Temperature in Drilling Procedures: A Comparative Laboratory Study with and without Lubrication. *International Journal of Biomedical and Biological Engineering* 1(11):816-819.
159. James TP, Chang G, Micucci S, Sagar A, Smith EL, Cassidy C (2014) Effect of applied force and blade speed on histopathology of bone during resection by sagittal saw. *Med Eng Phys* 36(3):364-370.
160. Palmisano AC, Tai BL, Belmont B, Irwin TA, Shih A, Holmes JR (2015) Heat accumulation during sequential cortical bone drilling. *J Orthop Res* 34(3):463-70.
161. Tehemar SH (1999) Factors affecting heat generation during implant site preparation: a review of biologic observations and future considerations. *Int J Oral Maxillofac Implants* 14(1):127-36.
162. Scarano A, Piattelli A, Assenza B, Carinci F, Di Donato L, Romani GL, Merla A (2011) Infrared thermographic evaluation of temperature modifications induced during implant site preparation with cylindrical versus conical drills. *Clin Implant Dent Relat Res* 13(4):319-23.
163. D'Hodet B, Ney T, Mohlmann H, Luckenbach A (1987) [Temperature measurements by infrared technology during drilling process for endosseous dental implants] Temperaturmessungen mit Hilfe der Infrarottechnik bei enossalen Fräsuren für dentale Implantate. *Z Zahnärztl Implantol* 3:123–30.
164. Benington IC, Biagioni PA, Crossey PJ, Hussey DL, Sheridan S, Lamey PJ (1996) Temperature changes in bovine mandibular bone during implant site preparation: an assessment using infra-red thermography. *J Dent* 24(4):263-7.
165. Kim SJ, Yoo J, Kim YS, Shin SW (2010) Temperature change in pig rib bone during implant site preparation by low-speed drilling. *J Appl Oral Sci* 18(5):522-7.
166. Oh HJ, Wikesjö UM, Kang HS, Ku Y, Eom TG, Koo KT (2011) Effect of implant drill characteristics on heat generation in osteotomy sites: a pilot study. *Clin Oral Implants Res* 22(7):722-6.

167. Marco M, Rodríguez-Millán M, Santiuste C, Giner E, Henar Miguélez M (2015) A review on recent advances in numerical modelling of bone cutting. *J Mech Behav Biomed Mater* 44:179-201.
168. Davidson SRH (1999) *Heat transfer in bone drilling*. Master Thesis, Institute of Biomaterials and Biomedical Engineering, University of Toronto, Canada.
169. Tu YK, Chen LW, Ciou JS, Hsiao CK, Chen YC (2013) Finite Element Simulations of Bone Temperature Rise During Bone Drilling Based on a Bone Analog. *J Med Biol Eng* 33:269-274.
170. Wang Y, Cao M, Zhao X, Zhu G, McClean C, Zhao Y, Fan Y (2014) Experimental investigations and finite element simulation of cutting heat in vibrational and conventional drilling of cortical bone. *Med Eng Phys* 36(11):1408-1415.
171. Plaskos C, Hodgson AJ, Cinquin P (2003) Modelling and Optimization of Bone-Cutting Forces in Orthopaedic Surgery. In: Ellis RE, Peters TM (Eds.) *Medical Image Computing and Computer-Assisted Intervention-MICCAI 2003*. Lecture Notes in Computer Science, Springer, Berlin, Vol. 2878, pp 254-261.
172. Alam K, Mitrofanov A, Silberschmidt V (2010) Thermal analysis of orthogonal cutting of cortical bone using finite element simulations. *Int J Exp Comput Biomech* 1(3):236–251.



## CHAPTER III

# Thermal analysis during bone drilling using rigid polyurethane foams: numerical and experimental methodologies\*

**Maria Goreti Fernandes**<sup>1</sup>, Elza Fonseca<sup>2</sup>, Renato Natal Jorge<sup>3</sup>

<sup>1</sup>INEGI, Faculty of Engineering, University of Porto, Portugal

<sup>2</sup>LAETA, INEGI, Department of Applied Mechanics, Polytechnic Institute of Bragança,  
Portugal

<sup>3</sup>LAETA, INEGI, Department of Mechanical Engineering, Faculty of Engineering, University  
of Porto, Portugal

*\*Journal of the Brazilian Society of Mechanical Sciences and Engineering. 2016 May  
38(7):1855-1863*

**DOI:** 10.1007/s40430-016-0560-4



## **Abstract**

Osteotomy or bone cutting is a common procedure in orthopaedic surgery, mainly in the treatment of fractures and reconstructive surgery. However, the excessive heat produced during the bone drilling process is a problem that counters the benefits of this type of surgery, because it can result in thermal osteonecrosis, bone reabsorption and damage the osseointegration of implants. The analysis of different drilling parameters and materials can allow to decrease the temperature during the bone drilling process and contribute to a greater success of this kind of surgical interventions. The main goal of this study was to build a numerical three-dimensional model to simulate the drilling process considering the type of bone, the influence of cooling and the bone density of the different composite materials with similar mechanical properties to the human bone and generally used in experimental biomechanics. The numerical methodology was coupled with an experimental methodology. The use of cooling proved to be essential to decrease the material damage during the drilling process. It was concluded that the materials with less porosity and density present less damage in drilling process. The developed numerical model proved to be a great tool in this kind of analysis.

**Keywords:** Temperature rise, Bone, Drilling, Drill bit, Finite element method.





## 1 Introduction

The drilling process in human bone is a common technique in many clinical procedures, such as surgical reconstruction, bone and implant fixation [1]. The success of bone-cutting surgery is measured according to the bone damage minimization during drilling. There are several studies related with the increase of the temperature during the cutting of the bone tissue. The heat generated is caused by friction between the cutting surface of the drill bit in contact with the hole and bone fragments formed during the drilling [2, 3]. When the temperatures obtained during drilling operation reached the limit supported by bone tissue, necrosis occurs [4, 5].

There are studies in the literature about to the registration of temperatures during bone drilling that indicate thermal necrosis in cortical bone when this one reached a temperature of 47 °C for 1 min [6, 7]. Other authors showed that temperature values above 55 °C for a period longer than 30 s can cause great irreversible lesions in bone tissue [6, 8]. Finally, Eriksoon and Albrektsson [9] concluded that heating up to 47 °C could be considered as the optimal limit that bone can withstand without necrosis. Currently, it is known that the generated heat in these processes is associated to the drilling parameters, such as drill speed, feed-rate, geometry of the drill bit, drill force, hole depth and also the bone density [4]. It is essential to understand and to improve the cutting conditions and all the variables involved in these processes to reduce the generated heat and consequently minimize the bone damage.

Several devices and techniques have been proposed to control the thermal damage and reduce the heat due to drilling process. Temperature measurement during drilling can be conducted using the infrared thermography that allows the measurement of the temperature detectable on the surface of a body [3, 10, 11] or thermocouples which provide a direct measurement [12-14]. While thermocouples detect only a single temperature point, the infrared techniques generate an overall thermal profile. In addition, the kind of bone model varies. Usually, ex vivo studies use bovine or porcine bone models, which exhibit variable structure. Therefore, synthetic foam bone blocks with different densities have been described [3, 15, 16]. These blocks are based on polyurethane and provide a uniform testing model simulating the properties of human bone.

Besides of the uniformity of the models, these materials provide consistent properties and are less susceptible to failures, making them preferable for investigations involving temperature measurements during drilling tests [16, 17]. Möhlhenrich et al. [16] studied how the bone density affects the temperature development in artificial bone and drill. They found that the thermal development depends on bone density and the temperature rise increases with increase of bone density. Gehrke et al. [15] also used synthetic blocks to study the temperature variation under different irrigation conditions. They found that double irrigation technique resulted in a smaller increase in temperature in the cortical bone model.

There have been many efforts by the researchers to develop experimental methodologies capable of predicting the generated heat during bone drilling. However, only few researchers have studied bone drilling numerically and experimentally. It is important the development of numerical models capable of simulating accurately the drilling process, being the numerical modelling of these processes still a challenge.

The main purpose of this study was to develop experimental and numerical methodologies to investigate the effect of bone density, the use of external cooling and assess the temperature distribution inside of the bone blocks. Experimentally, holes were made in composite materials with mechanical properties similar to those of human bone (cortical and cancellous bone). A set of thermocouples and a thermographic camera were used to measure the temperature distribution inside of the composite blocks and drill bit, respectively. Numerically, the present study proposes a three-dimensional computational model to simulate the thermal behaviour of the bone and the cutting tool during the bone drilling through a thermal transient analysis.

## 2 Experimental Methodology

The experimental setup used in this study measures the temperature rise during drilling bone process in four biomechanical test blocks in composite material, supplied by Sawbones [17]. Two test blocks represent the cortical bone (C) with different densities [C+D (0.80 g/cm<sup>3</sup>) or C-D (0.08 g/cm<sup>3</sup>)] and the other two test blocks represent the cancellous bone (T) also with different densities [T+D (0.32 g/cm<sup>3</sup>) or T-D (0.12 g/cm<sup>3</sup>)]. All test blocks have the following dimensions: 130 x 180 x 40mm (Figure 1).

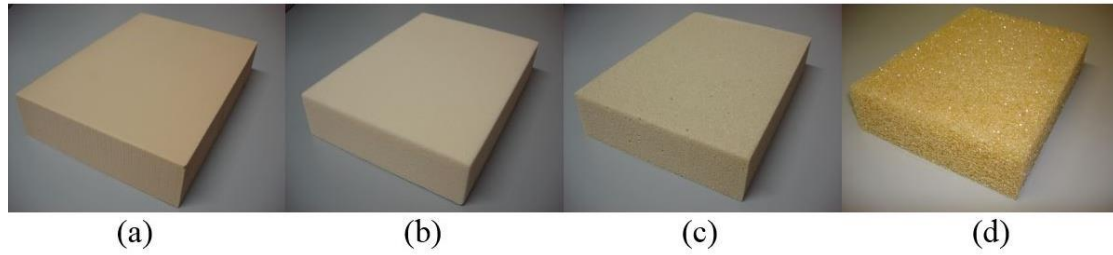


**Figure 1.** Test Blocks from Sawbones: (a) C+D, (b) C-D, (c) T+D, (d) T-D.

The chromel-alumel K-type thermocouples (Omega Engineering Inc., USA) with the temperature range of  $-200\text{ }^{\circ}\text{C}$  to  $1250\text{ }^{\circ}\text{C}$  were used for measuring the temperature inside of block into two opposite sides (A and B) and in adjacent positions to the drill bit. All thermocouples were connected to a data acquisition system (MGCplus). In these experiments, drilling in side holes were performed with diameter of 3.5 mm for the installation of thermocouples. In one side of block, the thermocouples were considered and placed at the same distance from drill bit (Side A), and the other side of block, thermocouples placed at different distances (Side B), (Figure 2).

The thermocouples were tagged for the identification of each channel and respective connection to data acquisition system (Table 1). This system allowed read the temperatures obtained within the block along the time.

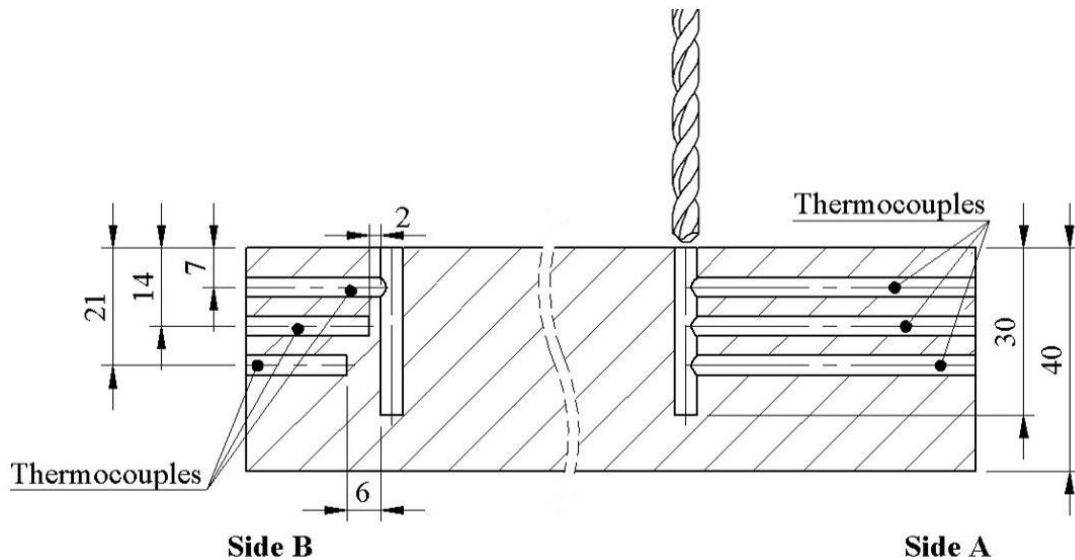


**Figure 2.** Schematic illustration of the thermocouples positions.

**Table 1.** Tagging of thermocouples.

Thermocouple	Designation
A/B-T	Side A or B, thermocouple depth 7 mm
A/B-M	Side A or B, thermocouple depth 14 mm
A/B-R	Side A or B, thermocouple depth 21 mm

The drill bit used in these experiments was made of stainless steel with 4 mm of diameter, point angle equal to  $118^\circ$  and helix angle of  $30^\circ$ . In total, 64 holes were made (16 holes in each biomechanical block). It is important to mention that during the drilling process in some holes at cortical bone (C+D) an external cooling system was used, by means pressurized air. The others biomechanical blocks present greater porosity and no external cooling was used. In these blocks the use of external cooling does not produce differences in temperature recording, since the heat dissipates out of hole more easily. For all the holes, the processing parameters as drill diameter, drill speed, feed-rate, etc., were considered as described in Table 2.

**Table 2.** Drilling processing parameters.

Processing parameters	
Drill diameter	4 mm
Hole depth	30 mm
Drill speed	800 rpm
Feed-rate	50 mm/min
Full time (drilling and cooling)	45 s + 55 s

For each drilling hole three readings within the block were performed, considering the depth of the hole and the distance between the drill and the thermocouple. The distance between the holes and the cooling time of drill bit were also considered, ensuring that the heating of each hole does not interfere with the temperature values of the other holes. Figure 3 shows the geometrical model of blocks used in these experiments and the distance between the holes.

During the bone drilling process, the temperature was measured in the surface of cutting tool with a thermographic camera (ThermaCAM 365, FLIR Systems) which was rigidly fixed to a tripod at a distance of 1.5 m from the drill bit. Temperatures were measured in real time and the thermal image data were transferred to a PC for simultaneous analysis in appropriated software (FLIR QuickReport Software, FLIR Systems).

The measured temperature is function of object surface conditions represented by the emissivity. In this case, the emissivity of stainless steel was considered to measure the temperature surface of the drill bit. All imposed camera parameters are listed in Table 3.

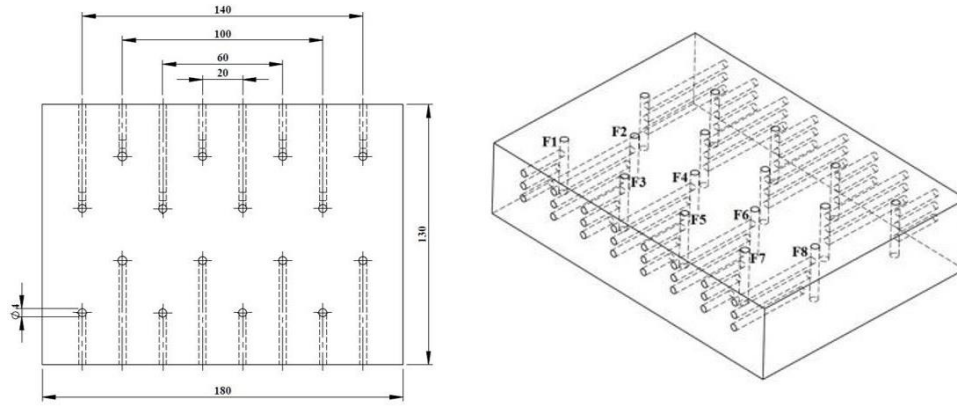


**Figure 3.** Geometrical model of block from Sawbones.

**Table 3.** Parameters used for thermal images acquisition.

Parameters	Value
Distance camera-bone block	1.5 m
Ambient temperature	20 °C
Emissivity $\epsilon_{\text{stainless steel}}$	0.70
Relative humidity	50%

Another important aspect is to protect the measured object from the influence of other near objects, i.e., from background radiation, that can change the thermal image by reflection from measure object surface. To avoid the possible of heat transmission from the surrounding objects, the area of interest was protected with a black cloth. The overview of the experimental setup used in this study is shown in Figure 4.

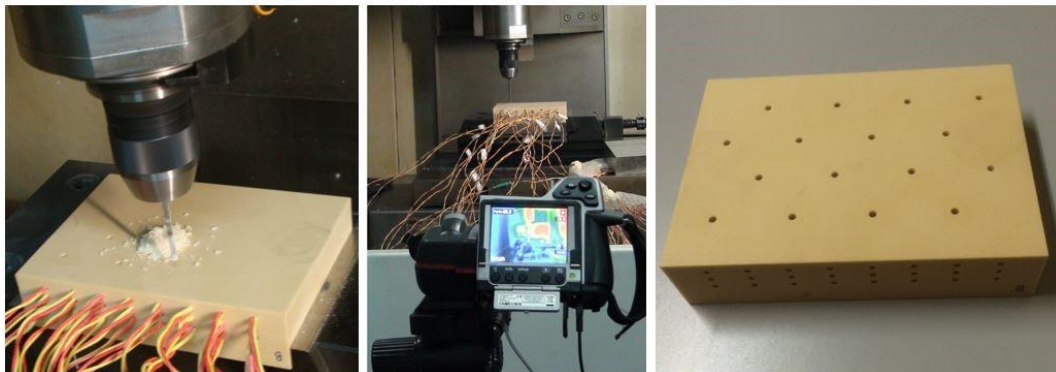


**Figure 4.** Drilling process of biomechanical blocks.

### 3 Numerical Analysis

In this study, a three-dimensional numerical model was used to simulate the heating inside of material during the drilling process. The numerical model represents an half of a biomechanical block of Sawbones with eight holes represented in Figure 3. The simulations were performed using the finite element method with ANSYS Multiphysics software Version 14.5 (ANSYS, Inc., Canonsburg, PA, USA). All material models were treated as isotropic thermal properties. The material properties for cortical bone, cancellous bone and the drill bit were considered in this analysis and are summarized in Table 4 [18-20].

**Table 4.** Thermal properties of the drill bit and bone.

Material	Density (kg/m <sup>3</sup> )	Conductivity (W/K m)	Specific heat (J/kg K)
Drill bit	7850	53.3	440
C+D	800	0.4	1260
C-D	80	0.4	1260
T+D	320	0.005	1570
T-D	120	0.005	1570

Mathematical models of heat conduction problems could be solved numerically. Using the finite elements, the main idea is discretizing the heat transfer equation and then solve an algebraic problem. The general equation for transient heat conduction calculation takes the form [21]:

$$\frac{\partial}{\partial x} \left( \lambda \frac{\partial T}{\partial x} \right) + \frac{\partial}{\partial y} \left( \lambda \frac{\partial T}{\partial y} \right) + \frac{\partial}{\partial z} \left( \lambda \frac{\partial T}{\partial z} \right) + \dot{Q} = \rho C \frac{\partial T}{\partial t} \quad (1a)$$

$$-\lambda \frac{\partial T}{\partial n} = h_{cr} (T - T_{\infty}) + \bar{q} \quad (1b)$$

where  $\lambda$  is the thermal conductivity,  $\dot{Q}$  the heat generated/unit volume,  $\rho$  the material density,  $C$  the specific heat,  $T$  the temperature,  $t$  the time and  $h_{cr}$  the combined radiation/convection heat transfer coefficient.

The temperature field which satisfies this equation satisfy the following boundary conditions: prescribed temperatures  $\bar{T}$ ; specified heat flux  $\bar{q}$ ; heat flux by convection, heat flux by radiation and the environment at the temperature  $T_\infty$ . Using finite elements to discretize the domain  $\Omega$ , a weak formulation weigh functions based on the Galerkin Method is used, giving a system of differential equations in the following form [21]:

$$\sum_{e=1}^{Nel} \left\{ \sum_j^m \left[ \int_{\Omega^e} \lambda \left( \frac{\partial N_i}{\partial x} \frac{\partial N_j}{\partial x} + \frac{\partial N_i}{\partial y} \frac{\partial N_j}{\partial y} + \frac{\partial N_i}{\partial z} \frac{\partial N_j}{\partial z} \right) d\Omega^e + \int_{\Gamma_{h^e}} h_{cr} N_i N_j d\Gamma_h^e \right] T_j + \sum_j^m \left[ \int_{\Omega^e} \rho C N_i N_j d\Omega^e \right] \frac{\partial T_j}{\partial t} = \int_{\Omega^e} N_i \dot{Q} d\Omega^e + \int_{\Gamma_{q^e}} h_{cr} N_i T_\infty d\Gamma_h^e - \int_{\Gamma_q^e} N_i \bar{q} d\Gamma_q^e \right\} \quad (2)$$

Here,  $Nel$  is the total number of the elements in the mesh,  $m$  is the number of nodes per element,  $N_i$  and  $N_j$  represent the shape functions of the problem. Using a finite difference technique to time discretization, the system of ordinary differential Eq. (2) results in the recurrence formulas:

$$C \frac{dT}{dt} + KT = F \quad (3)$$

The finite difference time discretization will lead to the following equation:

$$C \frac{dT}{dt} \approx C \left\{ \frac{T_{n+1} - T_n}{\Delta t} \right\} = (1 - \alpha) C \dot{T}_n + \alpha C \dot{T}_{n+1} \quad (4)$$

Where  $C$  is the global capacitance matrix,  $K$  the global conductance matrix,  $T$  the vector of nodal temperature,  $F$  the vector of thermal loads and  $\alpha$  is a constant parameter used for several time integration schemes. Through Eqs. (3) and (4), the general equation could be written as:

$$\left( \frac{C}{\Delta t} + \alpha K \right) T_{n+1} = \left[ \frac{C}{\Delta t} - (1 - \alpha) K \right] T_n + (1 - \alpha) F_n + \alpha F_{n+1} \quad (5)$$

In order to fully satisfy the conditions from Eq. 5, it is necessary to employ an iterative procedure in each time step.

In this algorithm a modified Newton-Raphson method is adopted. This procedure is also used in ANSYS program to solve the thermal and transient problem.

The numerical model was meshed with a 3D thermal solid element (SOLID 70) with eight nodes and a single degree of freedom, temperature, at each node. The mesh convergence tests were carried out to minimise the computational error. It was found that a meshed solid model comprises a total of 43654 elements is an optimum mesh regarding the accuracy and amount of calculations (Figure 5) [22].

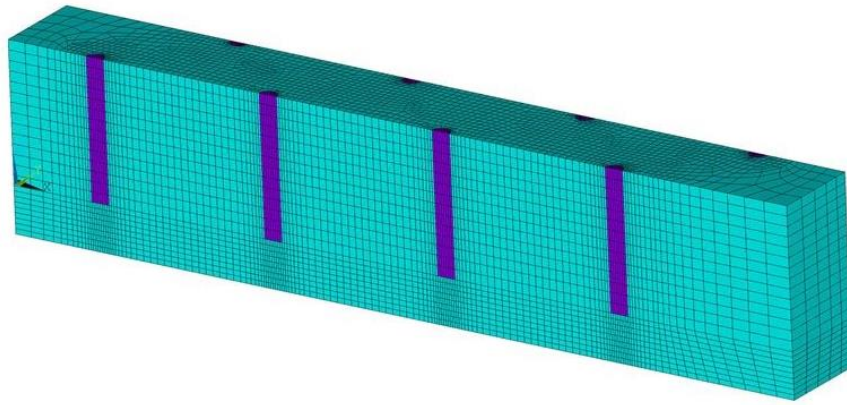


**Figure 5.** Finite element mesh to the numerical model.

The boundary conditions considered in this analysis are the convection in the upper bone surface and a prescribed temperature inside of the hole drill according to the real experimental conditions. The entire model (block and drill bit) is assumed to have the same initial temperature of 19 °C. The progress of the temperature rise in the drill bit was recorded from the thermal camera. An average of the registered temperature values in the different holes, through the drill time was considered in the numerical model. These curves were imposed as prescribed temperature on the surface of the drill bit. Figure 6 shows the evolution of the mean temperature recorded on the drill bit during the drilling process without external cooling system, for each block C+D, C-D, T+D and T-D, respectively.

In the holes made with external cooling system, the temperature was kept constant on the drill with values around 19 °C. For these holes a prescribed constant temperature in the surface of the drill bit was imposed. In all simulations a transient thermal analysis was employed and the thermal variation over time could be acquired by defining the time steps.



According to the times of drilling performed in the experimental process, for numerical model a total time of drilling equal to 800 s was established: 45 s of drilling and 55 s of cooling, for each eight holes.

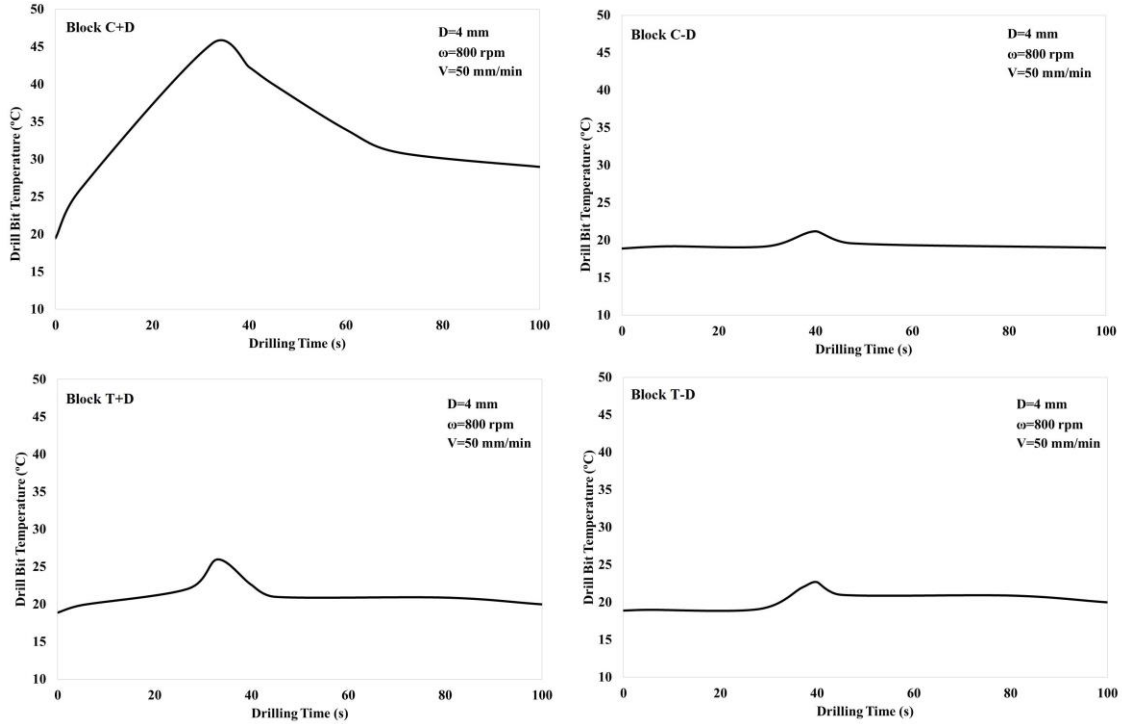


**Figure 6.** The mean value of temperature-time history in the drill bit during the drilling process.

## 4 Results and Discussion

As mentioned previously, there are several variables that can influence the heat generation during the drilling of the bone tissue. Through the biomechanical blocks provided by Sawbones (cortical and cancellous) it was possible to evaluate the temperature distribution considering different material densities and the use of external cooling system during the drilling process. To evaluate the influence of external cooling, only the block C+D was considered. The results for this type of material are graphically displayed. The experimental and numerical results are compared. In the numerical model the temperature values are obtained in different nodal positions in accordance with the positions of thermocouples as described in Figure 2. Figure 7 represents the temperatures obtained over time (drilling and cooling) for two holes in the block, with and without external cooling (the terminology used is the same as described in Table 1: *E* is for experimental and *N* for numerical results).

The results show that the obtained numerical temperatures in C+D have a similar behaviour to the experimental model. Since the heat generated along the drilling process is not easily driven out of the block, it is important to analyse the distribution of the temperature in the holes vicinity. It was confirmed that the temperature increases too quickly in the block region, adjacent to the hole, and decreases with the distance of the drilling hole. This event was expected because this kind of material (as the bone) is a bad heat conductor. Another relevant aspect in the results is the influence of using external cooling systems. In both models we observed that the use of external cooling in the cutting zone decreased aggression to the block, since the temperatures reached in these circumstances do not exceed 25 °C. In the block drilling without external cooling there is an increase of temperature to values between 30 °C and 40 °C. In general, all holes have temperatures between 18 °C and 40 °C, which means that the limit that can cause bone injury in tissues is not exceeded, as referred by Augustin et al. [23, 24].

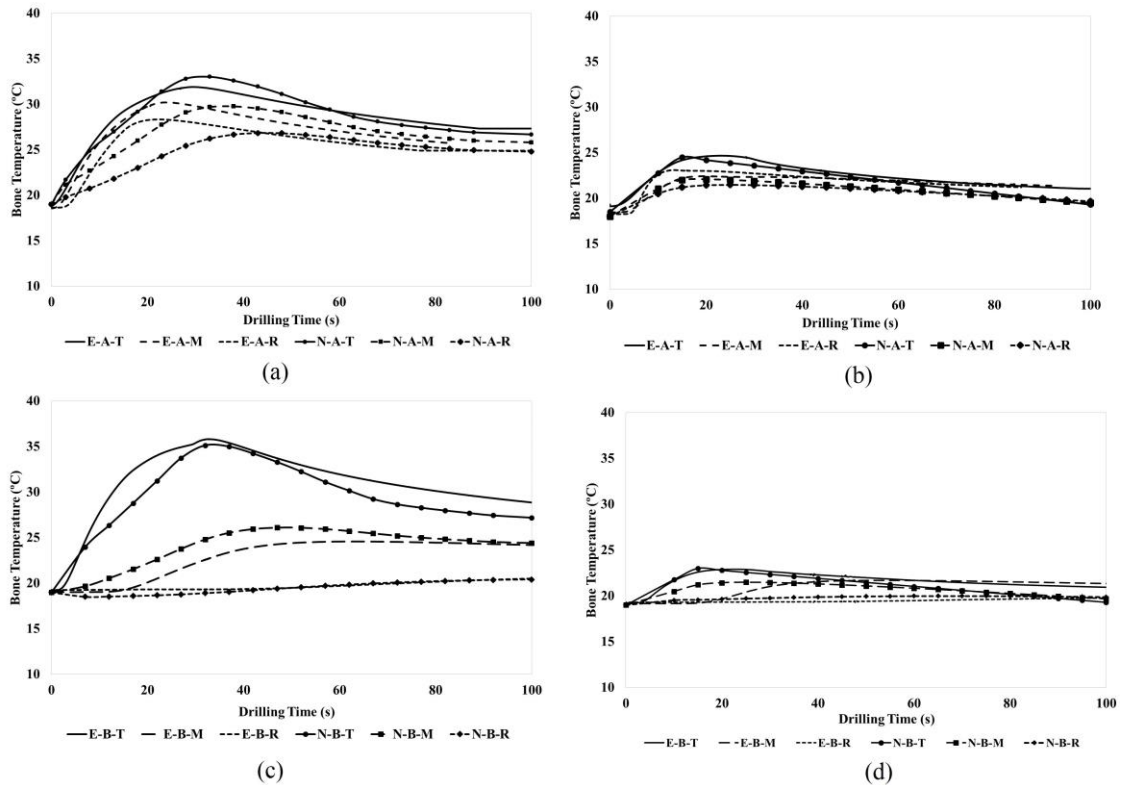


**Figure 7.** Time-temperature history in the block C+D: (a) side A, without external cooling, (b) side A, with external cooling, (c) side B, without external cooling, (d) side B, with external cooling.

Considering the remaining blocks (C-D, T+D, T-D) the type and the quality of bone tissue in processes of drilling bone were analysed. Figure 8 shows the temperature profiles

obtained in C+D, C-D, T+D and T-D respectively, for the same hole, at the time in which the bone tissue attains the more critical values of temperature in this hole.

In Figure 8 was observed that bone density caused great influences in the heating of the bone tissue. There are values of temperature between 30-43 °C in C+D, while that in the C-D does not exceed 22 °C. This event is explained because the cortical bone with less density (C-D) presents a greater porosity when compared with the cortical denser (C+D), allowing a drilling easier when imposed the same drilling parameters. The formation of bone fragments on the cut surface of the drill bit is also significantly smaller, avoiding the obstruction of the hole and in turn the reduction of heat during the drilling operation. Another aspect in the C+D block is a small heating in the holes previously performed. In the C-D model this event is not so obvious, because the heat dissipates easily throughout the model and to the outside of the hole. The temperature peak is also very close to the initial temperature of the block.

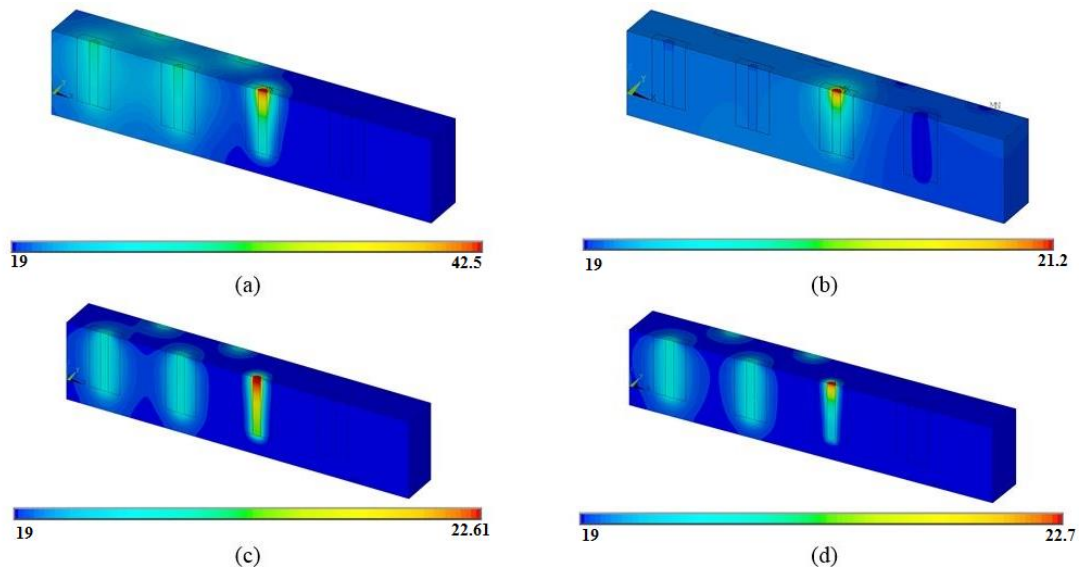


**Figure 8.** Temperature during drilling at 440 s: (a) C+D, (b) C-D, (c) T+D, (d) T-D.

As already been mentioned before, the type of bone tissue influences the temperature of drilling. The cancellous bones have a bone structure much more porous than block C+D and the temperature during drilling bone is different. This is explained by the difference in bone density. The enormous trabeculae of cancellous bone allow an easy drilling process and no many bone fragments are produced during the process.

Comparing the blocks T+D and T-D it is verified that there is no significant difference between the temperature values. Both blocks have temperatures around 19-22 °C.

The holes made in models C-D, T+D and T-D, present temperatures inside the bone almost constants, around 18-25 °C. In the literature, most of the works suggest that the temperature rise depends on bone density. Möhlhenrich et al. [16] also found that temperature increases with increase of bone density. However, they reported that the effect could be reduced with increasing drill diameter.

Table 5 shows the recorded average of the temperatures and the standard deviation for the methodologies mentioned in this study. In numerical model different nodal positions were considered for each hole, always respecting the distances of thermocouples in the experimental model.

**Table 5.** Bone temperature in °C for all blocks in study.

Blocks	Position of thermocouples	Experimental M $\pm$ SD		Numerical M $\pm$ SD	
		Side A	Side B	Side A	Side B
C+D (holes without external cooling)	T ( $n_A=4/n_B=4$ )	27.41 $\pm$ 2.99	30.78 $\pm$ 4.19	29.98 $\pm$ 3.60	29.98 $\pm$ 3.60
	M ( $n_A=4/n_B=4$ )	26.09 $\pm$ 3.39	23.79 $\pm$ 2.02	27.08 $\pm$ 2.71	24.87 $\pm$ 2.14
	R ( $n_A=3/n_B=4$ )	24.40 $\pm$ 3.54	20.10 $\pm$ 0.67	25.22 $\pm$ 2.31	20.69 $\pm$ 0.78
C+D (holes with external cooling)	T ( $n_A=4/n_B=4$ )	22.16 $\pm$ 1.45	22.08 $\pm$ 1.35	21.08 $\pm$ 1.51	21.8 $\pm$ 1.51
	M ( $n_A=4/n_B=4$ )	22.10 $\pm$ 1.51	21.11 $\pm$ 0.97	21.72 $\pm$ 1.42	21.19 $\pm$ 0.85
	R ( $n_A=4/n_B=4$ )	20.98 $\pm$ 1.44	19.47 $\pm$ 0.20	20.05 $\pm$ 1.23	19.83 $\pm$ 0.25
C-D	T ( $n_A=7/n_B=8$ )	19.35 $\pm$ 0.42	18.96 $\pm$ 0.18	19.34 $\pm$ 0.31	19.34 $\pm$ 0.31
	M ( $n_A=8/n_B=8$ )	19.12 $\pm$ 0.34	18.64 $\pm$ 0.10	19.28 $\pm$ 0.20	19.23 $\pm$ 0.16
	R ( $n_A=8/n_B=8$ )	19.07 $\pm$ 0.32	18.55 $\pm$ 0.03	19.23 $\pm$ 0.15	19.11 $\pm$ 0.07
T+D	T ( $n_A=8/n_B=7$ )	22.74 $\pm$ 1.88	22.95 $\pm$ 1.37	20.92 $\pm$ 0.86	20.92 $\pm$ 0.86
	M ( $n_A=8/n_B=8$ )	22.45 $\pm$ 2.09	21.36 $\pm$ 0.88	20.66 $\pm$ 0.71	19.86 $\pm$ 0.46
	R ( $n_A=8/n_B=8$ )	22.26 $\pm$ 1.30	19.83 $\pm$ 0.33	20.48 $\pm$ 0.68	18.94 $\pm$ 0.05
T-D	T ( $n_A=7/n_B=8$ )	20.25 $\pm$ 0.26	21.12 $\pm$ 0.30	20.14 $\pm$ 0.76	20.14 $\pm$ 0.76
	M ( $n_A=6/n_B=6$ )	20.07 $\pm$ 0.35	21.11 $\pm$ 0.54	19.94 $\pm$ 0.67	19.42 $\pm$ 0.39
	R ( $n_A=4/n_B=8$ )	20.06 $\pm$ 0.43	20.47 $\pm$ 0.20	19.80 $\pm$ 0.63	18.92 $\pm$ 0.02

*M* Mean value, *SD* Standard deviation,  $n_A$  number of samples in Side A,  $n_B$  number of samples in Side B

The results presented in Table 5 show agreement between the experimental and numerical methodology. In the different blocks, all thermocouples show a constant distribution of temperatures, with a tendency to decrease when the thermocouple is farthest from the hole. However, the difference of temperature in different thermocouples is minimal, especially in blocks with higher porosity (C-D, T+D and T-D). In blocks in which the porosity is significantly greater when compared with the C+D, is easier heat spread within the bone. In drilled holes carried out in higher porosity blocks, 55 s of cooling are enough to ensure that the generated heat of the previous holes are not transferred to the new ones.

To complement the obtained results, thermal imaging of the drill bit was also used, before and after the holes perforation. Figures 9 and 10 show the influence that density has on the distribution of temperatures in drilling processes.

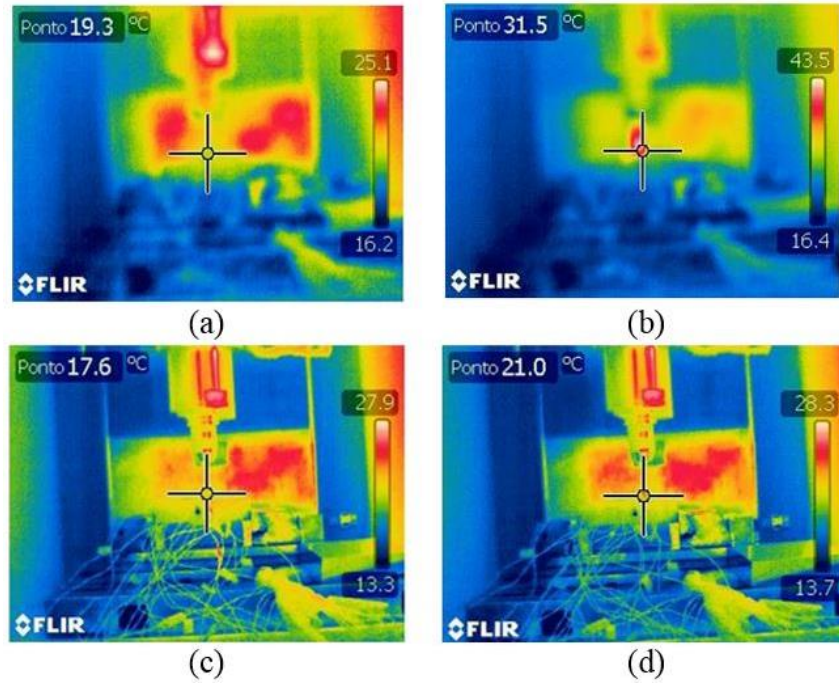


**Figure 9.** Thermal images of the drill bit, C+D: (a) before and (b) after drilling; C-D: (c) before and (d) after drilling.

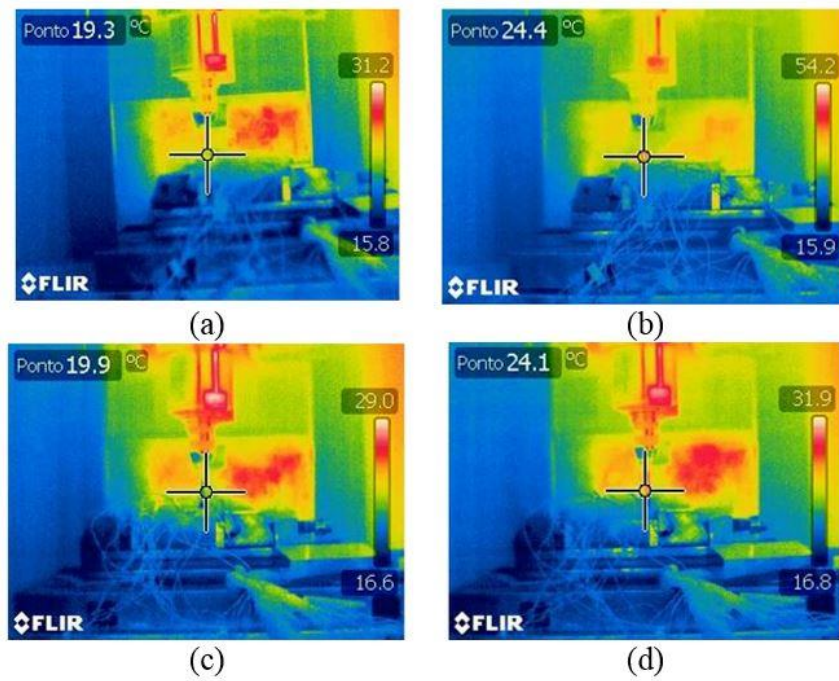


**Figure 10.** Thermal images of the drill bit, T+D: (a) before and (b) after drilling; T-D: (c) before and (d) after drilling.

## 5 Conclusions

In the processes of bone drilling there are variables that interfere directly in temperature values recorded during the bone drill. The control of these variables and the development of new methodologies of analysis is essential to understand how to maintain the integrity of the bone tissue in this type of process. The present study showed a numerical methodology that enabled it to obtain the temperature fields in bone drilling processes, considering the type of bone, the influence of external cooling system and the density. The numerical results are in accordance with the experimental results previously obtained. In block C+D it was found that the drilling operation performed with the cooling monitoring has a lower temperature when compared with the drilling carried out without any external agent. The type of material used in the process, quality and density involved are another appearance that significantly interfere with the recorded temperature. In holes made in blocks C-D, T+D and T-D there were no significant difference in the values of temperature, with very close values and not higher than 23 °C. Already in the block C+D values were observed between 30 °C to 40 °C, being known to decrease in temperature with the distance of the surface around the hole.

The numerical model presented in this study can be applied in various cases of drilling, considering different variables. The results are obtained quickly and allow a precise control of the involved variables.

## Acknowledgments

The author of this paper acknowledges the support of the Project NORTE-01-0145-FEDER-000022-SciTech-Science and Technology for Competitive and Sustainable Industries, cofinanced by Programa Operacional Regional do Norte (NORTE2020), through Fundo Europeu de Desenvolvimento Regional (FEDER).

## References

1. Li S, Wahab AA, Demirci E, Silberschmidt VV (2014) Penetration of cutting tool into cortical bone: Experimental and numerical investigation of anisotropic mechanical behaviour. *J Biomech* 47:1117-1126.

2. Staroveski T, Brezak D, Udiljak T. (2015) Drill wear monitoring in cortical bone drilling. *Med Eng Phys* 37:560-566.
3. Fernandes MG, Fonseca EMM, Natal R. (2015) Three-dimensional dynamic finite element and experimental models for drilling processes. *Proc IMechE Part L: J Materials: Design and Applications*, 0:1-9. DOI: 10.1177/1464420715609363 (In press).
4. Sezek S, Aksakal B, Karaca F (2012) Influence of drill parameters on bone temperature and necrosis: A FEM modelling and in vitro experiments. *Comp Mater Sci* 60:13-18.
5. Lundskog J (1972) Heat and bone tissue. An experimental investigation of the thermal properties of bone and threshold levels from thermal injury. *Scand J Plast Reconstr Surg* 6:5–75.
6. Tu YK, Chen LW, Ciou JS, Hsiao CK, Chen YC (2013) Finite Element Simulations of Bone Temperature Rise During Bone Drilling Based on a Bone Analog. *J Med Biol Eng* 33:269-274.
7. Eriksson AR, Albrektsson T (1983) Temperature threshold levels for heat induced bone tissue injury. A vital-microscopic study in the rabbit. *J Prosthet Dent* 50:101-107.
8. Hillery MT, Shuaib I (1999) Temperature effects in the drilling of human and bovine bone. *J Mater Process Technol* 92-93:302-308.
9. Eriksson AR, Albrektsson T (1984) The effect of heat on bone regeneration: An experimental study in the rabbit using the bone growth chamber. *J Oral Maxillofac Surg* 42:705-711.
10. Scarano A, Piattelli A, Assenza B, Carinci F, Di Donato L, Romani GL, Merla A (2011) Infrared thermographic evaluation of temperature modifications induced during implant site preparation with cylindrical versus conical drills. *Clin Implant Dent Relat Res* 13:319-323.
11. Augustin G, Davila S, Udiljak T, Vedrinar DS, Bagatin D (2009) Determination of spatial distribution of increase in bone temperature during drilling by infrared thermography: preliminary report. *Arch Orthop Trauma Surg* 129:703-709.
12. Chacon GE, Bower DL, Larsen PE, McGlumphy EA, Beck FM (2006) Heat production by 3 implant drill systems after repeated drilling and sterilization. *J Oral Maxillofac Surg* 64:265-269.

13. Misir AF, Sumer M, Yenisey M, Ergioglu E (2009) Effect of surgical drill guide on heat generated from implant drilling. *J Oral Maxillofac Surg* 67:2663-2668.
14. Alam K (2015) Experimental measurements of temperature in drilling cortical bone using thermocouples. *Scientia Iranica B* 22:487-492.
15. Gehrke SA, Bettach R, Taschieri S, Boukhris G, Corbella S, Del Fabbro M (2015) Temperature changes in cortical bone after implant site preparation using a single bur versus multiple drilling steps: an in vitro investigation. *Clin Implant Dent Relat Res* 17:700-707.
16. Möhlhenrich SC, Abouridouane M, Heussen N, Modabber A, Klocke F, Hölzle F (2015) Influence of bone density and implant drill diameter on the resulting axial force and temperature development in implant burs and artificial bone: an in vitro study. *Oral Maxillofac Surg* 20(2):135-142.
17. Sawbones-Worldwide Leaders in Orthopaedic and Medical Models, Available from: [www.sawbones.com](http://www.sawbones.com) Accessed 12 September 2014
18. Fonseca EMM, Magalhães K, Fernandes MGA, Barbosa MP, Sousa G (2014) Numerical Model of Thermal Necrosis due a Dental Drilling Process. In: R Natal, et al (eds) *Biodental Engineering II*, London: Taylor & Francis Group, CRC Press 2013, pp.69-73.
19. Huang C, Lui YC, Chen YC (2010) Temperature rise of alveolar bone during dental implant drilling using the finite element simulation. *Life Sci J* 7:68-72.
20. CEN (2005), Eurocode 3: Design of steel structures part 1-2: general rules - structural fire design.
21. Zienkiewicz OC, Taylor RL (2000) The Finite Element Method: Vol 1, 5th edn. Butterworth-Heinemann publisher, London.
22. Ansys mechanical APDL thermal analysis guide, release 15.0, 2014.
23. Augustin G, Davila S, Mihoci K, Udiljak T, Vedrina DS, Antabak A (2008) Thermal osteonecrosis and bone drilling parameters revisited. *Arch Orthop Trauma Surg* 128:71-77.
24. Augustin G, Davila S, Udiljak T, Staroveski T, Brezak D, Babic S (2012) Temperature changes during cortical bone drilling with a newly designed step drill and an internally cooled drill. *Int Orthop* 36:1449-1456.



## CHAPTER IV

# Three-dimensional dynamic finite element and experimental models for drilling processes\*

**Maria Goreti Fernandes**<sup>1</sup>, Elza Fonseca<sup>2</sup>, Renato Natal Jorge<sup>3</sup>

<sup>1</sup>INEGI, Faculty of Engineering, University of Porto, Portugal

<sup>2</sup>LAETA, INEGI, Department of Applied Mechanics, Polytechnic Institute of Bragança,  
Portugal

<sup>3</sup>LAETA, INEGI, Department of Mechanical Engineering, Faculty of Engineering, University  
of Porto, Portugal

*\*Proceedings of the Institution of Mechanical Engineers, Part L: Journal of Materials:  
Design and Applications. 2015 September 0(0):1-9*

**DOI:** 10.1177/1464420715609363



## **Abstract**

The main goal of this paper is to assess the mechanical damage in solid rigid foam materials with similar mechanical properties to the human bone induced by the cutting parameters. In the present study a three-dimensional (3D) dynamic finite element (FE) model was developed to simulate the drilling process in solid rigid foam materials and it was validated with experimental results. Using an explicit dynamic numerical simulation, it is possible to obtain large structural deformation with high load intensity in short time frame. The developed model is used to study the effects of different high intensity loads distribution in the solid rigid foam materials. Laboratory tests were produced using biomechanical test blocks instrumented with strain gauges in different surface positions during the drilling process. The comparison between the numerical and the experimental results enables the evaluation and improvements of the cutting process. It was concluded when the feed-rate is higher, the stresses and strains in the solid rigid foam material are lower. The developed numerical model proved to be a great tool in this kind of analysis and available to use in forthcoming tests.

**Keywords:** Drilling process, Solid rigid foam materials, Stresses, Damage.



## 1 Introduction

In medicine there are many surgical procedures that involve the penetration of a sharp tool into bone tissue, often entails a wide range of processes covering sawing, drilling and grinding [1-3]. The orthopaedic surgery, neuro-surgery, bone implant and repair operations are a few examples that involve these procedures [4]. The desired outcome of the bone-cutting surgery is dependent on many factors and the accuracy of the holes without mechanical and thermal damage to the bone and also to the surrounding tissue [5, 6]. Bone is considered a tough biological material; however, an excessive force generated by a cutting tool, can lead to formation of micro-cracks and fracture, and even cause permanent damage to the bone tissue that, in turn, can produce postoperative problems [4, 7].

Several studies have been published about specific problems that cause bone damage during the drilling process. One of these problems is the cut effort achieved during the process and it directly related with the drilling parameters [8-10]. Usually, the drilling procedures are performed using the conventional drill bit through hand drills, which means that the feed-rate is manually controlled by the surgeon. Thus, the cutting effort sensed by the surgeon is subjective and depends on the tool feed-rate, the bone quality and the type of the cut tool.

For better performance of the drilling procedures, it is essential to understand the mechanical behaviour of bones that leads to their failures and consequently to improve the cutting conditions. The finite element method (FEM) has been one of the most useful tools for simulate the drilling bone process and evaluate the tissue biomechanics during the drilling [11]. There are studies on literature that describe experimental tests and FE models to study the behaviour of the bone under several drilling conditions [12-14]. However, it is complicated to reach a numerical model to simulate the real drilled bone due to the complexity of the material properties inherent to the cutting material separation. According to the authors Marco et al. [12] the extensive number of variables involved in this procedures complicates the statement of concluding remarks and confirms the interest in to develop predictive tools for bone drilling, poorly developed to date.

To simplify the study, a three-dimensional (3D) dynamic model was built to simulate the drilling process in the solid rigid foam materials with mechanical properties similar to the human bone.

Bone is a heterogeneous material and can be approximated as a fibre-reinforced [14]. With an explicit dynamic simulation it is possible to obtain fast solution, large structural deformation and to apply high intensity loading in a short time frame. This model allows to prediction of bone drilling stresses as a function of drilled conditions, bit geometry and material bone model. The friction contact between the drill bit and the material, with the element removal scheme, are taken into account and allow advanced simulations of tool penetration and material removal. Currently, it is known that the cutting effort and the heat generated during the drilling process occurs due to the friction of the drill to the work piece interface. This operation transforms the applied cutting energy into heat energy that provoke mechanical and thermal damage on the bone tissue [15, 16]. Several studies in the literature have been relating the cutting parameters with the friction contact. Soriano et al. [9] and Krause [17] studied the effect of the feed-rate on the cutting force and they found that increasing the feed-rate decreased the cutting forces and specific cutting energy. This phenomena was attributed to the change in the frictional behaviour between the drill and the bone when the feed-rate increases. The improvement of the cutting parameters is essential to improve the bone drilling processes.

The model is also experimentally evaluated using biomechanical test blocks from Sawbones [18]. Each block was instrumented with strain gauges in different surface positions during the drilling process. The main purpose of this study was to evaluate different cutting parameters, namely three different feed-rates with a constant drill speed and consequently improve the drilling processes. The proposed 3D dynamic FE could be an important tool to the health professional support in cutting bone and an alternative to the experimental work without the use of associated biological materials. Through the experimental and numerical analysis, the present work supplies an important contributions in the modelling of bone cutting with special attention to the mechanical damage during the drilling. The analysis of mechanical damage for different feed-rates with a constant drill speed are an important contribution in further researches. The purpose of this article is to summarize a recent progress of the obtained results on the experimental and numerical models for drilling processes in relation to the others investigations developed by the authors of this work [8, 19, 20].

## 2 3D Dynamic FE Model

Considering the conventional drilling procedure, a 3D numerical model was developed using the ANSYS LS-DYNA. This software combines the LS-DYNA explicit FE program with the powerful pre- and post-processing capabilities of the ANSYS program. The numerical model consists of a set made up of a block and the drill bit, considering all involved process variables. The geometry of the drill bit was built in CAD software SolidWorks® (Dassault Systems S.A., France), similar to the HSS twist drill bit, having the diameter equal to  $\varnothing 4$  mm with a point angle of  $118^\circ$ . The block was modelled with dimensions (10 x 14 x 4) mm and material properties similar to the human bone, as shown in Figure 1.

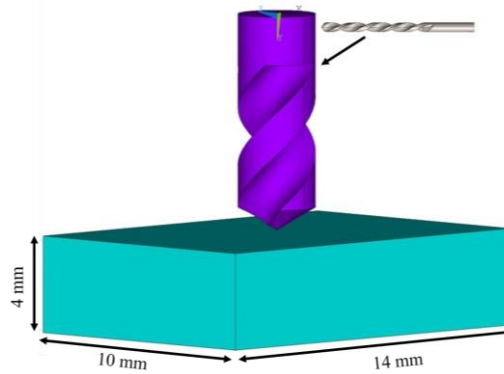


**Figure 1.** Geometric representation of the drill bit and the biomechanical block.

In this simulation, the main region of particular interest is located in the immediate vicinity of the drilled hole. The domain for numerical simulations in this part is specified as a cylinder with 6 mm in diameter and 4 mm in height. In simulations that involve high deformations and nonlinear material behaviour are important to take account the mesh sensitivity. The solid model was meshed using 3D Solid164 elements (eight nodes with three degrees of freedom at each node in X, Y, Z directions), only used for explicit dynamic analyses. Several meshes convergence study were carried out to obtain a more suitable model for this kind of simulation. Initially was constructed a FE model with uniform mesh density in all over model, but this had the disadvantage of increasing the computational time with findings rather vague. However, as the most important drilling part is located in the vicinity of the drilled place, a mesh size discretisation was applied with a size equal to 0.5 mm for the finite elements edge in this area. In the remaining block was used a coarse mesh, as show in Figure 2.

The biomechanical block was meshed with a total number of 16263 elements and the drill bit was modelled with a total number of 4638 elements.

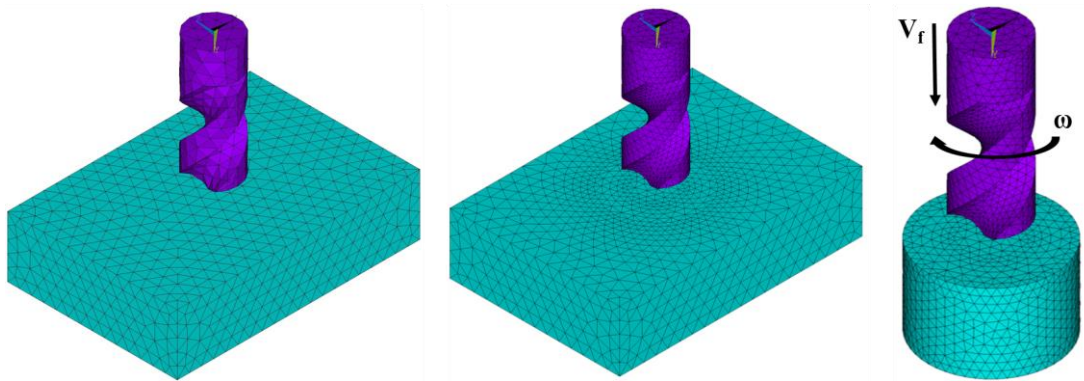


**Figure 2.** FE model of the drill bit, biomechanical block and applied boundary conditions.

In cutting simulations, the applied boundary conditions in the biomechanical block was kept fixed in all vertical faces, while the drill bit was constrained to move only about its own longitudinal axis with a specified drill speed ( $\omega$ ) and feed-rate ( $V_f$ ) downwards into the block, as represented in Figure 2. To explore the effects of feed-rate on the generated stresses, the simulations were performed using three feed-rates (25, 50 and 75 mm/min). The Table 1 presents all drilling parameters used in the FE analysis.

**Table 1.** Drilling parameters used in FE simulation.

Parameters	
Drill bit	Ø 4 mm, point angle 118°
Drill speed ( $\omega$ )	800 rpm
Feed-rate ( $V_f$ )	25, 50, 70 mm/min

## 2.1 Material properties

The material behaviour was performed by multi-linear description of the stress-strain curve observed experimentally in uniaxial tensile tests. The stress–strain tensile tests were recorded with an Instron 4485 universal testing machine using a constant loading speed of 0.25 mm/min [21]. The loading speed is defined as a change of the displacement per time interval and in general the non-metals should be tested at very low loading speeds. The obtained mean values through the tensile test were calculated and summarized in Table 2, for Young’s modulus, initial yield stress, tangent modulus and failure strain. The remaining parameters were taken from the literature [18, 19, 22].



To describe this material, the plastic-kinematic hardening model (Cowper-Symonds), which accounts for non-linear strain hardening and strain-rate sensitivity, was used [23]. This model is an elastic-plastic with strain rate dependency and failure, which includes isotropic and kinematic hardening plasticity [22, 24, 25]. The simulation of chip removal was defined by specifying a plastic failure strain in block component, and initiated by element deletion when the plastic strain of an element reached the limit. The formulation of this model is according the following equation [23, 26]:

$$\sigma_y = \left[ 1 + \left( \frac{\dot{\epsilon}^{1/P}}{C} \right) \right] (\sigma_0 + \beta E_p \epsilon_p^{eff}) \quad (1)$$

where  $\sigma_y$  is the yield stress,  $\sigma_0$  is the initial yield stress,  $\dot{\epsilon}$  is the strain rate,  $\beta$  is the hardening parameter,  $C$  and  $P$  are the Cowper–Symonds strain rate parameters,  $\epsilon_p^{eff}$  is the effective plastic strain, and  $E_p$  is the plastic hardening modulus which is dependent of the  $E$  Young's modulus and the  $E_{tan}$  tangent modulus given by:

$$E_p = \frac{E_{tan}E}{E - E_{tan}} \quad (2)$$

Isotropic and kinematic contributions may be varied adjusting the hardening parameter ( $\beta$ ) between 0 (kinematic hardening only) and 1 (isotropic hardening only) [22, 26]. The Cowper-Symonds model was adopted because it is one of the most typical used in the material formulation of human bones using finite element method and has the ability to represent the mechanical behaviour of materials [24, 27]. The drill bit was modelled as a rigid body in order to reduce the computing time and resources, with high stiffness (200–240 GPa) when compared with the solid rigid block material. The mechanical properties used in this work are summarized in Table 2.

## 2.2 Element removal and contact interactions

The hole generation during the drilling process was simulated by the element deletion that occurs when the plastic strain of an element reached the limit [8]. LS-DYNA provides specific types of contact and several criteria for removing elements during a numerical simulation. A Surface-to-Surface contact analysis was established between drill bit and biomechanical block. This contact is appropriate when a surface of one body penetrates

the surface of another body [26]. The Surface-to-Surface contact allows to choose contact options, such as Eroding contact. This algorithm allows one or both outer surfaces suffer damage to continue the simulation with the remaining internal elements [26]. The frictional contact between the drill bit and the biomechanical block is assumed to be governed by Coulomb's friction law. In accordance with results presented in the literature, the friction coefficient is assumed equal to 0.3 [28]. The numerical simulations require on average 48 h on a PC quad-core Intel I7-4790k with 16 GB RAM.

**Table 2.** Isotropic material properties and Cowper-Symonds parameters used in drilling simulations.

Properties	Block material	Drill bit
Density (kg/m <sup>3</sup> )	800	7850
Young's Modulus (GPa)	0.987	200
Poisson's ratio	0.3	0.3
Initial Yield Stress (MPa)	22.59	
Tangent Modulus (MPa)	0.91	
Hardening Parameter	0.1	
Cowper-Symonds model	C	2.5
	P	7
Failure Strain	0.05	

### 3 Experimental Setup

In the experimental setup were used several linear strain gauges (1-LY18-6/120,  $120\Omega \pm 0.35\%$  from HBM) in three biomechanical blocks, during the drilling procedure.

In total, 18 holes (6 holes in each block) with 30 mm of depth were made with instrumented strain gauges (Figure 3).

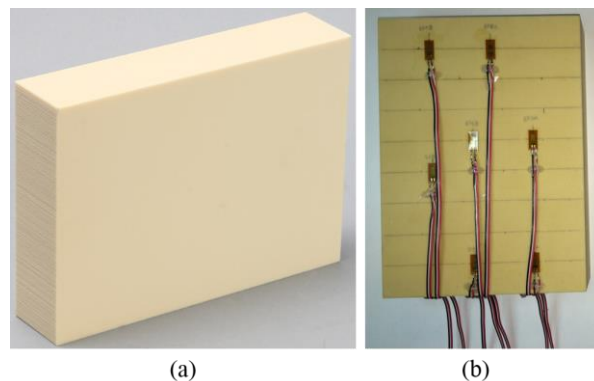


**Figure 3.** (a) Biomechanical test block from Sawbones and (b) instrumented block.

The strain gauges were tagged for each channel identification and respective connection to the data acquisition system (Spider8), shown in Table 3. This system allowed to read the strains and the stresses on of the blocks surface along the time. Figure 4 shows the block geometrical model used in the experiments and the identification of each hole. In order to allow a better comparison between the experimental and the numerical model, the same drilling parameters were chosen as described in Table 1. For each block was considered six holes with one different feed-rate, in order to evaluate the influence on the drilling process (Table 3). All the other parameters were considered as constant.

**Table 3.** Tagging of strain gauges.

Block ID	Designation
Bl <sub>1</sub>	H <sub>1</sub> to H <sub>6</sub> with $V_f = 25$ mm/min
Bl <sub>2</sub>	H <sub>1</sub> to H <sub>6</sub> with $V_f = 50$ mm/min
Bl <sub>3</sub>	H <sub>1</sub> to H <sub>6</sub> with $V_f = 75$ mm/min

$H_i$ : number of the hole;  $Bl_i$ : number of the block.

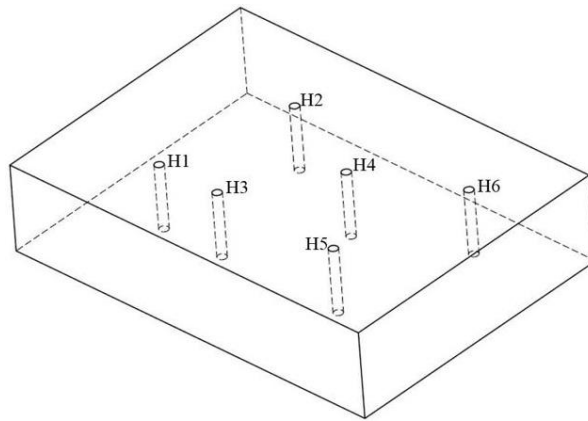


**Figure 4.** Geometrical model of the block and identification of the holes.

The drilling tests were performed in Mechanical Laboratory at Polytechnic Institute of Bragança using a computer numerically controlled (CNC) machine system with total control of the involved parameters. A conventional HSS twist drill bit was used to produce all holes, as described in Table 1. The distances between the edge of the drilled hole and the strain gauge were measured, as represented in Figure 5. The block surface was at room temperature (18 °C) with no interference in the strain measurements. Detailed results of the temperature measurements, in the surface and inside the block, could be obtained in previous publications from numerical and experimental tests [19, 20]. Figure 6 represents the numerical results of the temperatures on the block top surface in the drilled zone and

its immediate vicinity. As shown, the temperatures from a distance of the drill bit represent lower values at the end of the time test.

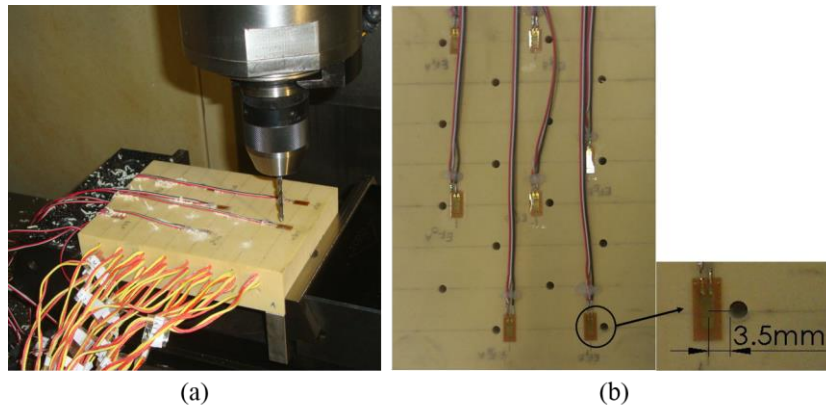


**Figure 5.** (a) Drilling process and (b) distance between the edge of the drilled hole and the stain gauge.

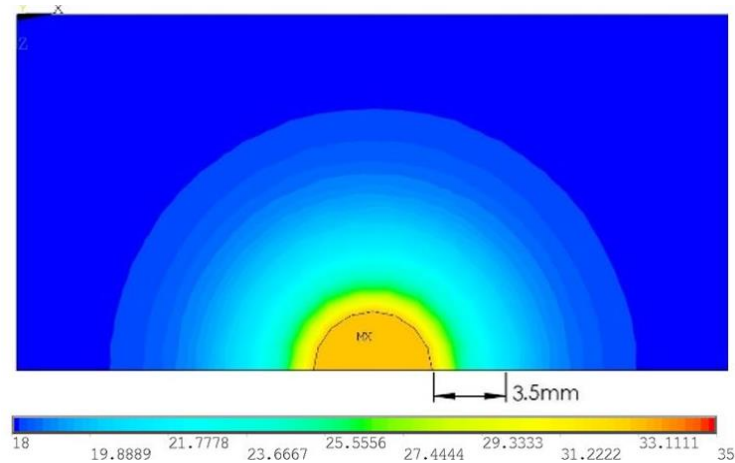


**Figure 6.** Temperature distribution on the block top surface.

## 4 Results and Discussion

The aim of this work was to investigate the levels of stresses induced in the solid rigid foam materials with similar mechanical properties to the human bone, caused during a cutting tool. The strains were obtained during the drilling depth using strain gauges and the generated normal stresses were calculated at the blocks surface.

In the numerical model were performed different simulations with the same feed-rates used in the experimental tests. For each feed-rate were considered different drilling times, considering the complete depth of the block (4 mm). Figures 7, 8 and 9 illustrate the von Mises stress distribution in the biomechanical blocks for different times instant of drilling

(0.5, 2 and 3.5 s). Obviously, for the same time instant the drilling depth is different at different feed-rates. A time equal to 3.5 s corresponds to the complete drill process when a feed-rate equal to 75 mm/min is used, while for the others feed-rates (25 and 50 mm/min) the end time for drill is greater.

The numerical results show that generated stresses in the material tend to increase with tool penetration. This behaviour was verified for all feed-rates. Also, for the same time instant was verified that the stresses increase with the increases of feed-rate. The results are acceptable, for the same time of drilling the depth is greater when higher feed speeds were used. Through the figures it can be seen that the maximum values of the von Mises stress for all feed-rates were verified in the drilled zone and its immediate vicinity.

In the drilled hole was verified that the elements have been removed when the yield stress and the plastic strain failure in the material were reached.

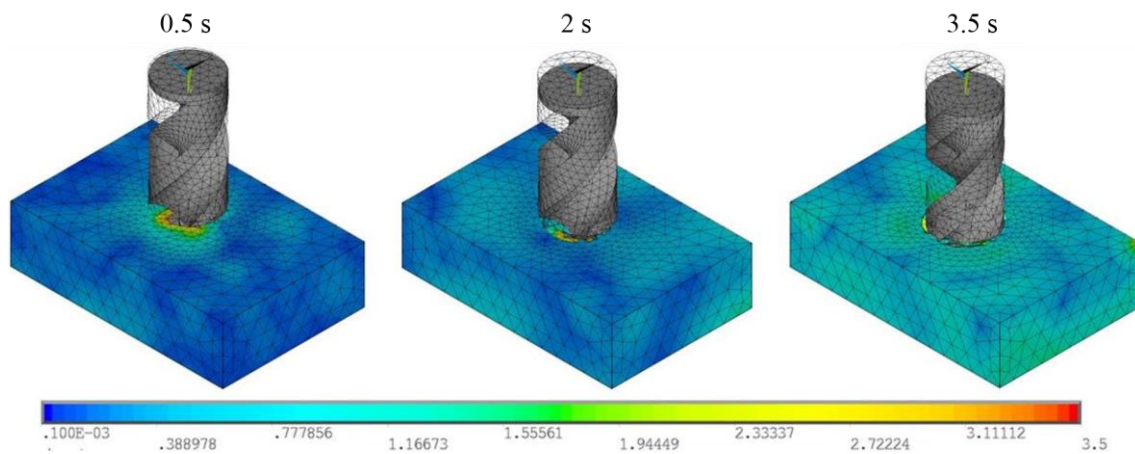


**Figure 7.** Distribution of von Mises stresses (MPa) at different point-in-times ( $V_f = 25$  mm/min).

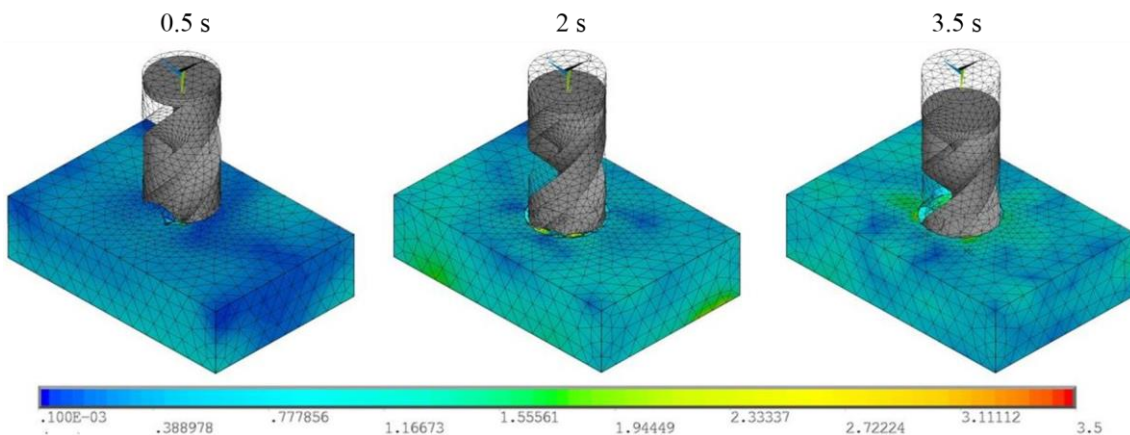


**Figure 8.** Distribution of von Mises stresses (MPa) at different point-in-times ( $V_f = 50$  mm/min).

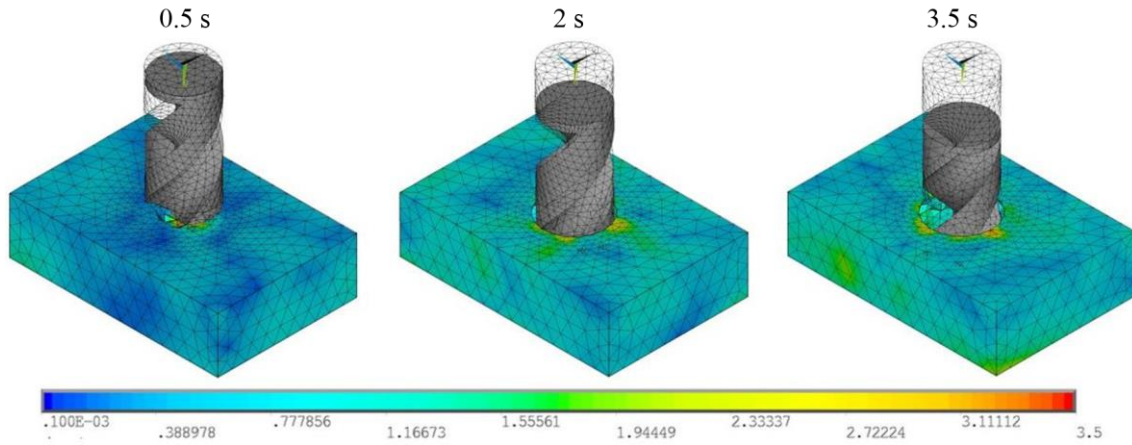


**Figure 9.** Distribution of von Mises stresses (MPa) at different point-in-times ( $V_f = 75$  mm/min).

In order to validate and to compare the numerical with experimental results, different nodal positions were considered and an average of the normal stresses were calculated. Figure 10 shows the mean and the standard deviation of normal stresses located near of each hole obtained experimentally and numerically, at different times instant of drilling. The calculated distance between the edge of the drilled hole and the strain gauge was also considered in both methodologies.

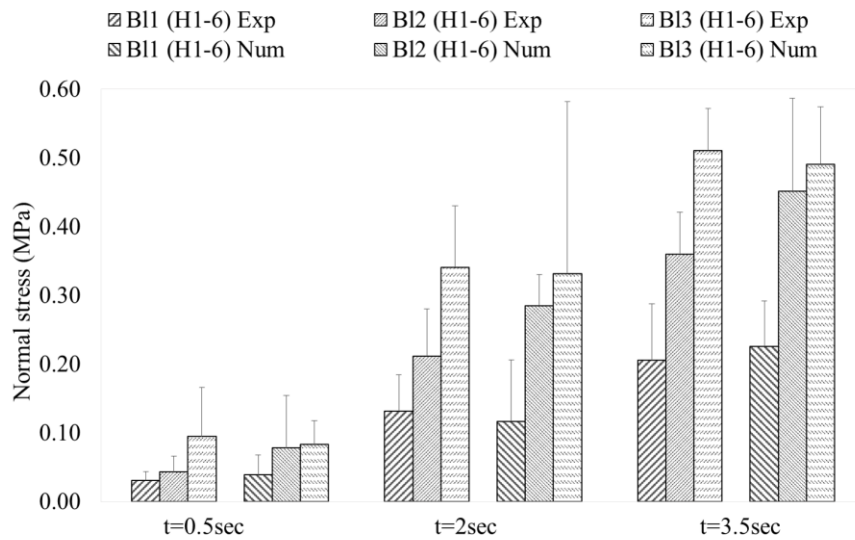


**Figure 10.** Comparison of normal stress (MPa) in numerical and experimental tests at different times of drilling.

According to the results presented in Figure 10 it was found in both methodologies that the stresses in the solid rigid foam materials increase with the increase of the feed-rate, for the same time instant.

Also in the experimental tests with the drill penetration, the level of normal stresses increases, reaching a maximum value when the drill bit penetrated completely in the block due the higher produced effort at the end of the process. The numerical model was validated using the experimental tests, and both methods are in agreement.

As previously indicated, the holes made in experimental tests were performed with a 30 mm of depth. The Figure 11 shows the stresses evolution in three different holes performed with feed-rates equal to 25, 50 and 75 mm/min, during the drilling time.

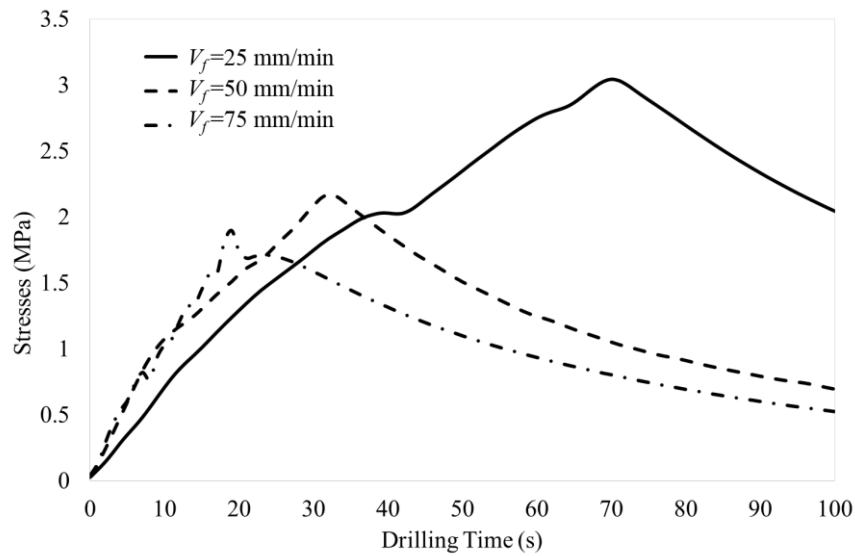


**Figure 11.** Variation of normal stresses for different feed-rates at depth = 30 mm.

As previous, Figure 11 shows that the generated stresses in the solid rigid foam material increase with tool penetration, reaching a maximum value when the drill bit penetrated completely the hole. The greater of the drilled hole depth, produces high stresses values generated in the block. Through of different feed-rates (25, 50 and 75 mm/min), it was found that the increase of feed-rate decreases the maximum generated stresses in the solid rigid foam material, as shown in Figure 11. Although at the start of drilling, the generated normal stresses are higher for higher feed-rates (75 mm/min), in the entire process are found higher stresses for lowest feed-rate (25 mm/min) because the drilling time also increase. The maximum value of the obtained stresses was approximately 3.5 MPa at the end of the drilling depth with a feed-rate equal to 25 mm/min.

## **5 Conclusions**

There are several studies in the literature about the influence of the different parameters in the bone drilling processes, however there is no clear agreement between different authors. In this study a 3D dynamic FE model was developed to simulate the conventional drilling in solid rigid foam material, with similar properties to the human bone. The presented model can simulate the drilling process with several parameters.

In addition, can to promote the damage determination in the material without the use of real biologic tissue. The numerical model allowed to evaluate the stresses distribution in the cutting region and in vicinity areas, obtained for different drilling parameters. In simultaneous, experimental tests were performed to obtain the stresses levels in the surface of the material. Based upon the numerical and experimental results, the following conclusions were obtained:

1. A drill bit with a higher feed-rate can reduce the stresses and strains in solid rigid foam materials during drilling;
2. The stresses increase with the tool penetration and, consequently with increasing of hole depth;
3. The normal stresses in the far hole regions were lower than near of the hole region;
4. The 3D dynamic FE model proved to be a great analysis tool to simulate the stress distribution in the material during the drilling process, useful to evaluate the performance of surgical tools as an alternative;
5. The numerical model could be applied in various cases of drilling, considering different variables and allowing to obtain quickly and accurate results in all involved cutting parameters.

## **Declaration of conflicting interests**

The author(s) declared no potential conflicts of interest with respect to the research, authorship, and/or publication of this article.

## **Funding**

The author of this paper acknowledges the support of the Project "Biomechanics: Contributions to the healthcare" co-financed by the Regional Operational Programme of



North (ON.2 - The New North), the National Strategic Reference Framework (NSRF), through the European Development Fund (ERDF) and also to the project UID/EMS/50022/2013 of LAETA financed by FCT.

## References

1. James TP, Chang G, Micucci S, Sagar A, Smith EL, Cassidy C (2014) Effect of applied force and blade speed on histopathology of bone during resection by sagittal saw. *Med Eng Phys* 36(3):364-370.
2. Fox MJ, Scarvell JM, Smith PN, Kalyanasundaram S, Stachurski ZH (2013) Lateral drill holes decrease strength of the femur: an observational study using finite element and experimental analyses. *J Orthop Surg Res* 8:29.
3. Tai BL, Zhang L, Zhang L, Wang A, Sullivan S, Shih AJ (2013) Neurosurgical bone grinding temperature monitoring. *Procedia CIRP* 5:226–230.
4. Li S, Wahab AA, Demirci E, Silberschmidt VV (2014) Penetration of cutting tool into cortical bone: experimental and numerical investigation of anisotropic mechanical behaviour. *J Biomech* 47(5):1117-1126.
5. Lughmani WA, Marouf KB, Ashcroft I (2015) Drilling in cortical bone: a finite element model and experimental investigations. *J Mech Behav Biomed Mater* 42:32-42.
6. Lughmani WA, Marouf KB, Ashcroft I (2013) Finite element modelling and experimentation of bone drilling forces. *J Phys Conf Ser* 451:012034.
7. Ebacher V, Guy P, Oxland TR, Wang R (2012) Sub-lamellar microcracking and roles of canaliculi in human cortical bone. *Acta Biomater* 8:1093-1100.
8. Fernandes MG, Natal R, Fonseca EMM (2015) Analysis of stresses in drilled composite materials. In: *IEEE 4th Portuguese Meeting on bioengineering (ENBENG)*, Porto, Portugal, pp. 1-4.
9. Soriano J, Garay A, Aristimuño P, Iriarte LM, Eguren JA, Arrazola PJ (2013) Effects of rotational speed, feed rate and tool type on temperatures and cutting forces when drilling bovine cortical bone. *Mach Sci Technol: An Int J* 17:611-636.
10. Fonseca EMM, Magalhães K, Fernandes MGA, Barbosa MP, Sousa G (2014) Numerical Model of Thermal Necrosis due a Dental Drilling Process. In: R Natal, et

- al (Eds) *Biodental Engineering II*, London: Taylor & Francis Group, CRC Press 2013, pp.69-73.
11. Qi L, Wang X, Meng MQ (2014) 3D Finite Element Modelling and Analysis of Dynamic Force in Bone Drilling for Orthopaedic Surgery. *Int J Numer Method Biomed Eng* 30:845-856.
12. Marco M, Rodríguez-Millán M, Santiuste C, Giner E, Henar Miguélez M (2015) A review on recent advances in numerical modelling of bone cutting. *J Mech Behav Biomed Mater* 44:179-201.
13. Alam K, Mitrofanov AV, Silberschmidt VV (2011) Experimental investigations of forces and torque in conventional ultrasonically-assisted drilling of cortical bone. *Med Eng Phys* 33:234-239.
14. Alam K, Mitrofanov AV, Silberschmidt VV (2009) Finite element analysis of forces of plane cutting of cortical bone. *Comp Mater Sci* 46:738-743.
15. Karaca F, Aksakal B, Kom M (2011) Influence of orthopaedic drilling parameters on temperature and histopathology of bovine tibia: An in vitro study. *Med Eng Phys* 33:1221-1227.
16. Karmani S (2006) The Thermal properties of bone and the effects of surgical intervention. *Curr Orthop* 52:20-58.
17. Krause WR (1976) *Mechanical effects of orthogonal bone cutting*. PhD Thesis, Clemson University, USA.
18. Sawbones-Worldwide Leaders in Orthopaedic and Medical Models, *Online Referencing*, [www.sawbones.com](http://www.sawbones.com) (2013, accessed 12 June 2015).
19. Fernandes MG, Vaz M, Natal R, Fonseca EMM (2015) Avaliação Térmica da Furação no Osso Cortical Com e Sem Irrigação. *APAET* 24:71-77.
20. Fernandes MG, Fonseca EMM, Jorge RN, Vaz M, Dias MI (2015) Composite materials and bovine cortical bone drilling: Thermal experimental analysis. In: J.F. Silva Gomes & S.A. Meguid (Eds.), *Proceedings of the 6th international conference on mechanics and materials in design*, Azores, Portugal, pp. 691-692.
21. Berzins A, Shah B, Weinans H, Summer DR (1997) Nondestructive measurements of implant-bone interface shear modulus and effects of implant geometry in pull-out tests. *J Biomed Mater Res* 34(3):337-340.
22. Li Z, Kindig MW, Kerrigan JR, Untaroiu CD, Subit D, Crandall JR, Kent RW (2010) Rib fractures under anterior-posterior dynamic loads: Experimental and finite-element study. *J Biomech* 43(2):228-234.

23. Cowper GR, Symonds PS (1957) *Strain hardening and strain rate effects in the impact loading of cantilever beams*. Applied Mathematics Report; Brown University, USA, p.28.
24. Asgharpour Z, Zioupos P, Graw M, Peldschus S (2014) Development of strain rate dependent material model of human cortical bone for computer-aided reconstruction of injury mechanisms. *Forensic Sci Int* 236:109-116.
25. Li Z, Kindig MW, Subit D, Kent RW (2010) Influence of mesh density, cortical thickness and material properties on human rib fracture prediction. *Med Eng Phys* 32:998-1008.
26. *ANSYS LS-DYNA user's guide, release 12.1*, ANSYS, Inc., Canonsburg, PA, 2009.
27. Hernandez C, Maranon A, Ashcroft IA, Casas-Rodriguez JP (2013) A computational determination of the Cowper-Symonds parameters from a single Taylor test. *Appl Math Model* 37(7):4698-4708.
28. Mellal A, Wiskot HW, Botsis J, Scherrer SS, Belser UC (2004) Stimulating effect of implant loading on surrounding bone. Comparison of three numerical models and validation by in vivo data. *Clin Oral Implants Res* 15(2):239-248.



## CHAPTER V

# Thermo-mechanical stresses distribution on bone drilling: Numerical and experimental procedures\*

**Maria Goreti Fernandes**<sup>1</sup>, Elza Fonseca<sup>2</sup>, Renato Natal Jorge<sup>3</sup>

<sup>1</sup>INEGI, Faculty of Engineering, University of Porto, Portugal

<sup>2</sup>LAETA, INEGI, Department of Applied Mechanics, Polytechnic Institute of Bragança,  
Portugal

<sup>3</sup>LAETA, INEGI, Department of Mechanical Engineering, Faculty of Engineering, University  
of Porto, Portugal

*\*Proceedings of the Institution of Mechanical Engineers, Part L: Journal of Materials:  
Design and Applications. 2017 January 0(0):1-10*

**DOI:** 10.1177/1464420716689337



## **Abstract**

In bone drilling, the temperature and the level of stresses at the bone tissue are function of the drilling parameters. If certain thresholds are exceeded, irreversible damages may occur on the bone tissue. One of the main challenges in the drilling process is to control the associated parameters and even more important, to avoid the surrounding tissue damage. In this study, a dynamic numerical model is developed to determine the thermo-mechanical stresses generated during the bone drilling, using the finite element method. The numerical model incorporates the geometric and dynamic characteristics involved in the drilling processes, as well the developed temperature inside the material. The numerical analysis has been validated by experimental tests using polyurethane foam materials with similar mechanical properties to the human bone. Results suggest that a drill bit with lower drill speed and higher feed-rate can reduce the strains and stresses in bone during the drilling process. The proposed numerical model reflected adequately the experimental results and could be useful in determination of optimal drilling conditions that minimize the bone injuries.

**Keywords:** Bone drilling, FE model, Temperature, Stresses, Feed rate, Drill speed





## 1 Introduction

The drilling process is one of the most frequent mechanical procedures in machining operations. The industrial concepts of productivity and surface integrity in material removal processes can be translated to medical applications. In the surgical context, the reduced drilling time is related to a short surgery in global time and the bone integrity is related to the absence of bone damage [1]. In recent years, several studies on bone drilling have been conducted, mainly focused to determine the effect of drilling parameters on the tissue integrity [2-7]. Currently it is well known that bone drilling process is a typical coupled thermo-mechanical problem. During the drilling, the heat generation occurs as a result of plastic deformation and friction along the cutting tool and the workpiece interface [8, 9]. Depending on the temperature rise magnitude and the exposure time in the drilling zone, heat generated may lead to hyperthermia and bone tissue combustion resulting in cell death (thermal necrosis) [10-12]. Besides of the negative thermal impact, high drill speed with higher cutting forces and tool vibrations can also cause damages on the bone microstructure, resulting in microcracks formation and bone fracture. The mechanical damage to bone cells could delay the healing process after the surgery, reducing the fixation strength and in some cases even the implant failure [9, 13, 14]. Piattelli et al. [15] reported eight cases of failed implants due to suspected thermally induced bone necrosis. Recently, Augustin et al. [2] reported that the implant failure rate for leg osteosynthesis ranges between 2.1% and 7.1% and it is higher than the failure rate upper limbs due to physiological pressure during locomotion.

The growing increase of bone drilling as a medical intervention and the importance of the associated problems have motivated the development of methodologies to find out effects of drilling parameters that minimize the bone injuries. However, there is a still lack of information with regard to the strain and thermal stresses distribution in bone tissue during drilling. Although in several methodologies have been proposed estimated values for bone temperature and cutting forces, none of them include the thermal stresses distributions on the bone. The large number of significant drilling parameters makes the study of bone drilling, through experiments, impracticable. The development of accurate numerical models is necessary in order to reproduce the factors that influencing the output variables (mainly temperature, drilling forces and surface integrity). In the literature, only a few numerical simulations have attempted to model the bone drilling.

Recently, Marcos et al. [1] has made a bibliographic review of the main contributions on the field of numerical modelling of bone cutting, including the bone drilling effect. They found that the numerical models are still far from clinical applications and there is a clear requirement for improvement the models available for drilling simulations. Most of the models presented in the literature were performed with limited parameters and using two-dimensional (2D) simulations, furthermore the analysis was not validated comparatively with experimental tests [6, 13, 16]. Experimentally, several techniques have been developed to measure the strain level in body surfaces during the drilling processes for many industrial applications, but have not widely used for medical situations. Usually, the strain level is measured using strain gauges and a data acquisition system from which the stresses can be calculated.

The present study was designed for the evaluation of thermo-mechanical stresses generated during the bone drilling, as function of different drilling parameters (drill speed, feed-rate, drill diameter and hole depth) and temperature changes during the process. A three-dimensional (3D) dynamic finite element (FE) model with the element removal scheme was developed to simulate the thermo-mechanical behaviour of the contact region between the drill bit and the bone tissue. The simulations were performed using the LS-DYNA program, as a nonlinear transient dynamic finite element. This program incorporates the dynamic characteristics involved in the process with the accurate geometrical considerations, as well the developed temperature inside the material. Physical problems involving severe loading conditions applied in a short time are best simulated with explicit dynamics solutions, like problems with nonlinearities, changing contact, failure or material separation. In addition, an experimental methodology was developed using solid rigid polyurethane foam materials (Sawbones, Pacific Research Laboratories, Inc., Vashon. WA, USA) as an alternative for human bone. The solid polyurethane foam of  $0.80 \text{ g/cm}^3$  density was selected for the cortical bone, which was approved by the American Society for Testing and Materials for a standard material for testing orthopaedic devices and instruments. The foams were instrumented with strain gauges to measure the level of strains on the surface during the drilling. Simultaneous, the temperature distribution on the foams surface and in the drill bit were measured with the thermography equipment. Inside of the foams material, at different positions from the drilling area, thermocouples were used to measure the temperature. The results of numerical simulations are discussed and compared with experimental results. The used methodologies in this study are an important contribution in the bone drilling modelling.

The incorporation of temperature data, as function of different drill speeds and feed-rates, and implemented as a prescribed temperature on the FE model provide not only the mechanical behaviour of the bone, but also the thermal-mechanical behaviour, with different feed-rates and drill speeds.

## **2 Thermo-mechanical Model of Drilling**

In this paper, a 3D FE model was developed using the explicit dynamic finite element code, LS-DYNA (LSTC, Livermore, CA, United State). The model aims to simulate the drilling process and to calculate the thermo-mechanical stress distribution in the bone material. The FE model consists of a set made up of a twist drill bit ( $\varnothing 4$  mm, point angle of  $118^\circ$  and a helix angle of  $30^\circ$ ) and a bone block with appropriate boundary conditions. The drill bit geometry was designed through the CAD software SolidWorks® (Dassault Systems S.A., France) and imported into LS-DYNA program for numerical simulation. The bone block was modelled with a rectangular shape with the following dimensions: 14 x 10 x 4 mm. For mesh generation, dual mesh density technology was used in order to improve the calculation accuracy and to reduce the processing time. The element size is critical for the computational cost of the simulation, solved with an explicit integration scheme. The selection of the element size should be stated ensuring equilibrium between computational efficiency and precision of the model [17]. Since the main part in this type of analysis is the bone region located in the immediate vicinity of the drilled hole, a circular disc with 6 mm of diameter was formed in this part and a mesh discretisation was applied with an element size of 0.5 mm to capture high stress gradients during the drilling process. In the remaining block was used a coarse mesh with an element size of 1 mm. To define those two densities, separate simulations were run to obtain better convergence and smooth contours, varying mesh densities were tried to find the optimal values that ensure the time of calculate and the stability of results. Previous mesh sensibility studies showed that the use of dual mesh density is a common practice in this kind of simulation to achieve both accuracy and time efficiency of the calculation [12, 18]. The element type chosen for the numerical model was the 3D Solid 164 (8 nodes with three degrees of freedom at each node in X, Y, Z directions), only used for explicit dynamic analysis. The final numerical model of the block and the drill bit were meshed with 20477 elements.

In the explicit analysis is important to define nodal groups called components to apply the loads. The whole FE model of the bone drilling along with the names of all its components are displayed in Figure 1(a).

Following the dynamics characteristics involved in these processes, the block was fixed on the bottom, while the drill bit movement was explicitly simulated via a dynamic FE approach to rotate and move only about its own longitudinal axis (Y axis) with a specific drill speed ( $\omega$ ) and feed-rate (V) vertically downwards into the bone block, as shown in Figure 1(b). To explore the effects of feed-rate and drill speed on the generated thermal stresses, the numerical simulations were performed using three different drill speeds (600, 800 and 1200 rpm) with a constant feed-rate of 50 mm/min, and three different feed-rates (25, 50 and 75 mm/min) with a constant drill speed of 800 rpm.

Thermal stress analysis is driven by strains generated in the structure by a temperature load. Through the temperature data obtained with experimental tests, the time temperature history was applied to the bone block component as a prescribed temperature load, producing the heating source effect inside of the block. The initial temperature of the bone block component was defined as 19 °C.

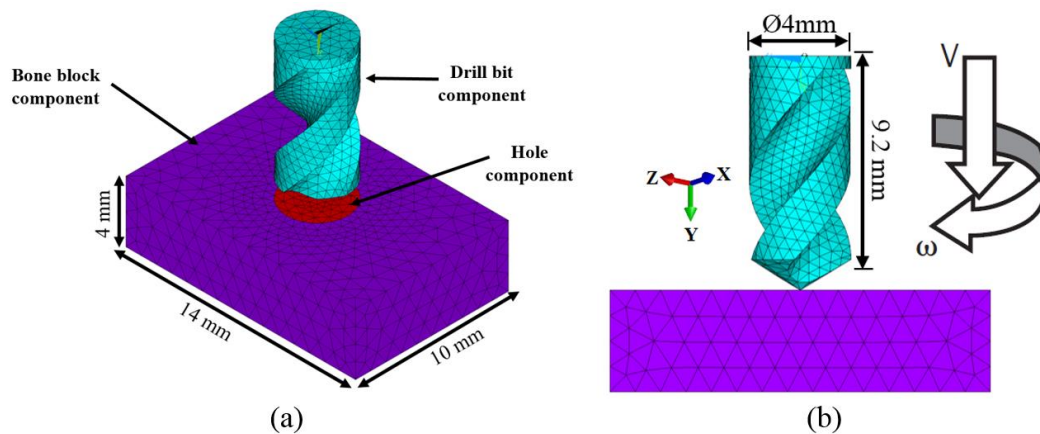


**Figure 1.** (a) FE model of drilling and (b) boundary conditions.

## 2.1 Material properties

It is well known that the FE simulation results are very sensitive to the material properties, and thus it is important to choose the most suitable material models in accordance with the analysis type. Materials subject to drilling are highly affected by large and high strain rates, which finally leads to failure. To define the bone block submitted to high impact deformation and the thermal expansion due to the temperature load, different material

models were implemented considering different components of the model. The material model for the bone block component was \*MAT\_ELASTIC\_PLASTIC\_THERMAL, which is the \*MAT type 4 in LS-DYNA material library. This model allows the definition of temperature dependent material coefficients in a thermo-elastic-plastic behaviour and take into account the thermal coefficient of expansion. The coefficient of thermal expansion allows the calculation of thermal strain and stress using the prescribed temperature data.

In the selection of material model for the hole component, it should be taken in consideration just the material models which consider the strain-rate with dependency of the materials plastic curve. According to the authors Skrlec and Klemenc [19], the three most common applied material models that consider the strain-rate effects are: Cowper-Symonds, Johnson-Cook and Zerilli-Armstrong. Since the Cowper-Symonds material model is simpler than the two others, considers the material failure and has been often applied in bone material models, we considered only this model in our research [20-22]. In the FE model, the Cowper-Symonds law is implemented through the \*MAT\_PLASTIC\_KINEMATIC (\*MAT type 3) in LS-DYNA material library. Yield stress according to the Cowper-Symonds material model is defined with equation (1) [23, 24]:

$$\sigma_y = \left[ 1 + \left( \frac{\dot{\varepsilon}}{C} \right)^{\frac{1}{P}} \right] (\sigma_0 + \beta E_p \varepsilon_p^{eff}) \quad (1)$$

where  $\sigma_0$  is the reference yield stress in MPa,  $\dot{\varepsilon}$  the strain rate in  $s^{-1}$ ,  $\beta$  is the hardening parameter (between 0 for kinematic hardening and 1 for isotropic hardening),  $C$  and  $P$  are the Cowper-Symonds strain rate parameters,  $\varepsilon_p^{eff}$  the effective plastic strain and  $E_p$  the plastic hardening modulus which is dependent of the Young's modulus and the  $E_{tan}$  tangent modulus given by:

$$E_p = \frac{E_{tan} E}{E - E_{tan}} \quad (2)$$

The mechanical properties of the bone block component and hole component were obtained from the uniaxial tensile tests and have been comprehensively defined in our

previous studies [25]. The remaining material properties were taken from literature [26-28]. The material parameters that consider the strain rate effects are not simply measured and determined, some of them are empirically determined through special experimental and optimisation process [19]. The drill bit was assumed to be a rigid body, since its stiffness is much higher than the bone. This is a practice way to reduce computational cost and resources involved in the drilling simulation. All the material properties used in the numerical analysis are listed in Table 1.

**Table 1.** Material properties and Cowper-Symonds parameters used in numerical simulations.

Properties	Block	Drill bit
Density (kg/m <sup>3</sup> )	800	7850
Young's Modulus (GPa)	0.987	200
Poisson's ratio	0.3	0.3
Thermal expansion coefficient (1/°C)	2.75e-5	
Initial Yield Stress (MPa)	22.59	
Tangent Modulus (MPa)	0.91	
Hardening Parameter	0.1	
Cowper-Symonds model	C	2.5
	P	7
Failure Strain	0.05	

In equation (2), the strain rate influences only the yield stress, which means that the plastic curves (the flow stress as a function of strain) are parallel [19]. The larger the strain rate, the higher the flow stress, as represented in Figure 2, according to the experimental data published in the literature for other materials [19].

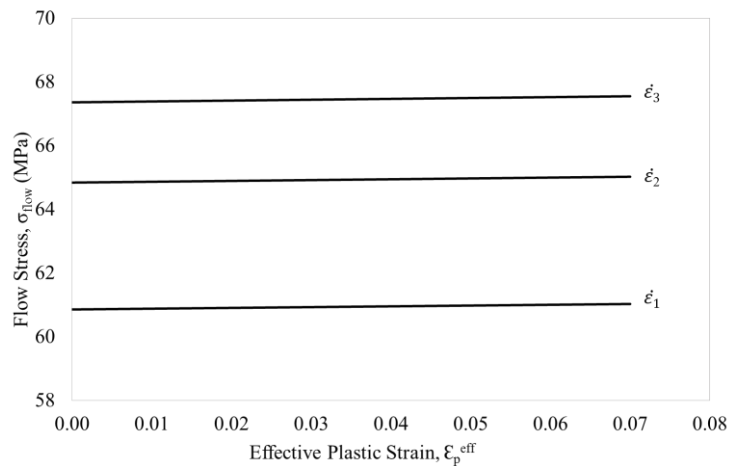


**Figure 2.** Flow stress for the Cowper-Symonds model.

## 2.2 Contact interaction and failure criteria

The contact algorithm was \*CONTACT\_ERODING\_SURFACE\_TO\_SURFACE, which is accessible in the LS-DYNA program [24]. This type of contact is used when a body surface penetrates the surface of another body. Eroding contact methods are suggested when solid elements involved in the contact definition are subject to erosion (element deletion) due to material failure criteria. The surface of the drill bit was classified as the contact surface. The target surfaces include all the block surfaces that will be contacted with drill bit. The friction behaviour between the drill bit and the block is assumed to be governed by Coulomb's friction law. In this case, for the frictional contact between the drill bit and the block a constant coefficient of friction of 0.3 was used [29, 30].

A failure criteria was applied to simulate the element removal and hole generation. As it was mentioned above, the approach of element erosion can be used to simulate the perforation when any element exceeds a specified plastic strain. These elements are deleted from the solution after they fail. Based on the bone properties, the failure strain reaching 0.05 is adopted as the criterion in the erosion algorithm implementation for the numerical simulation. Dynamic analysis was used with the simulation range subdivided into 15.000 time increments of  $8.0 \times 10^{-4}$  s. ANSYS/LS-DYNA requires very small time steps with many iterations to ensure stability of solution. Each simulation took about 68h to execute on a workstation with a quad-core Intel I7-4790k with 16 GB RAM.

## 3 Experimental Validation

An experimental methodology was executed to validate the numerical thermo-mechanical model of drilling. Solid rigid polyurethane foams were used as an alternative material to cortical bones, due its consistent and homogeneous structural properties [31, 32]. The samples were supplied in rectangular shape with the dimension of 130 x 180 x 40 mm and the material has a closed cell with density of  $0.80 \text{ g/cm}^3$  (Figure 3 (a)).

In order to validate the numerical model, the drilling tests were divided in two groups. For the first group, the holes were performed at drill speeds of 600, 800 and 1200 rpm with a constant feed-rate equal to 50 mm/min. In the second group, three different feed-rates (25, 50 and 75 mm/min) were applied throughout the drilling procedures, with a constant drill speed of 800 rpm.

Drillings were performed in the Mechanical Laboratory at Polytechnic Institute of Bragança. In total, 30 holes with 30 mm of depth were made at room temperature (without cooling) using a twist drill bit of 4 mm diameter, point angle equal to  $118^\circ$  and helix angle of  $30^\circ$ . A control of the drilling parameters was provided by a computer numerically controlled (CNC) system. All drills were used no more than fifteen times before being replaced with a new one. For each combination of parameters, the average of six drillings were used to present the results.

### 3.1 Strain measurement

Fifteen flexible linear strain gauges (1-LY18-6/120,  $120\ \Omega \pm 0.35\%$  from HBM) were attached on the blocks surface to measure the strain during the drilling process (Figure 3 (b)). The blocks were properly clean to create a uniform surface and the locations of the holes were marked to always keep the same distance of 3.5 mm, between the edge of the hole and the strain gauge. All strain gauges were identified for each channel and attached with bonding adhesive following the instructions of the manufacturer. Each lead wire was connected to the quarter bridge in a data acquisition system (Vishay Micro Measurements P3 Strain Indicator and Recorder).

Strain measurements were taken continuously during each step of the drilling procedure at once per second. The corresponding profiles of stresses versus drilling depth from the block surface were calculated.

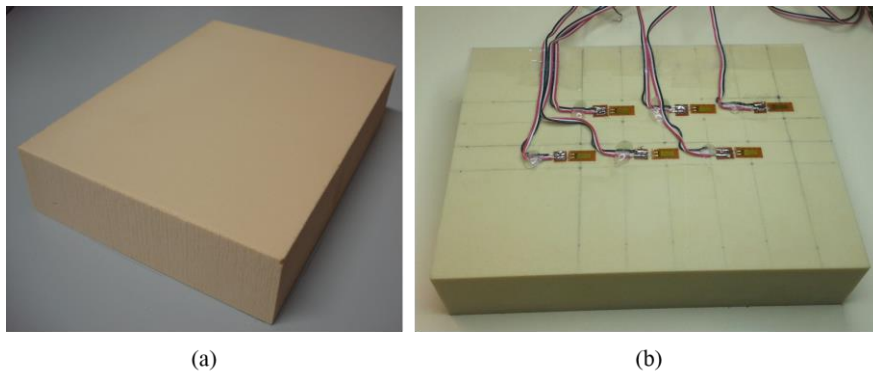


**Figure 3.** (a) Solid rigid polyurethane foam and (b) installation of the linear strain gauges.

### 3.2 Temperature control

Temperature measurement was carried out using two methods. In the first method, thermography (ThermaCAM 365, FLIR Systems) was used with the lens located at



distance of 1.5 m from the drilling area. This method allowed to obtain thermal images of the blocks and the drill bit surfaces, before and immediately after the drilling. The measured temperature is function of the surface conditions, represented by their emissivity. The imposed parameters to the camera during image acquisition are listed in Table 2.

**Table 2.** Parameters used for thermal images acquisition.

Parameters	
Distance camera-block surface	1.5 m
Room temperature	19 °C
Relative humidity	50%
Emissivity	$\epsilon_{\text{stainless steel}} = 0.70$
	$\epsilon_{\text{skin human}} = 0.98$

In the second method, a set of chromel-alumel K-type thermocouples (Omega Engineering Inc., Stamford, USA) installed close to the hole surface were used for measuring the temperature inside of the block.

The thermocouples with wire diameter of 3.5 mm were installed in two opposite sides of the block and at the same distance from the hole for all tests, as shown in Figure 4. After the thermocouples have been placed, the entrance of each hole was appropriately sealed with glue to fix the thermocouples and isolate them from external heat. All thermocouples were connected to a data acquisition system (HBM MGCplus) for the acquisition of temperature along the drilling time.

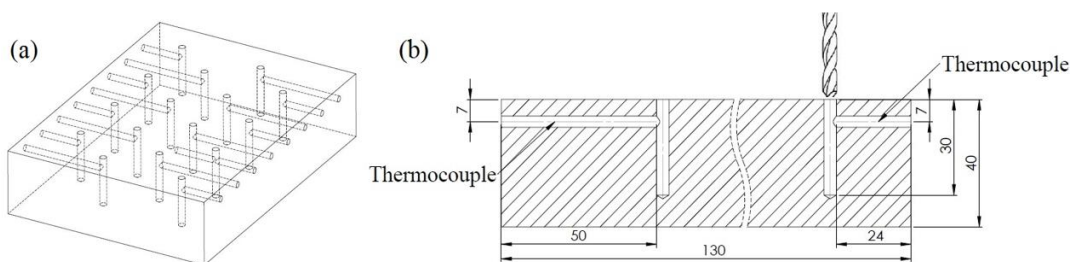


**Figure 4.** (a) Geometrical model and (b) thermocouples position.

The temperature rise inside of material during drilling was used as prescribed temperature in the FE model. An average of the registered temperature values in different holes through the drill time was considered. These curves were imposed as prescribed temperature on the bone block component. Figure 5 shows the evolution of the mean

temperatures recorded inside of the material considering the different drill parameters. As the numerical model was modelled with only 4 mm in height, the temperature data was collected only for the correspondent drilling times. For each feed-rate were considered different drilling times, ensuring the full block drilling.

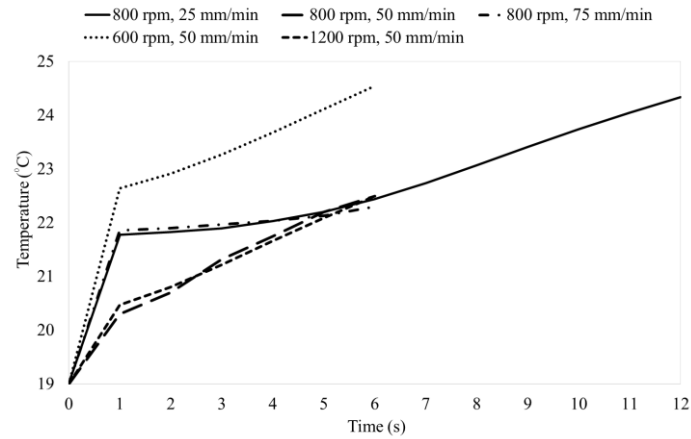


**Figure 5.** Temperature data applied in the Fe model.

Each block was prepared to accommodate eight holes with a distance between them of 20 mm. The complete experimental setup is shown in Figure 6. In this setup the position of the drill is fixed and a CNC machine was used to perform the holes. All experiments started from room temperature (approximately 19 °C) and the drilling direction was perpendicular to the block axis. Between successive experiments, sufficient time was allowed for the block and the drill bit to return to initial conditions.

Previous publications from numerical and experimental tests showed that temperature measurements, on the block top surface at 3.5 mm from the drilled zone, represent small values with no interference in the strain measurements [7, 25].

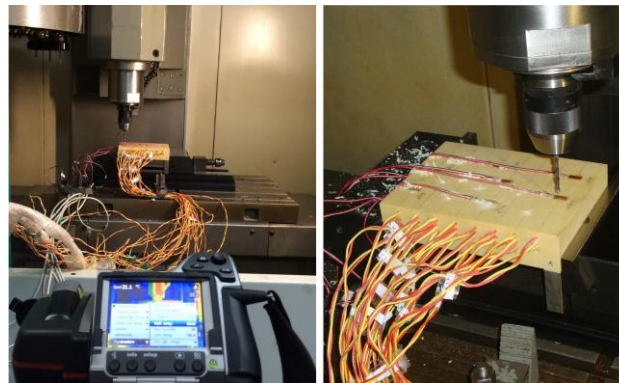


**Figure 6.** Experimental drilling process.

## 4 Results and Discussion

### 4.1 FE results

The ability to measure the thermo-mechanical stress is crucial to predict the behaviour of bone tissue during drilling and also to aiding in developing predictive capabilities by verifying models. The overall objective of this study was to analyse the thermo-mechanical stress as a function of the different drill parameters.

The results obtained by using the FE model are given under this section. Drilling depth of 3 mm was chosen to show the von-Mises stress distribution at different feed-rates and drill speeds in the numerical simulations. In order to evaluate each drill parameter individually, the drill speed was fixed at the value of 800 rpm to measure the effect of feed-rate and fixed at the value of 50 mm/min to measure the effect of drill speed.

Figure 7 presents the contours of von-Mises stress distribution in the bone drilling for each drill situation.

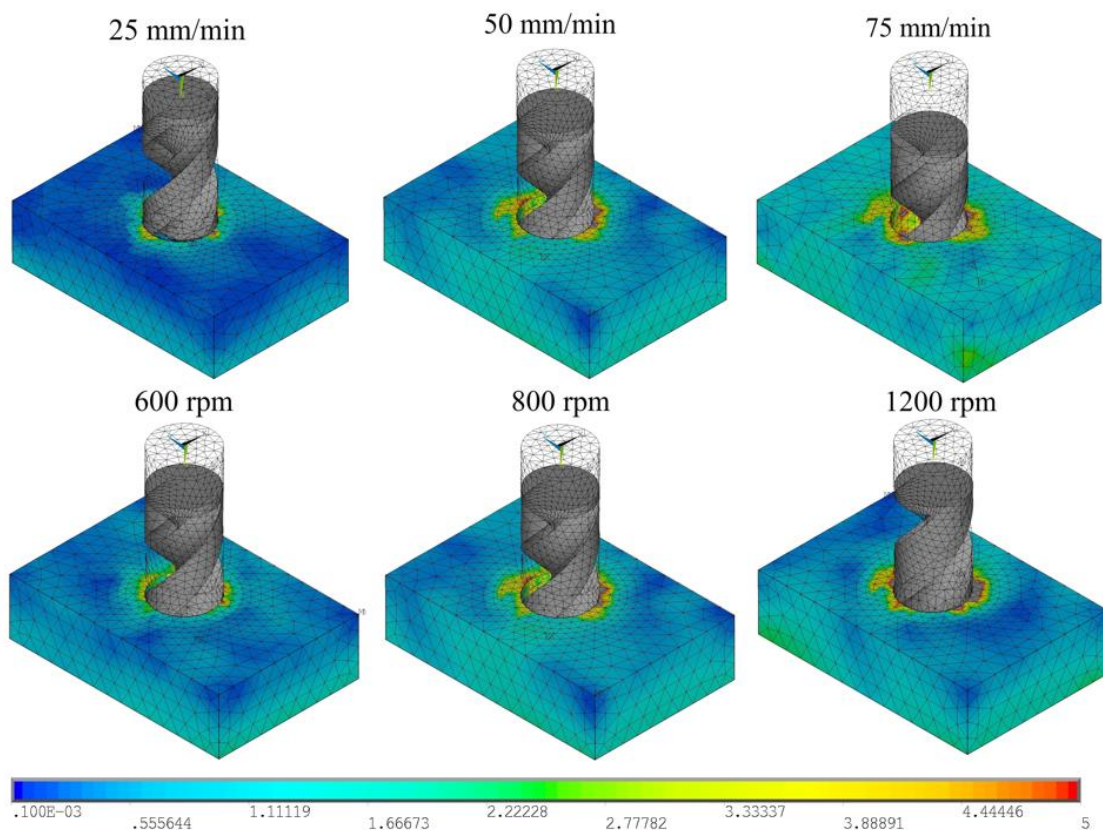


**Figure 7.** Distribution of von Mises stress (MPa) at different feed-rates and drill speeds (3 mm of depth).

For the same time instant was observed through the numerical results that the von Mises stresses increase with increases of feed-rate and drill speed. However, this trend becomes

more evident with regard to the feed-rate parameter. This may be explained in part by the differences between drilling depths at different feed-rates. For the same time instant, the holes made with a feed-rate equal to 75 mm/min reach a higher depth than feed-rates equal to 25 and 50 mm/min.

It is also important to point out that the maximum values of von-Mises stresses, for all numerical simulations were verified in the drilled zone and its immediate vicinity, exceeding the 5 MPa. During the numerical simulation, the elements in the drilled hole were removed when the plastic strain failure in the material was reached.

## 4.2 Experimental results and FE model validation

Experimental validation of numerical model was performed by comparing the results obtained in both models. The average of stress component ( $\sigma_{zz}$ ), which represents the normal stress on face perpendicular to the z axis, was calculated experimentally and compared with the numerical results at different drilling times. The distance between the edge of the drilled hole and the linear strain gauge, as well as the direction of the gauge were considered on the selection of the nodal points in the FE model. Figure 8(a) and (b) show the mean and standard deviation of normal stresses in one direction ( $\sigma_{zz}$ ) obtained in both methods at different drilling times. As well as to the numerical simulations, the drill speed was fixed at 800 rpm to measure the effect of feed-rate and fixed at 50 mm/min to measure the effect of drill speed.

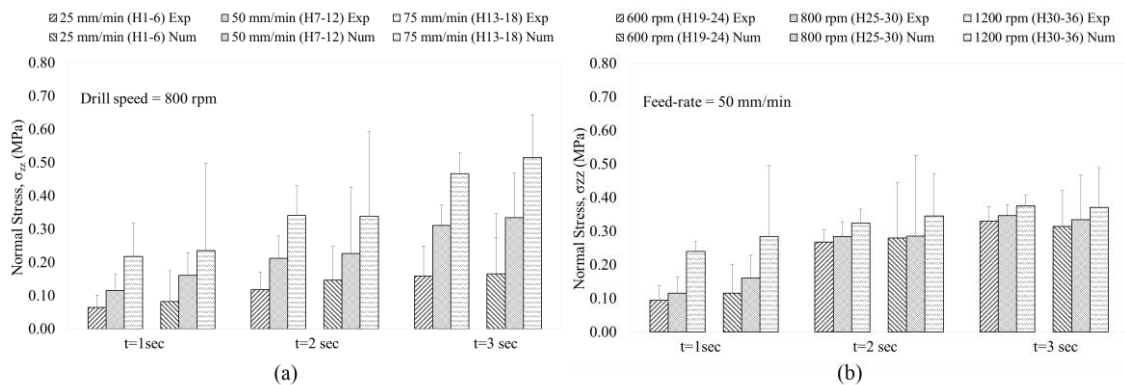


**Figure 8.** Normal stresses  $\sigma_{zz}$  (MPa) in experimental and FE models with (a) feed-rate and (b) drill speed.

Experimental and numerical results indicate strong relationship between either feed-rate, drill speed or drilling depth and the stress levels. Overall, it was observed that the normal stresses in drilling process increase with the increasing of feed-rate and drill speed, for

the same time instant. Regarding to the drilling depth, experimental and numerical results showed a clear trend for an increase in level of stresses with tool penetration along the time, reaching a maximum value when the drill bit penetrated completely the block. The greater of the drilled hole depth, the greater the normal stresses in the bone block.

After analysing the bone behaviour at different drilling times, it is also important to analyse at the end of the process. The effect of feed-rate and drill speed for the complete penetration of the block was examined. Figure 9(a) and (b) present the average of maximum normal stresses ( $\sigma_{zz}$ ) for both models analysed.

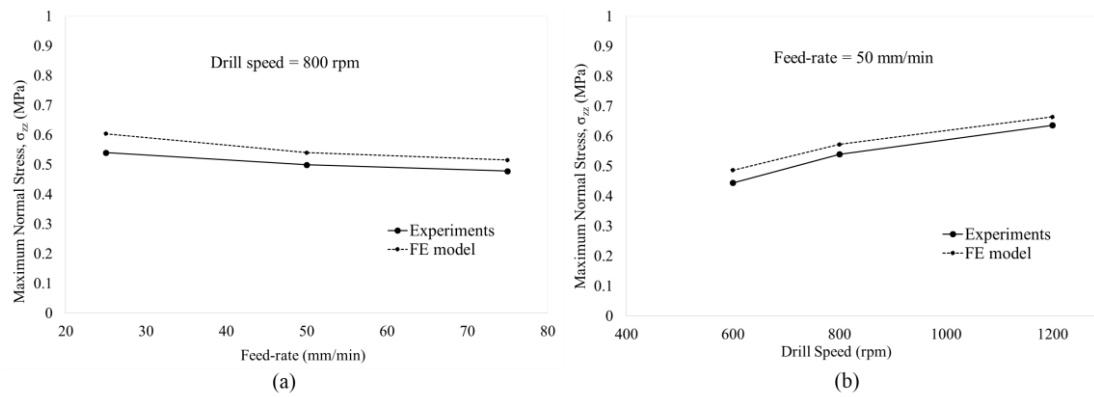


**Figure 9.** Maximum normal stresses  $\sigma_{zz}$  (MPa) with (a) feed-rate and (b) drill speed.

Analysing the entire process, it was observed that the maximum normal stresses retained the same behaviour with respect to the drill speed. Regarding to the feed-rate, the normal stresses decreased with the increase of feed-rate. Although at the start of drilling, the generated normal stresses are higher for higher feed-rates (75 mm/min), in the entire process are found higher stresses for lowest feed-rate (25 mm/min) because the drilling time also increases. In generally, the numerical results were validated and are in good agreement with experimental results.

## 5 Conclusions

In this paper, a three-dimensional thermo-elastic-plastic dynamic model based on finite element method was built to simulate the drill bit penetration into the bone tissue. Thermo-mechanical stresses involved in the drilling processes were obtained and compared with experimental tests. Based on numerical and experimental results, the following conclusions can be drawn:

- The thermo-mechanical stresses generated in the material increasing with tool penetration and, consequently, with increasing of hole depth;
- The normal stresses ( $\sigma_{zz}$ ) tend to decrease when the feed-rate is higher and increase when the drill speed is higher;
- The maximum values of von-Mises stresses are found in the drilled zone and its immediate vicinity for all situations;
- The results presented here demonstrate that the experimental methodology coupled to the developed numerical model are an effective procedure for evaluating thermo-mechanical behaviour of the contact region between the drill bit and the bone.

## Declaration of conflicting interests

The author(s) declared no potential conflicts of interest with respect to the research, authorship, and/or publication of this article.

## Funding

This research was supported by the Portuguese Foundation of Science and Technology under the research project UID/EMS/50022/2013. The third author acknowledges the funding of Project NORTE-01-0145-FEDER-000022 - SciTech - Science and Technology for Competitive and Sustainable Industries, cofinanced by Programa Operacional Regional do Norte (NORTE2020), through Fundo Europeu de Desenvolvimento Regional (FEDER).

## References

1. Marco M, Rodríguez-Millán M, Santiuste C, Giner E, Henar Miguélez M (2015) A review on recent advances in numerical modelling of bone cutting. *J Mech Behav Biomed Mater* 44:179-201.
2. Augustin G, Davila S, Mihoci K, Udiljak T, Vedrina DS, Antabak A (2008) Thermal osteonecrosis and bone drilling parameters revisited. *Arch Orthop Trauma Surg* 128:71-77.

3. Augustin G, Zigman T, Davila S, Udiljak T, Brezak D, Babic S (2012) Cortical bone drilling and thermal osteonecrosis. *Clin Biomech* 27:3313-325.
4. Fonseca EMM, Magalhães K, Fernandes MGA, Barbosa MP, Sousa G (2014) Numerical Model of Thermal Necrosis due a Dental Drilling Process. In: R Natal, et al (eds) *Biodental Engineering II*, London: Taylor & Francis Group, CRC Press 2013, pp.69-73.
5. Lee J, Ozdoganlar B, Rabin Y (2012) An experimental investigation on thermal exposure during bone drilling. *Med Eng Phys* 34:1510-1520.
6. Sezek S, Aksakal B, Karaca F (2012) Influence of drill parameters on bone temperature and necrosis: A FEM modelling and in vitro experiments. *Comput Mater Sci* 60:13-18.
7. Fernandes MG, Fonseca EMM, Natal R (2016) Thermal analysis during bone drilling using rigid polyurethane foams: numerical and experimental methodologies. *J Braz Soc Mech Sci Eng* 38:1855-1863.
8. Dogu Y, Aslan E, Camuscu N (2006) A numerical model to determine temperature distribution in orthogonal metal cutting. *J Mater Process Technol* 171(1):1-9.
9. Staroveski T, Brezak D, Udiljak T (2015) Drill wear monitoring in cortical bone drilling. *Med Eng Phys* 37:560-566.
10. Lee J, Rabin Y, Ozdoganlar OB (2011) A new thermal model for bone drilling with applications to orthopaedics surgery. *Med Eng Phys* 33:1234-1244.
11. Karaca F, Aksakal B, Kom M (2011) Influence of orthopaedic drilling parameters on temperature and histopathology of bovine tibia: An in vitro study. *Med Eng Phys* 33(10):1221-1227.
12. Li X, Zhu W, Wang J, Deng Y (2016) Optimization of bone drilling process based on finite element analysis. *Appl Therm Eng* 108:211-220.
13. Li S, Wahab AA, Demirci E, Silberschmidt VV (2014) Penetration of cutting tool into cortical bone: Experimental and numerical investigation of anisotropic mechanical behaviour. *J Biomech* 47:1117-1126.
14. Pandey RK, Panda SS (2015) Optimization of multiple quality characteristics in bone drilling using grey relational analysis. *J Orthop* 12:39-45.
15. Piattelli A, Piattelli M, Mangano C, Scarano A (1998) A histologic evaluation of eight cases of failed dental implants is bone overheating the most probable cause? *Biomaterials* 19(7-9):683-690.

16. Sugita N, OsaT, Aoki R, Mitsuishi M (2009) A new cutting method for bone based on its crack propagation characteristics. *CIRP Annals-Manuf Techn* 58(1):113–118.
17. Soldani X, Santiuste C, Muñoz-Sánchez A, Miguélez MH (2011) Influence of tool geometry and numerical parameters when modelling orthogonal cutting of LFRP composites. *Compos: Part A* 42(9):1205-1216.
18. Lughmani WA, Marouf KB, Ashcroft I (2015) Drilling in cortical bone: a finite element model and experimental investigations. *J Mech Behav Biomed Mater* 42:32-42.
19. Škrlec A, Klemenc J (2016) Estimating the Strain-Rate-Dependent Parameters of the Cowper-Symonds and Johnson-Cook Material Models using Taguchi Arrays. *Stroj Vestn J Mech e* 62:220-230.
20. Asgharpour Z, Zioupos P, Graw M, Peldschus S (2014) Development of strain rate dependent material model of human cortical bone for computer-aided reconstruction of injury mechanisms. *Forensic Sci Int* 236:109-116.
21. Hernandez C, Maranon A, Ashcroft IA, Casas-Rodriguez JP (2013) A computational determination of the Cowper-Symonds parameters from a single Taylor test. *Appl Math Model* 37(7):4698-4708.
22. Snedeker JG, Niederer P, Schmidlin FR, Farshad M, Demetropoulos CK, Lee JB, Yang KH (2005) Strain-rate dependent material properties of the porcine and human kidney capsule. *J Biomech* 38(5):1011-1021.
23. Cowper GR and Symonds PS (1957) *Strain hardening and strain rate effects in the impact loading of cantilever beams*. Applied Mathematics Report; Brown University, p.28.
24. *ANSYS LS-DYNA User's Guide, Release 12.1*, ANSYS, Inc., Canonsburg, PA, 2009.
25. Fernandes MG, Fonseca EMM, Natal R (2015) Three-dimensional dynamic finite element and experimental models for drilling processes. *Proc IMechE Part L: J Materials: Design and Applications* 0:1-9. Doi: 10.1177/1464420715609363 (in press)
26. Li Z, Kindig MW, Kerrigan JR, Untaroiu CD, Subit D, Crandall JR, Kent RW (2010) Rib fractures under anterior-posterior dynamic loads: Experimental and finite-element study. *J Biomech* 43(2):228-234.
27. Sawbones-Worldwide Leaders in Orthopaedic and Medical Models, *Online Referencing*, [www.sawbones.com](http://www.sawbones.com) (2013, accessed 12 September 2016).



28. Ranu HS (1987) The thermal properties of human cortical bone: an in vitro study. *Eng Med* 16:175-176.
29. Mellal A, Wiskot HW, Botsis J, Scherrer SS, Belser UC (2004) Stimulating effect of implant loading on surrounding bone. Comparison of three numerical models and validation by in vivo data. *Clin Oral Implants Res* 15(2):239-248.
30. Tu YK, Chen LW, Ciou JS, Hsiao CK, Chen YC (2013) Finite Element Simulations of Bone Temperature Rise During Bone Drilling Based on a Bone Analog. *J Med Biol Eng* 33:269-274.
31. Kim YY, Choi WS, Rhyu KW (2012) Assessment of pedicle screw pullout strength based on various screw designs and bone densities-an ex vivo biomechanical study. *Spine J* 12:164-168.
32. Liu D, Zhang XJ, Liao DF, Zhou JJ, Li ZQ, Zhang B, Wang CR, Lei W, Kang X, Zheng W (2016) Biomechanical Comparison of Pedicle Screw Augmented with Different Volumes of Polymethylmethacrylate in Osteoporotic and Severely Osteoporotic Synthetic Bone Blocks in Primary Implantation: An Experimental Study. *Biomed Res Int* 2016:1-8.



## CHAPTER VI

# Thermal analysis in drilling of *ex vivo* bovine bones\*

**Maria Goreti Fernandes**<sup>1</sup>, Elza Fonseca<sup>2</sup>, Renato Natal Jorge<sup>3</sup>, Mário Vaz<sup>3</sup>, Maria Isabel Dias<sup>4</sup>

<sup>1</sup>INEGI, Faculty of Engineering, University of Porto, Portugal

<sup>2</sup>LAETA, INEGI, Department of Applied Mechanics, Polytechnic Institute of Bragança,  
Portugal

<sup>3</sup>LAETA, INEGI, Department of Mechanical Engineering, Faculty of Engineering, University  
of Porto, Portugal

<sup>4</sup>CITAB, University of Trás-os-Montes e Alto Douro, Vila Real, Portugal

*\*Journal of Mechanics in Medicine and Biology. 2017 August 17(5):1750082-16*

**DOI:** 10.1142/S0219519417500828



## Abstract

Bone drilling is a common procedure in Medicine, mainly in traumatology and orthopaedic procedure for fractures fixation and in reconstructive surgery. The success of this surgical procedures is dependent on many factors, namely, on heat generation control during the bone drilling. The main concern in bone drilling is the mechanical and thermal damage of the bone induced by inappropriate parameters such as drill speed and feed-rate during the drilling. This study focuses on the temperature generated during drilling of cortical bone tissue (bovine origin) and solid rigid polyurethane foams with similar mechanical properties to the human bone tissue. Different parameters such as drill speed, feed-rate and hole depth were tested. All results showed that improvement of the drilling parameters and the drill temperatures can be estimated. It was concluded that when the drill speed and feed-rate were higher, the bone temperature increase was lower. The obtained results of temperature in the drilling process of polyurethane foam blocks or bovine bone were compared with a good agreement in between both.

**Keywords:** Drilling process, Temperature, Polyurethane foam block, *Ex vivo* bovine bone



## 1 Introduction

Bone drilling is an essential step in many surgical procedures, such as bone fracture reconstruction with resource to metallic implants, predrilling for screws placement or insertion of external fixators, and other techniques in orthopedic surgery [1, 40]. The success of such procedures is dependent upon the quality of the drilling process and has the purpose of minimizing the associated injury to the surrounding tissue. However, complications could occur during bone drilling, such as mechanical and thermal damage of bone and also to the surrounding tissue [35]. One of the main problems is the generated heat during bone drilling, due to shearing of the material and friction between the cutting surface of the drill bit in contact with the surrounding bone tissue and possible bone fragments formed during the drilling procedure [2-4]. When the obtained temperatures during the drilling operation reach the limit supported by bone tissue, bone necrosis could occur [5, 6]. The level of thermal damage to the living bone tissue is related to the magnitude of temperature elevation and the time to which the bone tissue is exposed to the damaging temperatures [7, 11, 31]. For recording the heat generated in real time, the scientific literature has only referred to two methods until now. The use of thermocouples, which enable direct measurements or indirect estimating by infrared thermography. Although thermocouple technology is well established, the results of the studies on its use are still not uniform [8]. One of the problems of this technology is its ability to detect local temperatures only. The present technology does not allow the production of an overall thermal profile or the measurement of heat that has leaked. This problem does not exist with infrared thermography, which is described as being more accurate and with a lower probability of error [8, 9]. Whenever possible and so as to reach more accurate results, both methodologies must be used in association.

Nowadays, there are many studies in the literature regarding the recording of temperatures reached during bone drilling processes. Eriksson and Albrektsson [10], for example, concluded that the threshold levels for thermal necrosis in the living rabbit bone tissue were set at 47 °C for 1 minute of heat exposition time. Lundskog [6] also carried out his studies on rabbits and concluded that a temperature of 55 °C for a period of 30 s could cause the irreversible death of the bone cells.

Bonfield and Li [7] demonstrated that irreversible bone changes occur when dog femoral bone tissue were heated to 56 °C *in vivo*. These results reflect the importance of the bone drilling studies when improving the chances of avoiding thermal necrosis.

Currently, it is known that the generated temperature during bone drilling is directly associated with the drilling parameters, such as drill speed, feed-rate, drill bit geometry, drill force, hole depth and also bone density [6, 11]. Control of these parameters is essential to improve the drilling conditions, reduce the generated heat and to minimize the bone damage. Based on temperature measurements, several studies have been carried out to assess various parameters that influence surgical drilling into bone [1, 12, 13, 34, 36-39]. However, the complexity of the process and the extensive number of variables involved complicates the statement of concluding remarks. Experimental models coupled to other methodologies, such as computational models, has been a common practice in this type of analysis. Recently, Marco et al. [14] has made a bibliographic review of the main contributions in modelling of bone cutting, including the drilling process. They concluded that the majority of the works involve the finite element method. Some models only include thermal issues assuming the application of a heat source without simulation of chip removal, but in other works, chip removal is simulated. Our recent studies have also demonstrated the importance of these numerical models in the analysis of drilling processes. Thermal and dynamic models were developed and validated based on experimental models of bone drilling [32, 35].

For the experimental models, the vast majority of models use biological materials to relate bone temperature with drilling parameters. A variety of cortical and cancellous bone types have been evaluated in surgical drilling studies, such as bovine and porcine [4, 12, 15, 16]. However, it is difficult to define a good method in such circumstances as the bone is a complex anisotropic biological tissue, with organic and inorganic components. The interaction of different components accounts for its complex mechanical and thermal properties, which are difficult to study due to sensitivity, test conditions and preparation of the specimens [17, 18]. Therefore, the ideal procedure is to replace the biological materials by engineering materials. In comparison with biological test materials, biomechanical test in standard materials do not require as many repetitions or the use of elaborate statistical tools [4].

For this propose, there are a variety of synthetic bone materials available but polyurethane foam manufactured by Sawbones (Sawbones, Pacific Research Laboratories, Inc., Vashon. WA, USA) has been the most extensively material used in medical experiments,



especially in surgical reconstruction, fracture fixation and drilling testing. The uniformity and consistency of its material properties makes rigid polyurethane ideal for comparative testing of various surgical procedures, medical devices and implants [19]. To date, just a relatively few number of researches have directly compared bone drilling into biological tissues and synthetic bones. Although these surrogates are becoming increasingly used, a comparison of generated heat during bone drilling in bovine versus synthetic bone has not been performed, yet.

The main goal of this study was to analyse the temperature variation in the drilling processes and determine the effects of some variables with the objective of helping health professionals, by ensuring drillings within a safe zone and hence ensuring not damaging of bone tissue. For this purpose, feed-rate, drill speed and hole depth were evaluated during the drilling of fresh bovine bones and solid rigid polyurethane foams. During the drilling process in polyurethane foam blocks, the temperature was measured using thermocouples inside the material, and a thermographic camera was used to capture the surface temperature in the drill bit. In bovine bones only, the thermographic camera was used to measure the temperature in drill bit.

## **2 Temperature Evolution in the Drilling of *ex vivo* Bovine Bones and Foam Blocks**

As previously indicated, the complex mechanical and thermal properties and the variation of the properties from samples taken from different bones of the skeleton, and from different individuals of the same species, outcome in variations in the measured temperature, although subject to identical drilling conditions in repeated tests.

In order to isolate inhomogeneity and anisotropy effects in the specimen and conduct the experimental tests in an effective manner, drillings in *ex vivo* bovine bones and solid polyurethane foams have been selected for the first stage of the experiments.

### **2.1 Bovine bones samples preparation**

In the *ex vivo* study, fresh samples of bovine femur were used. The bovine bone was chosen because it is one of the animal bones that most similarly replicates the characteristics of human bone tissue, and it has been shown that it can be used as a

substitute for human bone [20, 41]. All samples were obtained from a local butchery, where they had been previously cleaned (muscle removed), as shown in Figure 1.

The bones were obtained after the death of the calves, with age of 9-12 months (no animals were sacrificed specifically for the purpose of the current study).



**Figure 1.** Samples preparation for the experimental tests in *ex vivo* bovine bones.

The experimental tests were performed a few days after obtaining of the bone samples. In this case it is important to prepare and preserve the femurs correctly (frozen at -20 °C after wrapped with gauze swabs in physiological saline solution) and keep the properties until the day of the tests. In order to retain the mechanical and thermo-physical properties, the samples were prepared according to the guidelines established by Ref. [42]. All samples were kept moist in saline solution with gauze swabs and stored in plastic bags at -4 °C. Before the tests, bone samples were removed from freezer and completely thawed at room temperature for 24 h.

Since higher temperatures are obtained in the cortical tissue, through a hacksaw, the bone epiphysis were removed just keeping the mid-diaphysis columns (Figure 2). The periosteum and bone marrow were also removed from the outer surface of the bone samples, as it clogs the drill flutes [21].

The bone pieces have the approximate dimension of 120-150 mm in length with an average thickness of the cortical wall of 7-9 mm. A total of eight test samples were prepared from the femur bones and each sample was numbered and divided to accommodate approximately six holes with 20 mm of distance between them.

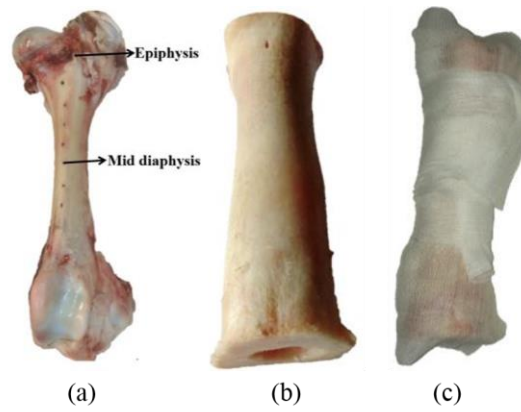


**Figure 2.** Fresh bovine femur (a), sample cut from mid-diaphysis (b) and wrapped with gauze swabs in physiological saline solution (c).

## 2.2 Experimental setup in bovine bones samples

The overall experimental setup includes a temperature measurement system, a computer numerically controlled (CNC) machine for a constant processing with controlled parameters and a conventional HSS twist drill bit with 4 mm of diameter and a point angle equal to  $118^\circ$ .

The temperature system is based on the use of a thermal camera (ThermaCAM 365, FLIR Systems) which has been rigidly fixed to a tripod at a distance of 1.5 m from the drilling area. This method allowed to obtain thermal images of the bone and drill bit surface, before and immediately after drilling. Temperatures were measured in real time and the thermal image data were transferred to a PC for simultaneous analysis in appropriate software (FLIR QuickReport Software, FLIR Systems). The measured temperature is function of the surface conditions, represented by their emissivity. The imposed parameters to the camera during image acquisition are listed in Table 1.

**Table 1.** Parameters used for the thermal image acquisition.

Parameters	Value
Distance camera-drill bit surface	1.5 m
Room temperature	19 °C
Emissivity $\epsilon$	$\epsilon_{\text{stainless steel}} = 0.70$ ; $\epsilon_{\text{skin human}} = 0.98$
Relative humidity	50%

An experimental procedure was designed to evaluate the effects of drill parameters as well as to compare the results obtained with those obtained from synthetic bones. The overview of the experimental setup used in this study is shown in Figure 3.

All the drilled holes were carried out on femoral diaphysis at room temperature without cooling. For the successive holes, a sufficient time was allowed for the bone and the drill bit to return to the initial conditions.

The parameters used in all experimental tests are condensed in Table 2. Parameter combinations were selected to investigate either the influence of drill speed and temperature variation between biological tissues and synthetic bones.



**Figure 3.** Drilling operations of bovine bones.

### 2.3 Experimental setup in polyurethane foam blocks

To the drilling operations in the solid rigid polyurethane foams, two biomechanical test blocks supplied by Sawbones were chosen due to comparable mechanical properties to the human bone tissue. Foams are available in a range of sizes and densities.

In this study, the foam density of  $0.80 \text{ g/cm}^3$  (50 pcf) was selected, as representing the cortical bone, which was approved by the American Society for Testing and Materials for testing orthopaedic devices and instruments. These materials are used as an alternative testing medium to human cadaver bone and offer consistent and uniform physical properties that eliminate the variables encountered when testing human cadaver bones [22]. The polyurethane foam blocks have the same dimensions (130 x 180 x 40 mm) and were identified as BL<sub>1</sub> and BL<sub>2</sub> in accordance with different drilling parameters (Figure 4).



**Figure 4.** Biomechanical foam blocks: BL1 and BL2.

The drilling procedure used to drill the foams blocks was the same used in the drilling of bovine bones. Several holes were made using a set of parameters and the temperature variation was obtained with the thermal camera at a distance of 1.5 m from the drilling area, as show in Figure 5.

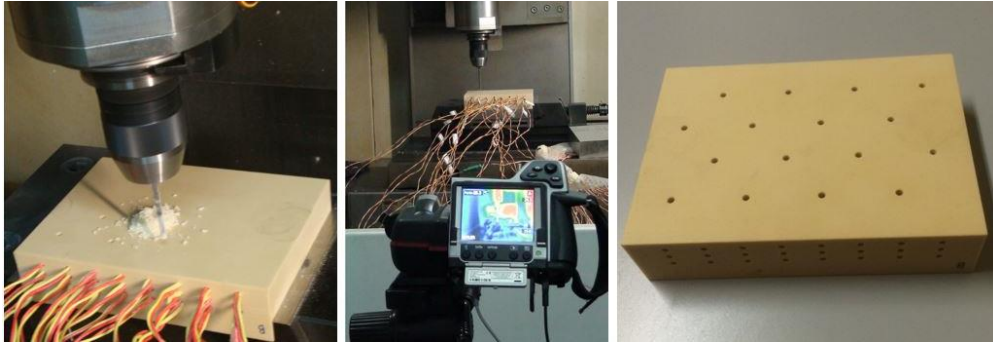


**Figure 5.** Drilling process of biomechanical blocks.

The parameters considered in the drilling of *ex vivo* bovine bones and polyurethane foam blocks are presented in Table 2. All drilling tests were performed through customized automated system with total control of the involved parameters.

**Table 2.** Parameters used in drilling tests.

Parameters	Foam block		<i>Ex vivo</i> bovine bones	
	Bl <sub>1</sub>	Bl <sub>2</sub>	Samples 1,2,3,4	Samples 5,6,7,8
Drill diameter (mm)	4	4	4	4
Drill point angle (°)	118	118	118	118
Depth of the holes (mm)	8	8	8	8
Drill speed, $\omega$ (rpm)	800	900	800	900
Feed rate, V (mm/min)	50	50	50	50

## 2.4 Analysis of the experimental results: bovine bones and foam blocks

By using the thermographic camera the temperature generated in the drill bit during the drilling of the bovine femur and polyurethane foams was studied. It is a fact that the resistance of cortical bone tissue with friction causes temperature increase in bone tissue. The cellular damage and thermal necrosis in cortical bone caused by heat during drilling is reported to be evident at temperatures of 50 °C [2, 15, 23]. The main advantage of a thermal camera is the ability to measure a whole temperature field. Furthermore, there are no concerns regarding proper contact or precise placement.

In this section, only the effect of drill speed and the temperature variation between different materials were investigated. The temperature variation was calculated and compared by subtracting the recorded temperature ( $T_R$ ) with the initial temperature of the drill bit ( $T_0$ ) before each hole ( $\Delta T$  (°C) =  $T_R - T_0$ ). The results were summarized using means and standard deviations. Table 3 shows the mean values obtained in different holes made with a drill speed of 800 and 900 rpm and a constant feed-rate of 50 mm/min.

**Table 3.** Variation of temperature from drill bit, before and after drilling.

Statistics	Foam block		<i>Ex vivo</i> bovine bones	
	Bl <sub>1</sub>	Bl <sub>2</sub>	Samples 1,2,3,4	Samples 5,6,7,8
M ± SD	(n=8) 68.95 ± 2.60	(n=5) 69.88 ± 2.00	(n=19) 39.47 ± 3.73	(n=25) 39.78 ± 2.08
[Range]	[65.9-73.6]	[66.8-71.8]	[32.3-45.90]	[35.55-47.02]

*M* Mean value, *SD* Standard Deviation, *n* number of holes

The bone blocks used in this study have been specifically designed to reproduce the physical properties of the cortical bone in terms of mechanical properties. The physical features of these synthetic bone are homogeneous throughout their volume, so as to obtain a good standardization of the procedures and to avoid possible mistakes in the temperature measurements. However, due to natural inhomogeneity of the animal origin bone tissue, there might be differences between such model and the *ex vivo* situation. Comparing the results obtained in both conditions, it was found that the temperature in the cutting tool is higher in holes made in polyurethane foam blocks, when compared with holes made in bovine femurs. These results were within what was expected, since the biomechanical blocks have a uniform platform over the whole model. The samples of bovine femur have an irregularly geometry, with different cortical thickness along its diaphysis. Moreover, this is a fresh biological material with lower temperature inside, when compared with foams blocks.

The own structure of the bone tissue itself provides a natural cooling to the cutting tool that block foam cannot offer. With regard to the drill speed, it was found that increasing the drill speed from 800 rpm to 900 rpm did not promote any significant change in the temperature during drilling. The temperature variation is slightly higher in holes made with 900 rpm, however no significant difference was observed.

### 3 Temperature Evolution Inside of the Bone

In order to study the temperature distribution inside the bone tissue, thermocouples were used in the polyurethane foam blocks. For this purpose, two biomechanical blocks with the same characteristics used in the previous tests were chosen and identified as B13 and B14. During the drilling process, the temperature was evaluated inside the blocks by thermocouples and in the drill bit surface by thermal camera. In this section the effect of different drill speeds, feed-rates and hole depth were studied.

#### 3.1 Temperature measurement system

Bone temperature registers were performed at selected sites on the foam blocks. To measure the temperature inside the blocks several thermocouples (K-type, precision 0.4%) with the range of  $-270^{\circ}\text{C}$  to  $1200^{\circ}\text{C}$  were used. The thermocouples were placed in two opposite sides of the blocks and in adjacent positions to the drill bit. On one side of the block, the thermocouples were placed at the same distance from the drill bit (Side A), and on the other, thermocouples were placed at different distances (Side B), as shown in Figure 6.

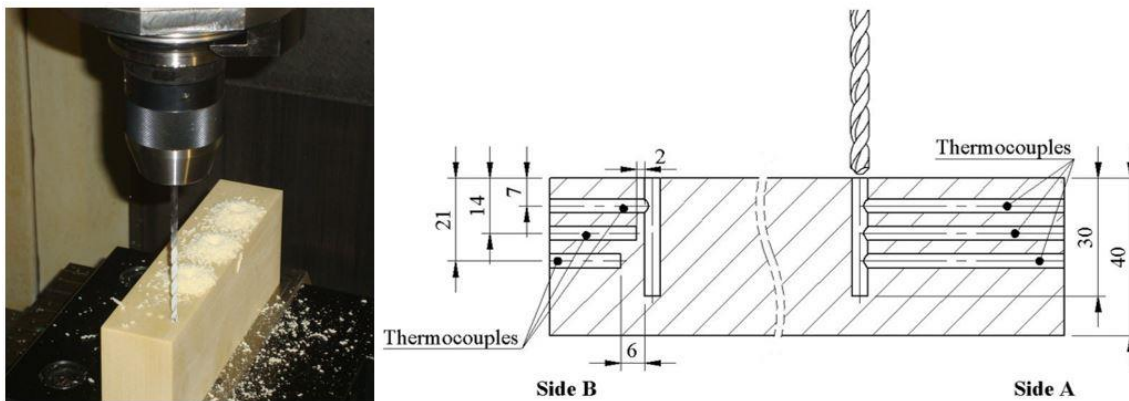


**Figure 6.** Polyurethane foam block and illustration of the thermocouple positions.

All thermocouples were tagged accordingly for each channel identification and respective connection to data acquisition system (Table 4). This experimental setup allowed to measure the temperatures within the blocks at different distances of the holes and along the drilling procedure duration time.

**Table 4.** Thermocouple labelling.

Thermocouple	Description
A/B-T	Side A or B, drilling depths of 7 mm
A/B-M	Side A or B, drilling depths of 14 mm
A/B-R	Side A or B, drilling depths of 21 mm

In accordance with the previous tests, the thermal camera was placed at the same distance from the drilling area and the holes were made with a CNC machine with total control of the parameters. For this study, different feed-rates and drill speeds were considered in order to evaluate their influence on the drilling process (Table 5). All the other parameters were considered as a constant.

**Table 5.** Parameters used in drilling experiments.

Parameters	Foam block	
	Bl <sub>3</sub>	Bl <sub>4</sub>
Drill diameter (mm)	4	4
Drill point angle (°)	118	118
Depth of the holes (mm)	30	30
Drill speed, $\omega$ (rpm)	600, 800, 1200	800
Feed rate, $V$ (mm/min)	50	25, 50, 75
Thermocouples	Yes	Yes
Thermal camera	Yes	Yes

### 3.2 Temperature evolution inside of the polyurethane foam blocks

Through the thermocouples placed inside of the blocks at different distances it was possible to evaluate the temperature distribution throughout the drilling time, using different feed-rates with a constant drill speed and also different drill speeds with a constant feed-rate.

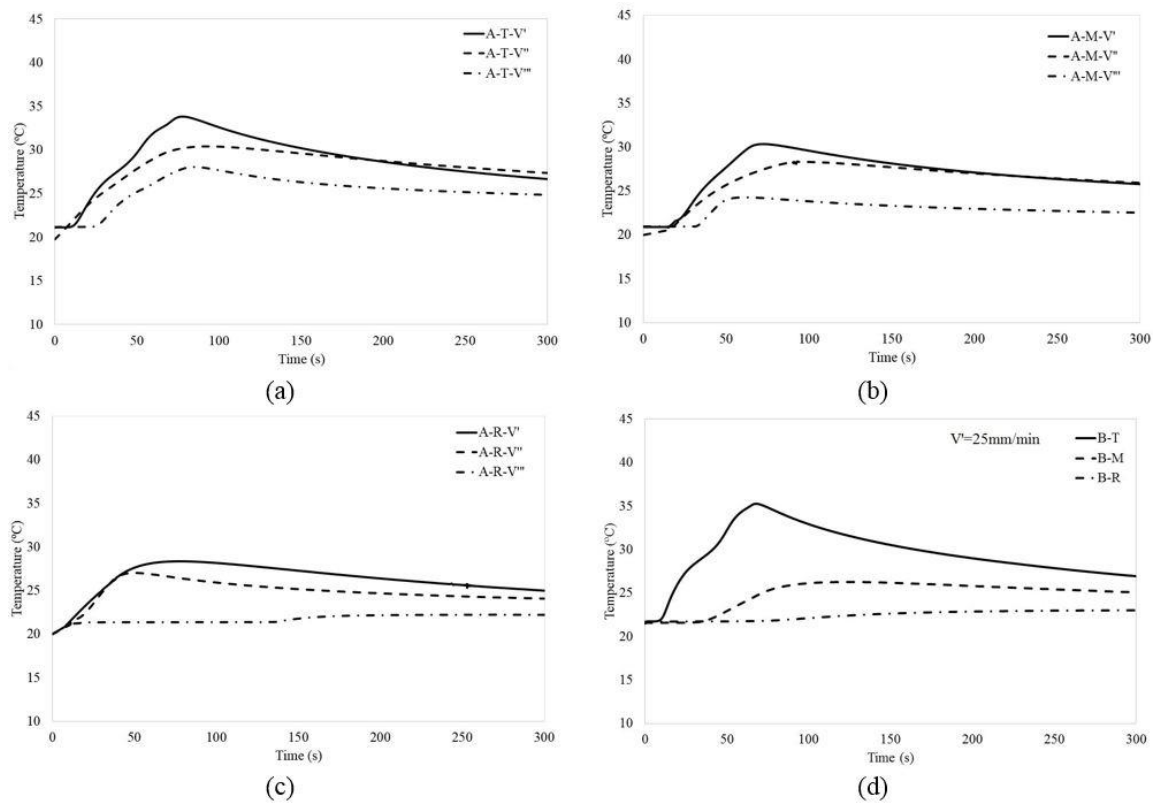
In Figure 7, graphs (a), (b) and (c) represent the obtained temperatures at different positions of thermocouples (Side A), for nine holes made with 30 mm of the depth; feed-rate:  $V' = 25$  mm/min,  $V'' = 50$  mm/min and  $V''' = 75$  mm/min; and a constant drill speed:  $\omega = 800$  rpm. The last graph (d) represents the typical curves of the temperature, at different positions of the thermocouples in Side B for one drilled hole. The results were obtained for a feed-rate equal to 25 mm/min and constant drill speed ( $\omega = 800$  rpm).

Figure 7 allows to explain the influence of feed-rate in drilling process of the polyurethane foam blocks.



It is concluded that the increase in feed-rate causes lesser increase of the temperature in the polyurethane foam block. The same trend can be found in others studies using bovine and porcine bones [4, 6, 23-26, 38].

Comparing the levels of temperature for different feed-rates, it was observed that when the feed-rate was increased from 25 mm/min to 50 mm/min, the temperature decreased in about 10.23% and when the feed-rate was increased from 25 mm/min to 75 mm/min the temperature decreases in about 17.23%. The feed-rate represents the time of the heat source around the bone wall. Thus, the growth of feed-rate increases the rate of heat generation but reduces the drilling time, which leads to a decrease of the total heat generated.



**Figure 7.** Temperature evolution at different feed rates and positions of thermocouples.

Different positions of thermocouples allowed concluding that the temperature decrease when the thermocouple is farthest from the hole.

This event was expected because the polyurethane foam as well as bone material are bad heat conductors. In addition, this was confirmed in a study conducted by Lee et al. [4] that included a precise positioning of multiple thermocouples during drilling of bovine

femurs. They concluded that the highest temperatures were recorded in the thermocouples closest to the drilled hole.

For all thermal histories, it was also noted a similar trend with time; first an increase in time, reaching a peak (maximum) value, and then a slow decay. According to the authors Eriksson et al. [10], the maximum temperature was far below critical level in all combinations of feed-rates during drilling.

In the Figure 8, graphs (a) and (b) represent the temperatures obtained at different positions of thermocouples (Side A), for two holes performed with 30 mm of depth; drill speed:  $\omega' = 600$  rpm and  $\omega'' = 1200$  rpm; and a constant feed-rate:  $V'' = 50$  mm/min.

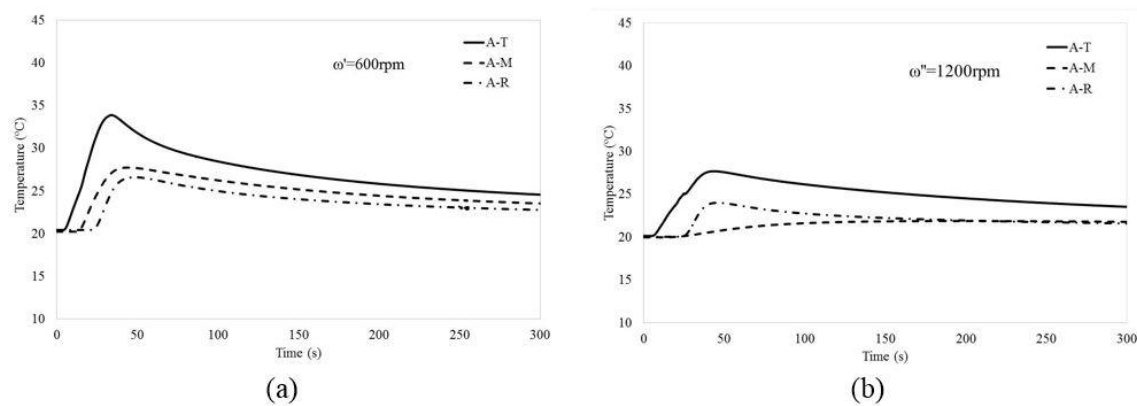


**Figure 8.** Temperature evolution at different drill speeds.

As show in Figure 8, the change in temperature also depends on the drill speed at a constant feed-rate. The temperature decreased in about 22.83% with increasing drill speed from 600 rpm to 1200 rpm. However, the literature review on the drill speed during bone drilling suggest no consistent trend. Some researchers suggest low drilling speed [4, 6, 13, 23, 27] while others suggest a decrease in the temperature with the increase of drill speed [15, 26, 28]. The majority of the studies recommend high drill speed with larger force for minimum heat generation [11]. According to the author Karmani [29], a possible factor in the temperature variation relationship and drill speed is that the rotational speed of a manual electric drill also depends on the force applied.

Abouzgia and James [30] measured the operating speeds of various drills and found them to be at times as low as 50% of the operating speed depending on the applied force. Therefore, apparent rotational speeds may not be the actual speeds.

Drilling depth also influences the temperature generated during drilling. Comparing the holes made with 8 mm and 30 mm of the depth, significantly higher temperatures were

recorded for the holes with 30 mm. The increase of the temperature with an increasing in the hole depth is explained by the friction effect. The frictional resistance offered by the compact cortical bone to the drill causes increases in temperature, while the thermal effect propagates to farther distances in the bone tissue samples. Similar conclusions were reached by the authors Hillery and Shuaib [15], Karaca et al. [26] and Lee et al. [4].

The present study is an experimental approach of selected drilling parameters on the heat generated during the drilling of bovine and synthetic bone. Several studies have been performed to analyse the temperature rise during drilling of animal bones, however no studies have exactly compared these results with commercially available artificial bones used in biomechanical studies. The validations of the experiments have been carried out by repeating the tests taking into account the selected drilling conditions and comparing the results with published scientific articles with similar approaches. Previous experimental and numerical methods developed by the authors of this work also allowed to compare and confirm the current results.

## 4 Conclusions

In this study, temperature measurement systems were introduced to record real-time temperature changes during the drilling of ex vivo bovine bones and polyurethane foam blocks with different parameters. In our work, the comparison between the results, using different materials in similar drilling conditions, allows to obtain a confident level in the quality of the results with a same trend of conclusions. This research demonstrated that the appropriate combinations of different drill parameters can produce temperatures far below the critical values. It was concluded that when the feed-rate and the drill speed are higher, the increase of the bone temperature is lower and, independently, the maximum drill temperature increased with the increasing of hole depth. The values of temperature in the drilling process of ex vivo bone tissue were lower than the drilling process of solid rigid polyurethane foams, as expected. Through this study the application of high drill speeds are suggested, as well as high feed-rates and the reduction in contact area between the drill and bone. The polyurethane foam blocks have proved to be an appropriate material to test the bone drilling conditions with no need to resort to the biological tissues.

The obtained conclusions are similar using different materials with different methodologies (experimental, numerical or both), and the results trend have a good correspondence, according the measured values which compare means and standard deviations. Furthermore, increasing the amount of information from different measurements, the uncertainty of the results decreases with the results from the statistical calculation. The authors continue to develop more tests (experimental and numerical) to confirm the level of confidence and their results.

Automated drilling system with synthetic bone materials can be developed to minimize human error during bone drilling and reduce the incidence of osteonecrosis in the surrounding cortical bone tissue. With this research and with continuing to develop new methods to reduce the undesired mistakes during the bone drilling process in the surgical applications, we intend to contribute to the knowledge on the best drilling conditions.

## **Acknowledgments**

This research was supported by the Portuguese Foundation of Science and Technology under research project UID/EMS/50022/2013.

## **Conflict of interest statement**

The authors declare that no conflicts of interest associated with the presented work.

## **References**

1. Li S, Wahab AA, Demirci E, Silberschmidt VV (2014) Penetration of cutting tool into cortical bone: Experimental and numerical investigation of anisotropic mechanical behaviour. *J Biomech* 47:1117-1126.
2. Eriksson AR, Albrektsson T, Albrektsson B (1984) Heat caused by drilling cortical bone. Temperature measured in vivo in patients and animals. *Acta Orthop Scand* 55:629-631.
3. Bachus KN, Rondina MT, Hutchinson DT (2000) The effects of drilling force on cortical temperatures and their duration: an in vitro study. *Med Eng Phys* 22:685-691.

4. Lee J, Ozdoganlar B, Rabin Y (2012) An experimental investigation on thermal exposure during bone drilling. *Med Eng Phys* 34:1510-1520.
5. Sezek S, Aksakal B, Karaca F (2012) Influence of drill parameters on bone temperature and necrosis: A FEM modelling and in vitro experiments. *Comp Mater Sci* 60:13-18.
6. Lundskog J (1972) Heat and bone tissue. An experimental investigation of the thermal properties of bone and threshold levels from thermal injury. *Scand J Plast Reconstr Surg* 6:5-75.
7. Bonfield W, Li CH (1968) The temperature dependence of the deformation of bone. *J Biomech* 7:323-329.
8. Möhlhenrich SC, Modabber A, Steiner T, Mitchell DA, Hölzle F (2015) Heat generation and drill wear during dental implant site preparation: systematic review. *Br J Oral Maxillofac Surg* 53:679-689.
9. Scarano A, Piattelli A, Assenza B, Carinci F, Donato LD, Romani GL, Merla A (2011) Infrared thermographic evaluation of temperature modifications induced during implant site preparation with cylindrical versus conical drills. *Clin Implant Dent Relat Res* 13:319-323.
10. Eriksson AR, Albrektsson T (1983) Temperature threshold levels for heat induced bone tissue injury. A vital-microscopic study in the rabbit. *J Prosthet Dent* 50:101-107.
11. Pandey RK, Panda SS (2013) Drilling of bone: A comprehensive review. *J Clin Orthop Trauma* 4:15-30.
12. Alam K, Mitrofanov AV, Silberschmidt VV (2009) Finite Element Analysis of Forces of Plane Cutting of Cortical Bone. *Comput Mater Sci* 46:738-743.
13. Xiashuang L, Wei Z, Junqiang W, Yuan D (2016) Optimization of bone drilling process based on finite element analysis. *Appl Therm Eng* 108:211-220.
14. Marco M, Rodríguez-Millán M, Santiuste C, Giner E, Henar Miguélez M (2015) A review on recent advances in numerical modelling of bone cutting. *J Mech Behav Biomed Mater* 44:179-201.
15. Hillery MT, Shuaib I (1999) Temperature effects in the drilling of human and bovine bone. *J Mater Process Technol* 92:302-308.
16. den Dunnen S, Mulder L, Kerkhoffs GM, Dankelman J, Tuijthof GJ (2013) Waterjet drilling in porcine bone: The effect of the nozzle diameter and bone architecture on the hole dimensions. *J Mech Behav Biomed Mater* 27:84-93.

17. Zelenov ES (1985) Thermophysical properties of compact bone. *Mech Compos Mater* 21:1092-1095.
18. Augustin G, Zigman T, Davila S, Udiljak T, Brezak D, Babic S (2012) Cortical bone drilling and thermal osteonecrosis. *Clin Biomech* 27:3313-325.
19. Shim V, Boheme J, Josten C, Anderson I (2012) Use of polyurethane foam in orthopaedic biomechanical experimentation and simulation. In: F. Zafar & E. Sharmin (Eds.), *Polyurethane*, InTech, pp.171-200.
20. Vashishth D, Tanner KE, Bonfield W (2000) Contribution, development and morphology of microcracking in cortical bone during crack propagation. *J Biomech* 33:1169-1174.
21. Jacob CH, Berry JT, Pope MH, Hoagland FT (1976) A study of bone machining process. *J Biomech Eng* 9:343-349.
22. Sawbones-Worldwide Leaders in Orthopaedic and Medical Models, Available from: [www.sawbones.com](http://www.sawbones.com) (2015). Accessed 11 March 2015.
23. Augustin G, Davila S, Mihoci K, Udiljak T, Vedrina DS, Antabak A (2008) Thermal osteonecrosis and bone drilling parameters revisited. *Arch Orthop Trauma Surg* 128:71-77.
24. Shin HC, Yoon YS (2006) Bone temperature estimation during orthopaedic round bur milling operation. *J Biomech* 39:33-39.
25. Augustin G, Davila S, Udiljak T, Vedrina DS, Bagatin D (2009). Determination of spatial distribution of increase in bone temperature during drilling by infrared thermography: preliminary report. *Arch Orthop Trauma Surg* 129:703-9.
26. Karaca F, Aksakal B, Kom M (2011) Influence of orthopaedic drilling parameters on temperature and histopathology of bovine tibia: an in vitro study. *Med Eng Phys* 33:1221-1227.
27. Vaughan RC, Peyton FA (1951) The influence of rotational speed on temperature rise during cavity preparation. *J Dent Res* 30:737-744.
28. Sharawy M, Misch CE, Weller N, Tehemar S (2002) Heat generation during implant drilling: the significance of motor speed. *J Oral Maxillofac Surg* 60:1160-1169.
29. Karmani S (2006) The thermal properties of bone and the effects of surgical intervention. *Curr Orthop* 20:52-58.
30. Abouzgia MB, James F (1997) Temperature rise during drilling through bone. *Int J Oral Maxfac Implants* 12:342-52.

31. Bedrettin CS, Guhan D, Bahar G, Ergun K, Imad S (2009) Effects of irrigation temperature on heat control in vitro at different drilling depths. *Clin Oral Implants Res* 20(3):294-8.
32. Fernandes MG, Fonseca EMM, Natal R (2016) Thermal analysis during bone drilling using rigid polyurethane foams: numerical and experimental methodologies. *J Braz Soc Mech Sci Eng* 38: 1855-1863.
33. Fernandes MG, Fonseca EMM, Natal RJ (2016) Influence of Bone Drilling Parameters on the Thermal Stress Distribution. In: J.F. Silva Gomes and S.A. Meguid (Eds.), *Proc 5th Int Conf Integrity-Reliability-Failure*, Porto, Portugal, pp. 517-528.
34. Fernandes MG, Fonseca EMM, Natal R (2017) Thermo-mechanical stresses distribution on bone drilling: Numerical and experimental procedures. *Proc IMechE Part L: J Mater Des Appl* 0(0):1-10. doi: 10.1177/1464420716689337 (in press)
35. Fernandes MG, Fonseca EMM, Jorge RN (2015) Three-dimensional dynamic finite element and experimental models for drilling processes. *Proc IMechE Part L: J Mater Des Appl* 0(0):1-9. doi: 10.1177/1464420715609363 (in press).
36. Fernandes MG, Natal R, Fonseca EMM (2015) Analysis of stresses in drilled composite materials. In: *IEEE 4th Portuguese Meeting on bioengineering (ENBENG)*, Porto, Portugal, pp. 1-4.
37. Fernandes MG, Fonseca EMM, Jorge RN, Vaz M, Dias MI (2015) Composite materials and bovine cortical bone drilling: Thermal experimental analysis. In: J.F. Silva Gomes & S.A. Meguid (Eds.), *Proc 6th Int Conf Mechanics and Materials in Design*, Azores, Portugal, pp. 691-692.
38. Fernandes MG, Natal RJ, Fonseca EMM, Dias MI (2016). Temperature assessment in the drilling of *ex vivo* bovine and porcine cortical bone tissue. In: Natal Jorge et al. (Eds), *Proc Int Conf Clinical and BioEngineering for Women's Health*, CRC Press, Taylor & Francis Group, London, pp. 159-163.
39. Tu YK, Chen LW, Ciou JS, Hsiao CK, Chen YC (2013) Finite Element Simulations of Bone Temperature Rise During Bone Drilling Based on a Bone Analog. *J Med Biol Eng* 33:269-274.
40. Feldmann A, Anso J, Bell B, Williamson T, Gavaghan K, Gerber N, Rohrbach H, Weber S, Zysset P (2016) Temperature Prediction Model for Bone Drilling Based on Density Distribution and In Vivo Experiments for Minimally Invasive Robotic Cochlear Implantation. *Ann Biomed Eng* 44(5):1576-1586.

41. Campana V, Milano G, Pagano E, Barba M, Cicione C, Salonna G, Lattanzi W, Logroscino G (2014) Bone substitutes in orthopaedic surgery: from basic science to clinical practice, *J Mater Sci: Mater Med* 25:2445–2461.
42. Yuehuei HA, Christopher VB (2000) General considerations of mechanical testing. In: Yuehuei HA, Robert AD (Eds), *Mechanical testing of bone and the bone-implant interface*. New York: CRC Press, pp. 119-131.



## CHAPTER VII

# *Ex vivo* experimental and numerical study of stresses distribution in human cadaveric tibiae\*

**Maria Goreti Fernandes**<sup>1</sup>, Elza Fonseca<sup>2</sup>, Renato Natal Jorge<sup>3</sup>, Maria Cristina Manzanares Céspedes<sup>4</sup>

<sup>1</sup>INEGI, Faculty of Engineering, University of Porto, Portugal

<sup>2</sup>LAETA, INEGI, Department of Applied Mechanics, Polytechnic Institute of Bragança, Portugal

<sup>3</sup>LAETA, INEGI, Department of Mechanical Engineering, Faculty of Engineering, University of Porto, Portugal

<sup>4</sup>Laboratory of Arthroscopic and Surgical Anatomy, Human Anatomy and Embryology Unit, Department of Pathology and Experimental Therapeutics, Faculty of Medicine and Health Sciences, University of Barcelona, Barcelona, Spain

\*Submitted to an International Journal (under review), May 2017



## Abstract

The mechanical behaviour of bone tissue subject to drilling processes has been recently reviewed due to its increased clinical interest. However, no published data exist regarding stress analysis during the bone drilling involving real (*ex vivo*) human bones. The inherent difficulties to perform this process and to collect human bones lead to a lack of information about this subject. The use of the finite element method (FE) models can allow numerical simulations of drilling processes and analyse the tisular bone behaviour during drilling. Numerical models have been proposed to simulate the bone drilling, but none of them represent the real human bone geometry. In this study, a new elasto-plastic dynamic FE model of bone drilling was developed using the real geometry of human cadaveric tibia obtained with a handheld 3D scanner. In addition, the FE model was validated with experimental tests on human cadaveric tibiae. Different drilling conditions from experimental tests were simulated in order to study the stress distribution during drilling. The developed FE model was in good agreement when compared with experimental tests. Results suggest that the use of lower drill speed and higher feed-rate lead to a decrease in the stress level of the treated tibial bone. The developed FE model can be used for future studies, using different drilling parameters, and cover not only the mechanical behaviour of human cadaveric tibiae bone analysis, but also the study of the thermal aspects.

**Keywords:** Human tibia, Cadaver, Drilling, Stresses, Numerical model, Experimental model



## 1 Introduction

Bone drilling is required in about 95% of orthopaedic surgical procedures to correct bone deformities, implanting prosthetics and immobilize fractures [1]. Orthopaedic treatments involving drilling procedures have been increasing as a result of patients ageing, or due to injuries related to sports, transport accidents or falls from height. Although the drilling procedures have integrated modern tools and methods, they are usually carried out with a manual controlled hand-piece by the surgeon. It means that the success of bone drilling and the postoperative recovery are associated with human perception and tool attributes so there is opportunity for improvement.

Thermal and mechanical damage are the major problems associated with the bone drilling processes [2]. The temperature due to friction between cutting tool and bone tissue, and the forces produced during drilling have a negative impact on the outcome of the procedure. Temperature increase limits bone viability due to the reduction of the proteins related with the regeneration processes [3, 4] and thermal bone cell damage [4], while the excessive cutting efforts may result in drill overrun [5], formation of cracks and fractures [6].

Recently, a comprehensive review of the relevant investigations carried on bone drilling has been published as well as a study of the influence of drilling on thermal necrosis [7, 8]. Most of the research focused on thermal damage involves artificial or animal bones as testing materials. Despite its similarities, animal bones are not equal to the human bones. This inherent variation in biological, anatomical, mechanical and thermal properties of specimens from different origins results in differences in the results subject to identical drilling conditions in repeated experiments [9]. However, few researchers have actually studied surgical drilling in human bone [10, 11]. Although the experiments resulted in various conclusions, there is a lack of information on the mechanical bone damage, especially about the strain and stress distribution in bone tissue during drilling and its surface integrity.

From the numerical modelling point of view, only a few number of models are available in literature to address issues related with bone drilling. Marco et al. [12] conducted a literature review with main contributions on bone cutting modelling, including bone drilling with special attention to the bone mechanical behaviour. These authors concluded that there is a need for improvement of models available for drilling simulations.

In spite of major efforts, there is still no adequate and realistic model that can fully describe the materials behaviour and its damage under drilling conditions. The numerical complexity and expensive computational cost of these models is their major challenge and drawback. Validated finite element models using human bones could potentially reduce the experimental effort necessary for the improvement of the drilling processes and predict in an efficient manner the influence on drilling parameters.

This paper presents a three-dimensional (3D) dynamic elasto-plastic FE model using a real geometry of human cadaveric tibia, captured by 3D handheld scanner. The model allows to predict the strain and stress fields generated during human bone drilling, as a function of drill bit geometry and others drilling parameters. A failure criterion is taken into account to allow advanced simulations of drill bit penetration and material removal. The model has been tested and experimentally evaluated using human cadaveric tibiae. Experimentally, each human cadaveric tibia was instrumented with strain gauges in different surface positions to measure the strains under different drilling conditions. The findings of this survey complement previous research developed by our team [13-16], contributing significantly to the knowledge of drilling processes. No FE drilling models based on real geometry of human bones have been reported in the literature so far.

## **2 Materials and Methods**

### **2.1 Numerical model of human tibia**

Two non-embalmed bone samples were extracted from human cadaveric tibiae (two females). The samples were obtained with the permission of the author's institutional research ethics board and were processed in the Body Donors Service and Dissection Room of the University of Barcelona. Due to the limitation of the cadaveric bone sources, whenever possible, donor medical histories were accessed to verify the absence of bone pathology. The samples were sectioned from the medial condyle to the medial malleolus with a band saw. The average length of the tibial diaphysis samples was 209 mm with an average cortical thickness of 3.5 mm as shown in Figure 1.



**Figure 1.** Human cadaveric tibiae and sample dimensions.

Considering the realistic geometry of the human bone, the FE model has been developed based on the bone surfaces recorded by using a 3D portable handheld scanner. The scans were exported as 3D computational surface meshes in Stereolithography (STL) format for post-processing (Figure 2 (b)).

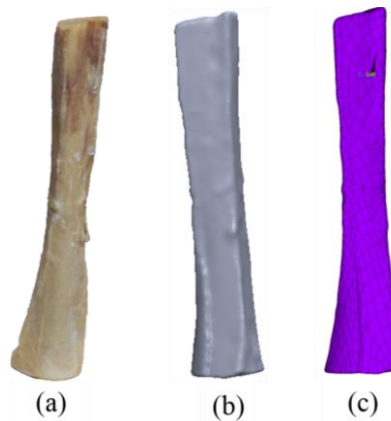


**Figure 2.** (a) Human cadaveric tibia, (b) 3D CAD model and (c) FE model.

The complete FE model includes a part of cortical and trabecular tibial bone, and it involves also a 4 mm diameter twist drill bit with a point angle of  $118^\circ$  and a helix angle of  $30^\circ$ . Initially the FE model of tibial diaphysis was developed with full size (Figure 2 (c)). However, it was noted that the complete model requires a high computational cost and resources. To overcome these problems, the FE model of tibia was reduced as shown in Figure 3. The developed model was configured in accordance with a conventional orthopaedic drilling surgery. The drill bit has an imposed rotational motion (drill speed,  $\omega$ ) and feed movement (feed-rate,  $V$ ).

The bottom surface of the human tibia was fully constrained, while the two lateral edges were constrained in the x-plane due to the material symmetry. The parameters combinations have been chosen considering our experimental setup. Three different drill speeds and feed rates were used for a feed depth of 5 mm, and are described in the next sub-section. The thermal issues are not accounted in these models, due to the numerical calibration obtained at a distance equal to 3.5 mm to the hole edge perforation, so the drill thermal effect in this vicinity vanishes.

Through the explicit dynamic finite element code, solid elements (SOLID164) were used in the model. Conditional stability is the only concern about explicit integration, requiring a very small time step. Thus the element size should be defined under the point of view of both accuracy and time efficiency of the calculation. Based on previous meshes analysis [17, 18] and our previous studies [13, 15], the model was meshed with an edge element length of 1 mm (Figure 3 (b)). This element size ensures the mesh independent results, the calculation accuracy and the reduction of computational requirements (CPU, RAM and running time).

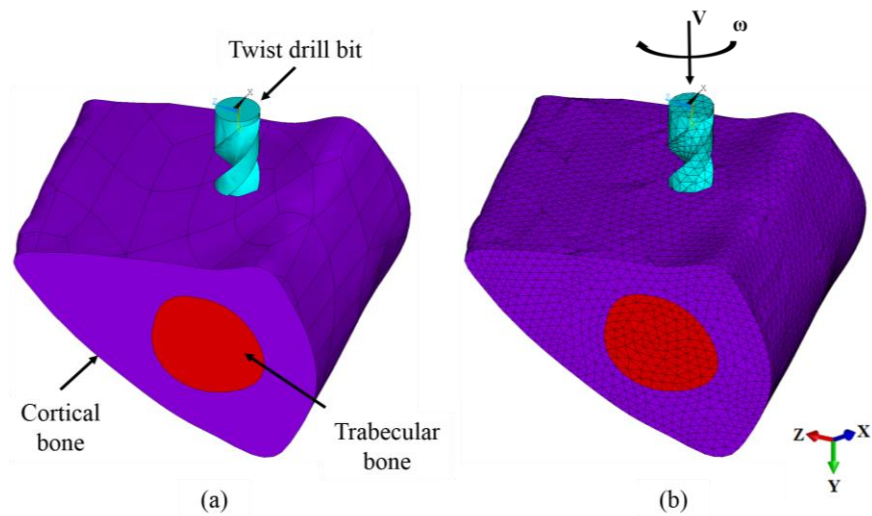


**Figure 3.** (a) FE model of bone drilling and (b) mesh and boundary conditions.

### 2.1.1 Material and constitutive models

Explicit dynamic FE code to simulate drilling processes requires the use of an accurate and reliable model to represent the constitutive material behaviour under large deformations due to drilling conditions. According to the literature, the three most commonly applied material models which consider the strain-rate effects are: Cowper-Symonds, Johnson-Cook, and Zerilli-Armstrong [19].



Following our previous studies, it was opted for the Cowper Symonds model [13, 15]. This model is often used to describe a non-elastic behaviour bone tissue allowing the element deletion and "separating" the material applying a failure strain criterion [20, 21]. In addition, Cowper-Symonds model implementation with strain-rate dependency is versatile, since it may be generally applied to any set of stress-strain data that maintains a consistent material curve shape at various strain-rates, a behaviour which is typical for most biological materials [21]. Cowper-Symonds law is implemented in the finite element program and is determined with the following parameters: Young's modulus  $E$ , Poisson's number  $\nu$ , tangent modulus  $E_{tan}$ , effective plastic strain  $\varepsilon_p^{eff}$ , hardening coefficient  $\beta$  (between 0 for kinematic hardening and 1 for isotropic hardening), material density  $\rho$ , and the parameters  $C$  and  $P$  that describe the dependency of the yield stress  $\sigma_y$  on the strain rate  $\dot{\varepsilon}$ , according to the following equation [22]:

$$\sigma_y = \left[ 1 + \left( \frac{\dot{\varepsilon}}{C} \right)^{\frac{1}{P}} \right] \left( \sigma_0 + \beta \frac{E_{tan} E}{E - E_{tan}} \varepsilon_p^{eff} \right) \quad (1)$$

Mechanical properties of the cortical and trabecular regions were selected based on the literature [23-25]. Table 1 summarizes all properties used in the finite element model. In the numerical simulations, bone marrow is neglected due to its low load transmission properties [23]. The drill bit was a high speed steel (HSS) and was assumed as absolutely rigid (no distortion).

**Table 1.** Material properties and Cowper-Symonds parameters.

Properties	Cortical bone	Trabecular bone	Drill bit
Density (kg/m <sup>3</sup> )	1850	1000	7850
Young's Modulus (GPa)	17	0.4	200
Poisson's ratio	0.3	0.3	0.3
Initial Yield Stress (MPa)	125	10	
Tangent Modulus (MPa)	1000	25	
Hardening Parameter	0.1	0.1	
Cowper-Symonds model			
	$C$	360.7	360.7
	$P$	4.605	4.605
Failure Strain	0.016	0.134	

### 2.1.2 Contact and material failure criteria

In our FE simulations, contacts were modelled using the surface to surface contact eroding algorithm, which is accessible in the finite element program. This algorithm was established between drill bit, cortical bone and trabecular bone. The surface of cutting tool was identified as the contact surface while the target surfaces include the cortical and trabecular surfaces which are brought into contact with drill bit. Eroding contact types are recommended whenever solid elements involved in the contact definition are subject to erosion (element deletion) due to material failure criteria. Coulomb friction law was assumed to model the cutting tool/workpiece contact zones. A value of  $\mu=0.3$  was adopted, which had been used by other authors [26]. The hole generation during drilling was simulated through the eroding contact algorithm together with an integrated failure model, in which way all failed solid elements are deleted and contact surfaces can be automatically updated to the next layer of specimen elements. In this case, the elements are deleted from the solution when exceed a specified plastic strain. Based on the properties described in Table 1, failure strain reaching 0.016 and 0.134 are adopted as the criterion in the erosion algorithm implementation for the cortical and trabecular bone, respectively.

The dynamic analysis was performed using an explicit direct-time-integration procedure and thereby avoids the need for matrix evaluation, assembly and decomposition at each time step as required by many implicit time-integration algorithms. The FE program automatically examines the finite element mesh and material properties in order to determine an appropriate time step size for numerical stability, using a stability scale factor which is 0.90 by default. This time step size is then automatically adjusted throughout the transient analysis to account for contact and local material and geometric nonlinearities [27].

## 2.2 Experimental validation

The FE model validation was made using experimental tests in human cadaveric tibiae. It was decided that the most efficient method of measuring the strain level at the bone surface during drilling was to locate several strain gauges as close as possible to the drilled zone. Therefore, each sample was instrumented with three linear strain gauges (1-LY18-6/120,  $120\Omega \pm 0.35\%$  from HBM) to estimate the level of strain at the *facies medialis* flat tibial surface. To promote the strain gauge bond, the bone surface was prepared by stripping of the periosteum in the area to which the strain gauge was implanted.

To promote the uniformity of results, all gauges were mounted in identical locations, considering the same distance of 3.5 mm between the edge hole and the strain gauge (Figure 4). Single strain gauge is used to measure the strain in one direction. Wire leads were soldered to the strain gauge contacts and connected to an acquisition data system (Vishay Micro Measurements P3 Strain Indicator and Recorder). This system allowed to read the strains over time during each step of the drilling.

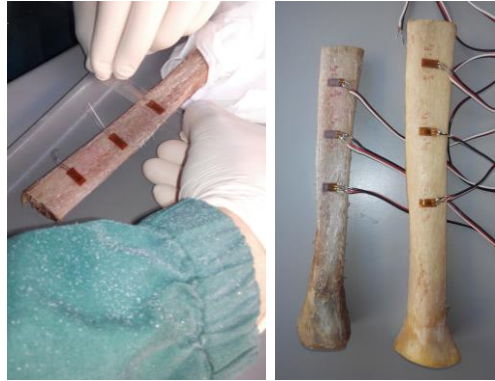


**Figure 4.** Instrumentation of human bone tibiae.

To determine the strain and stress during bone drilling, twelve holes were performed using a vertical drilling machine with a twist drill bit ( $\varnothing 4$  mm, point angle of  $118^\circ$  and helix angle of  $30^\circ$ ) and using two different drill speed: 900 and 1370 rpm. The combinations of parameters have been chosen considering the existing clinical practice based on hand-held drilling devices. In clinical practice, the drilling operations are blind in nature with unknown hole depth and feed-rate. Therefore, our drilling tests were performed in the same way. However, all holes were carried out by the same operator for one operative standardization. To obtain the feed-rate for each drilled hole, drilling time and hole depth were measured with an appropriate depth gauge and the average of feed-rates in each human cadaveric tibia were calculated. For the holes made with a drill speed of 900 rpm was obtained a mean feed-rate of 0.325 mm/s, while the holes performed with 1370 rpm was obtained a mean value of 0.241 mm/s.

The tests were conducted at room temperature ( $23^\circ\text{C}$ ) without applying cooling at the drilling zone. The complete experimental setup for bone drilling is shown in Figure 5.

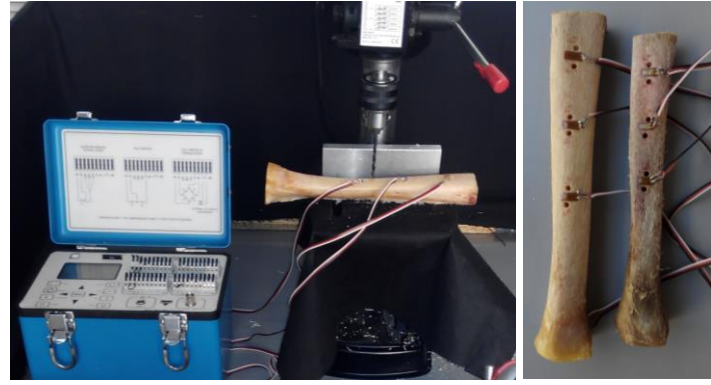


**Figure 5.** Experimental setup on human cadaveric tibiae.

### 3 Results and Discussion

FE models are a promising and effective tool in assessing bone injury and in best clinical practices establishment. The numerical model built in this study has been developed to best represent the human cadaveric bone, as well as to predict the stresses distribution under different drilling conditions. The geometry of the bone regions were directly scanned from the handheld 3D scanner of the bone sample which was actually tested. The variations of the von Mises stress occurring on the human tibia at different drill speeds and feed-rates are illustrated in Figure 6. Since the simulations were performed at different feed-rates, a fixed value of drilling depth (2.5 mm) was selected as the best way to evaluate the effect of drill speed on stress generated during drilling.

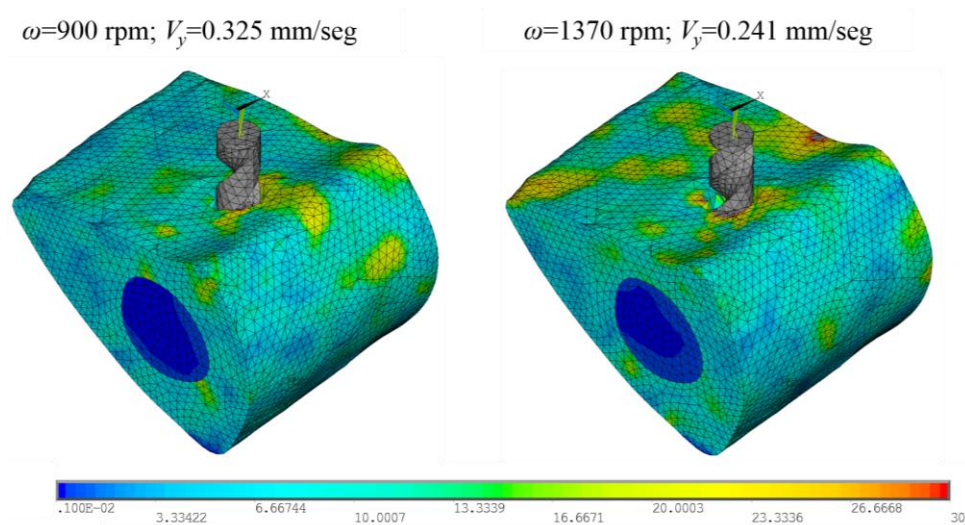


**Figure 6.** Comparison of the von Mises stresses (MPa) obtained for drill speeds of 900 and 1370 rpm and 2.5 mm drilling depth.

The first point of interest from Figure 6 is the difference between the stress level occurring in the drill speed of 900 rpm and 1370 rpm. Considering the same range of contour levels and colours for both models, and a fixed value of drilling depth, the equivalent stresses increase with increasing drill speed. A cutting tool with higher drill speed will remove the material more rapidly, i.e. the number of cuts and the amount of friction between the drill and the human bone will be relatively increased and, in turn, correlate with higher accumulated friction energy. This can increase the stress generation on the bone tissue. Additionally, the maximum stress values are located at the drilling zone and tend to decrease with the distancing from this area. Certainly, the highest stress concentration appears at the intersection of drill bit helixes and hole border, where the work material is undergoing higher equivalent strain. Therefore, it is here that bone failures generally develop. Current numerical results for stress generation at different drill speeds are compared to our already published works with synthetic bone and followed the same trend [13, 15].

### 3.1 Comparison of the numerical and experimental results

In the numerical simulations a maximum drilling depth of 3 mm was established, considering the average cortical thickness of human cadaveric tibia and the required solution time. Experimentally, average values of linear strain ( $\epsilon_{zz}$ ) and the calculated normal stress ( $\sigma_{zz}$ ) from Hooke Law's, in z direction, were obtained thus allowing the comparison with numerical results. Numerically, a set of finite elements were selected at a distance of 3.5 mm from the edge of drilled hole (according to the area covered by the strain gauge in the experimental tests) and the mean values in the same direction were evaluated. The results obtained in both methodologies are given in Figure 7. In order to provide an overview on mechanical behaviour of the human bone during drilling, Figure 7 (a) represents the mean values and standard deviation of results for different drilling steps (1, 2 and 3 s) while Figure 7 (b) shows the mean values of maximum normal stress, considering the established final drilling depth (3 mm).

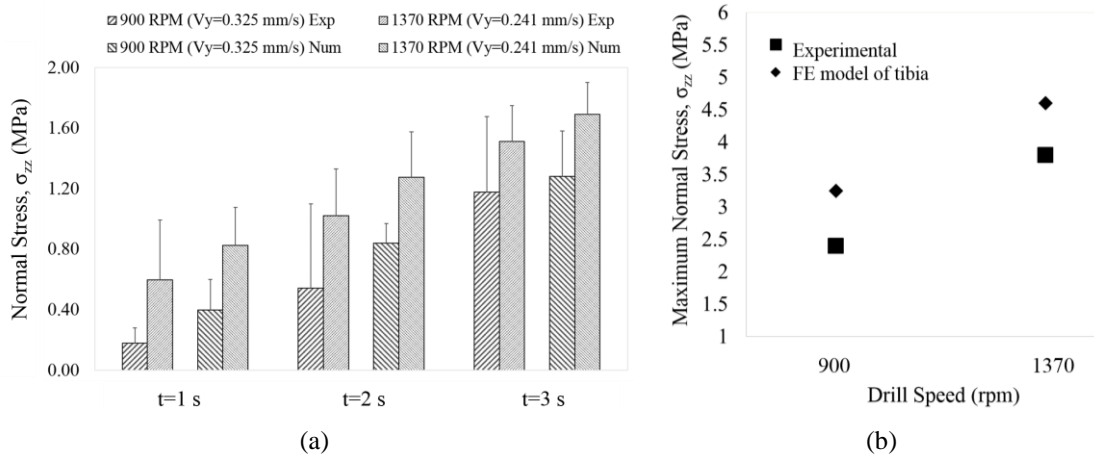


**Figure 7.** Comparisons of normal stress (MPa) from FE model and experiments at different drilling steps (a) and at maximum drilling depth of 3 mm (b).

Figure 7 shows significant differences between the different drilling parameters, showing the importance of considering an appropriate drill speed and feed-rate in the orthopaedic surgeries. Figure 7 (a) represents that the stress levels in the human bone increasing over drilling time. It is expected that the higher the drilling time, the greater will be the stress distribution on human bone tissue. As has already been observed in numerical results, the Figure 7 (b) clarify, once again, that the maximum values of drilling stress increase with increasing of drill speed. It is also essential to highlight that the feed-rate, manually controlled, decreased from 0.325 to 0.241 mm/s, when the drill speed increase from 900 to 1370 rpm. Combining these two parameters, it was also observed that the stress generation increases for the lowest values of feed-rate. Similar behaviour was reported in our previous studies using synthetic bone with properties similar to the human cadaveric bone [26, 27]. As the value of the drilling depth is fixed, this trend may be explained by the fact that the slower feed-rate translates into a longer friction time between the drill bit and the human bone tissue, leading to more accumulated friction energy and a higher rise in bone stress levels. By comparing the results obtained through the numerical simulations and experimental tests, it is found that there is a good agreement between them.

## 4 Conclusions

This article analyses the stress generation during bone drilling under different parameters and using the dynamic explicit finite element method with experimental validation. The

developed FE model provides a new, enhanced approach of bone drilling models based on complex and real geometries, which is able to predict the mechanical behaviour of human bone tissue.

The main conclusions of this study can be presented as follows:

- for both methods, a drill bit with a lower drill speed and higher feed-rate can reduce the level of stresses in the human cadaveric tibiae during drilling;
- in all drilling situations, the stresses increase with the drilling time and, consequently, with the increase of the hole depth;
- in the von Mises stresses obtained from the numerical study, the maximum stress occurs on the drilling zone and its immediate vicinity. The maximum von Mises stress value is always located at the intersection of drill bit helixes and hole walls regardless of the drilling parameters;
- a good agreement is achieved between the mean values of the experimental and numerical results.

Based on all results and discussion, it can be shown that the use of FE human bone drilling models, based on dynamic analysis were calibrated and validated, especially for the assessment of stress distribution around the drilling zone. These models can be used as an important tool for the health professionals to plan an accurate safe surgery with rapid post-surgery recovery.

## Acknowledgments

This research was supported by the Portuguese Foundation of Science and Technology under research project UID/EMS/50022/2013. The authors gratefully acknowledge the generosity of the body donors.

## Conflict of interest statement

The authors declare that no conflicts of interest associated with the presented work

## References

1. Accini F, Díaz I, Juan J (2016) Using an admittance algorithm for bone drilling procedures. *Comput Methods Programs Biomed* 123:150-158.

2. Alam K, Khan M, Silberschmidt VV (2014) 3D Finite-Element Modelling of Drilling Cortical Bone: Temperature Analysis. *Journal of Medical and Biological Engineering* 34(6):618-623.
3. Gupta V, Pandey PM (2016) Experimental investigation and statistical modeling of temperature rise in rotary ultrasonic bone drilling. *Med Eng Phys* 38(11):1330-1338.
4. Eriksson RA, Albrektsson T, Magnusson B (1984) Assessment of bone viability after heat trauma: a histological, histochemical and vital microscopic study in the rabbit. *Scand J Plast Reconstr Surg Hand Surg* 18:261-8.
5. Brett PN, Baker DA, Taylor R, Griffiths MV (2004) Controlling the penetration of flexible bone tissue using the stapedotomy microdrill. *Proc IMechE Part I: J Systems and Control Engineering* 218(5):343-351.
6. Ebacher V, Guy P, Oxland TR, Wang R (2012) Sub-lamellar microcracking and roles of canaliculi in human cortical bone. *Acta Biomater* 8(3):1093-100.
7. Augustin G, Zigman T, Davila S, Udilljak T, Brezak D, Babic S (2012) Cortical bone drilling and thermal osteonecrosis. *Clin Biomech* 27:3313-325.
8. Pandey RK, Panda SS (2013) Drilling of bone: A comprehensive review. *J Clin Orthop Trauma* 4:15-30.
9. Lee J, Ozdoganlar B, Rabin Y (2012) An experimental investigation on thermal exposure during bone drilling. *Med Eng Phys* 34:1510-1520.
10. Natali C, Ingle P, Dowell J (1996) Orthopaedic bone drills-can they be improved? Temperature changes near the drilling face. *J Bone Joint Surg Br* 78(3):357-62.
11. Hillery MT, Shuaib I (1999) Temperature effects in the drilling of human and bovine bone. *J Mater Process Technol* 92-93:302-308.
12. Marco M, Rodríguez-Millán M, Santiuste C, Giner E, Henar Miguélez M (2015) A review on recent advances in numerical modelling of bone cutting. *J Mech Behav Biomed Mater* 44:179-201.
13. Fernandes MG, Fonseca EMM and Natal R. Three-dimensional dynamic finite element and experimental models for drilling processes (2015) *Proc IMechE Part L: J Materials: Design and Applications*. Doi: 10.1177/1464420715609363 (in press).
14. Fernandes MG, Fonseca EMM and Natal R (2016) Thermal analysis during bone drilling using rigid polyurethane foams: numerical and experimental methodologies. *J Braz Soc Mech Sci Eng* 38:1855-1863.
15. Fernandes MG, Fonseca EMM and Jorge RN (2017) Thermo-mechanical stresses distribution on bone drilling: numerical and experimental procedures. *Proc IMechE*



*Part L: J Materials: Design and Applications*. Doi: 10.1177/1464420716689337 (in press)

16. Fernandes MG, Fonseca EMMM, Natal R, Vaz M, Dias MI (2017) Thermal analysis in drilling of ex vivo bovine bones. *J Mech Med Biol* 17(3):1750082-16.
17. Lughmani WA, Marouf KB, Ashcroft I (2015) Drilling in cortical bone: a finite element model and experimental investigations. *J Mech Behav Biomed Mater* 42:32-42.
18. Li X, Zhu W, Wang J, Deng Y (2016) Optimization of bone drilling process based on finite element analysis. *Appl Therm Eng* 108:211-220.
19. Škrlec A, Klemenc J (2016) Estimating the Strain-Rate-Dependent Parameters of the Cowper-Symonds and Johnson-Cook Material Models using Taguchi Arrays. *Stroj Vestn J Mech e* 62:220-230.
20. Hernandez C, Maranon A, Ashcroft IA, Casas-Rodriguez JP (2013) A computational determination of the Cowper-Symonds parameters from a single Taylor test. *Appl Math Model* 37(7):4698-4708.
21. Snedeker JG, Niederer P, Schmidlin FR, Farshad M, Demetropoulos CK, Lee JB, Yang KH (2005) Strain-rate dependent material properties of the porcine and human kidney capsule. *J Biomech* 38(5):1011-1021.
22. Cowper GR and Symonds PS (1957) Strain hardening and strain rate effects in the impact loading of cantilever beams. Applied Mathematics Report; Brown University, p.28.
23. Quenneville CE, Dunning CE (2011) Development of a finite element model of the tibia for short-duration high-force axial impact loading. *Comput Methods Biomech Biomed Engin* 14(2):205–212.
24. Burstein AH, Reilly DT, Martens M (1976) Aging of bone tissue: mechanical properties. *J Bone Joint Surg Am* 58(1):82-6.
25. Iwamoto M, Miki K, Tanaka E (2005) Ankle skeletal injury predictions using anisotropic inelastic constitutive model of cortical bone taking into account damage evolution. *Stapp Car Crash J* 49:133-56.
26. Mellal A, Wiskot HW, Botsis J, Scherrer SS, Belser UC (2004) Stimulating effect of implant loading on surrounding bone. Comparison of three numerical models and validation by in vivo data. *Clin Oral Implants Res* 15(2):239-248.
27. Hallquist JO (2006) LS-DYNA Theory Manual, Livermore Software Technology Corporation.



## **CHAPTER VIII**

### **Concluding Remarks and Future Directions**



## 8.1 Introduction

The aim of the study presented in this thesis was improving the understanding of the main thermal and mechanical characteristics, involved in the bone drilling processes, in order to reduce the risk of bone damage. All obtained experimental data, theoretical and numerical analyses on the bone response under different drilling conditions, have provided the basis for the development of new models able to predict, not only the thermal bone response, but also the mechanical behaviour. This last chapter presents the main statements, conclusions and some topics that should be subject of future analysis and further development.

## 8.2 Conclusions and remarks

Clinical surgeries that involve drilling of bone tissue has been increasing. Although the drilling procedures have come a long way through improvements, and implementation of modern tools, the controversies and doubts related to the effect of drilling parameters on bone response still prevail. Studies assessing the risk of bone damage during drilling has increasingly attracted the attention of researchers. The vast majority of them, analysed the gradient of temperature and cutting force, with the aim to avoid unnecessary damage and improve drilling quality during the process. However, there has not been a systematic study that included the measurement of temperatures, strains and stresses, during the drilling in different materials, as synthetic, animal and human bone. From the point of view of engineering, drilling is associated with the conversion of mechanical work energy into thermal energy. Primary sources of this thermal energy are plastic deformation and shear failure of bone tissue and friction during the machining process. In light of this, it is also important analyse all the mechanical issues involved in this processes.

In this thesis, a comprehensive literature review was presented, with particular emphasis on the used methods and obtained results, particularly, to point out what are the contradictions, limitations, concerns or faults. Based on the literature, the following conclusions, limitations and challenges were found:

- the most techniques and methodologies studied, present the effects of different drilling parameters on the temperature rise and the obtained drilling forces during bone drilling. However, mechanical damage and strain level produced during the drilling bone are an

important aspect to be considered in these procedures. Strain measurements from extensometers located on bone surface, near of the drill bit, require a delicate and rigorous instrumentation process, who needs to be considered in this type of studies. In addition, few experimental studies have examined surgical drilling in human bone, and no studies have inquired into this aspect for the strains and stresses in the bone tissue;

- there is no full agreement about the exact and ideal drilling parameters. Several studies recommend the use of high drill speeds, feed-rates and larger drilling forces for minimum temperature rise. In this context, attention should be given to the bone and tissues involved. Different surgeries (such as orthopaedic, dental surgery, among others) require different drilling parameters;

- cooling systems have been pointed out as the most important factor to avoid bone necrosis. However there are no clear recommendation of which one is better system to the bone drilling;

- concerning to the drill bit geometry, most of the researches recommended the use of quick helix with split point and large point angle, between  $100^{\circ}$  to  $120^{\circ}$ . This geometry allows efficient removal of the fragments and minimizes friction during bone drilling;

- from a numerical point of view, most of the FE models only include thermal issues assuming the application of a heat source without simulation of fragments removal. In this kind of approach is commonly used simple constitutive models (isotropic, elastic-plastic) and simplistic representations of bone geometry. The development of FE models based on the real geometry of bone and all real drilling characteristics is one of the challenges in this field.

Considering the above literature review and their limitations, the most relevant contributions of this thesis were:

- an extensive experimental test campaign on different test materials (polyurethane foams with mechanical properties similar to the human bone, bovine femurs and human cadaveric tibiae) as well as, the combined experimental approach to obtain temperatures and strain distribution during bone drilling. This was the first comprehensive set of experimental results, to analyse of bone stresses during drilling, in simultaneous with the temperature level in the drill bit and in bone material;

- an extensive numerical research of the thermomechanical behaviour of bone tissue during drilling was conducted. An extension of dynamic elasto-plastic models for bone

drilling was proposed and compared with our experimental results. In addition, new dynamic models based on real geometry of human bone are introduced and validated. This numerical approach easily allows the inclusion of different drilling parameters or different material characteristics to predict the damage on bone tissue;

- experimental and numerical analysis demonstrated that the appropriate combinations of different drill parameters can reduce the risk of thermal and mechanical damage of bone tissue. In general, it was found that the maximum temperature, strain and stress increase with the increasing drill speed and, independently, decrease with the increasing feed- rate. The use of cooling system and materials with less porosity and density lead to a decrease in bone temperature during drilling;

- the proposed numerical models were validated with the experimental tests and a good correlations was found. The ability to determine, in a simple way, the thermomechanical behaviour of bone under different drilling conditions is a valuable input for the health professionals and their patients.

### **8.3 Future directions**

The author sees this thesis as a lever to new developments and improvements with several research fronts. There are main future perspectives that could follow this thesis:

- the development of robotics and navigation systems applicable on the operating room. These systems would permit the use of precise drilling parameters, minimizing human error;

- the development of more methods that analyse the effects of cooling systems and predicting advantages and possible use of all;

- the developments of new tests to analyse the use of coatings on the cutting tools. The use of appropriate coatings could be useful to reduce friction and, in turn, reduce the thermal and mechanical damage on the bone tissue;

- the development of studies to analyse the effect of different drilling parameters on the micro drilling of bone and its benefits on bone damage;

- numerically, the further development of models at the micro-scale level, in order to study the thermal and mechanical bone damage. Subsequently, the comparative study between these models with those already existing in the macroscopic scale.





## **APPENDIXES**



### Autorização de Compilação

Elza Maria Morais Fonseca e Renato Manuel Natal Jorge na qualidade de coautores do artigo “Thermal analysis during bone drilling using rigid polyurethane foams: numerical and experimental methodologies” publicado na revista *Journal of the Brazilian Society of Mechanical Sciences and Engineering*, declaram que autorizam a inclusão do mesmo na dissertação de doutoramento da candidata Maria Goreti Antunes Fernandes, intitulada “Analysis of bone damage during drilling processes”

Porto, 17 de Maio de 2017



(Elza Maria Morais Fonseca)

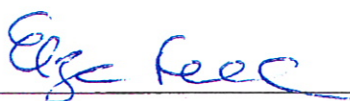


(Renato Manuel Natal Jorge)

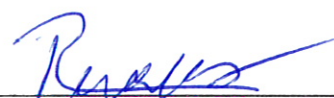
### Autorização de Compilação

Elza Maria Morais Fonseca e Renato Manuel Natal Jorge na qualidade de coautores do artigo “Three-dimensional dynamic finite element and experimental models for drilling processes” publicado na revista *Proceedings of the Institution of Mechanical Engineers, Part L: Journal of Materials: Design and Applications*, declaram que autorizam a inclusão do mesmo na dissertação de doutoramento da candidata Maria Goreti Antunes Fernandes, intitulada “Analysis of bone damage during drilling processes”

Porto, 17 de Maio de 2017



(Elza Maria Morais Fonseca)



(Renato Manuel Natal Jorge)

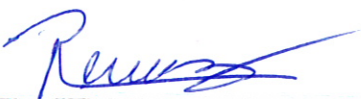
### Autorização de Compilação

Elza Maria Morais Fonseca e Renato Manuel Natal Jorge na qualidade de coautores do artigo “Thermo-mechanical stresses distribution on bone drilling: numerical and experimental procedures” publicado na revista *Proceedings of the Institution of Mechanical Engineers, Part L: Journal of Materials: Design and Applications*, declaram que autorizam a inclusão do mesmo na dissertação de doutoramento da candidata Maria Goreti Antunes Fernandes, intitulada “Analysis of bone damage during drilling processes”

Porto, 17 de Maio de 2017



(Elza Maria Morais Fonseca)

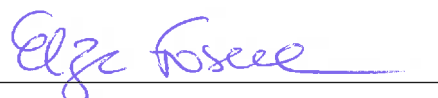


(Renato Manuel Natal Jorge)

### Autorização de Compilação

Elza Maria Morais Fonseca, Renato Manuel Natal Jorge, Mário Augusto Pires Vaz e Maria Isabel Ribeiro Dias na qualidade de coautores do artigo “Thermal analysis in drilling of *ex vivo* bovine bones” publicado na revista *Journal of Mechanics in Medicine and Biology*, declaram que autorizam a inclusão do mesmo na dissertação de doutoramento da candidata Maria Goreti Antunes Fernandes, intitulada “Analysis of bone damage during drilling processes”

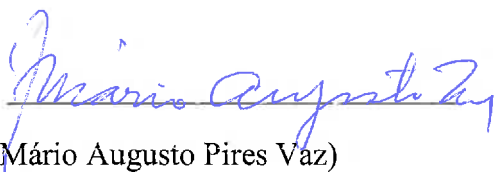
Porto, 17 de Maio de 2017



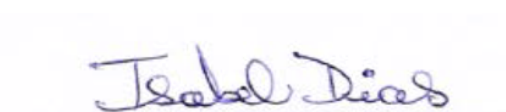
(Elza Maria Morais Fonseca)



(Renato Manuel Natal Jorge)



(Mário Augusto Pires Vaz)

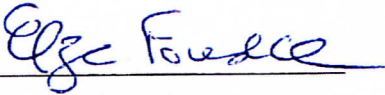


(Maria Isabel Ribeiro Dias)

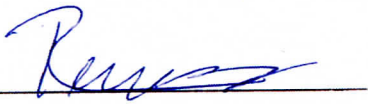
### Autorização de Compilação

Elza Maria Morais Fonseca, Renato Manuel Natal Jorge e Maria Cristina Manzanares Céspedes na qualidade de coautores do artigo “*Ex vivo* experimental and numerical study of stresses distribution in human cadaveric tibiae” submetido para publicação na revista *Computer Methods in Biomechanics and Biomedical Engineering*, declaram que autorizam a inclusão do mesmo na dissertação de doutoramento da candidata Maria Goreti Antunes Fernandes, intitulada “Analysis of bone damage during drilling processes”

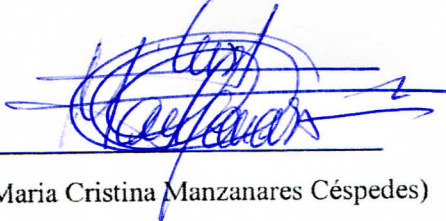
Porto, 17 de Maio de 2017



(Elza Maria Morais Fonseca)



(Renato Manuel Natal Jorge)



(Maria Cristina Manzanares Céspedes)